Penn Libraries
UNIVERSITY of PENNSYLVANIA

University of Pennsylvania
ScholarlyCommons

Master of Environmental Studies Capstone Projects   Department of Earth and Environmental Science

8-1-2006

The Influence of Urban Street Characteristics on Pedestrian Heat Comfort Levels in Philadelphia

Masayoshi Oka
University of Pennsylvania, moka@alumni.upenn.edu

Follow this and additional works at: http://repository.upenn.edu/mes_capstones

The Influence of Urban Street Characteristics on Pedestrian Heat Comfort Levels in Philadelphia

Abstract

This article describes relationships between selected physical characteristics of urban streets and pedestrian-level heat. It also identifies conditions that are particularly vulnerable to the summer heat. Field measurements of ambient temperatures 1 m above the ground were collected over sidewalks, green spaces, and parking lots in high density commercial and residential areas. Panel autoregression (PAR) analysis was then used to assess significant contributors, and prediction equations were developed. These explained over 90% of the total observed variation. The prediction equations were then used with a geographic information system (GIS) to create a cartographic map of hot and cool areas for a particular study site. The results indicate that planting trees can reduce ground ambient temperatures. Moreover, a cartographic map is effective tool for identifying heat vulnerable areas. This study offers a more comprehensive spatial scale analysis and most explicit prediction map than other studies to date.

The Influence of Urban Street Characteristics on Pedestrian Heat Comfort Levels

in Philadelphia

Masayoshi Oka, M.S.

Master of Environmental Studies

Department of Earth and Environmental Science

University of Pennsylvania

August, 2006

Capstone Project

Advisors

Frederick N. Scatena, Ph.D.   (Department of Earth and Environmental Science)

C. Dana Tomlin, Ph.D.   (Department of Landscape Architecture and Regional Planning)

TABLE OF CONTENTS

CONTEXT

PREFACE

The study presented in this paper was conducted as part of a research project examining the causes and effects of "urban heat islands" in Philadelphia. Conducted by faculty at the University of Pennsylvania and the Philadelphia Department of Public Health, the goal of that project was to explore causal relationships between observed levels of heat-induced morbidity and characteristics of the city's physical and social environment associated with the urban heat island effect.

This paper is encompasses one part of that project. It examines how physical characteristics of urban settings influence microclimate. To characterize this influence at a fine scale, differences among microclimates are expressed in terms of a physiological index that also represents human comfort. This assessment of human comfort is presented as a manuscript entitled "The Influence of Urban Street Characteristics on Pedestrian Heat Comfort Levels in Philadelphia" that will be submitted to the *Journal of American Planning Association* (*JAPA*). The format of this manuscript follows the specific guideline to fulfill *JAPA* requirements.

Due to the space limitations imposed on this submission, it does not include detailed background information, descriptions, or explanations. Those are presented separately in a context section and several appendices.

Title:

The Influence of Urban Street Characteristics on Pedestrian Heat Comfort Levels in Philadelphia

Author:

Masayoshi Oka

Biographical Sketch:

Oka is the recent graduate of the Master of Environmental Studies in the Department of Earth and Environmental Science at the University of Pennsylvania. His primary interests relate to characteristics of the physical and social environments of cities that are associated with urban heat islands. His research involves the application of spatial analytical techniques in urban environments.

Word Count for the main text: 4,951 words

Title:

The Influence of Urban Street Characteristics on Pedestrian Heat Comfort Levels in Philadelphia

Abstract:

This article describes relationships between selected physical characteristics of urban streets and pedestrian-level heat. It also identifies conditions that are particularly vulnerable to the summer heat. Field measurements of ambient temperatures 1 m above the ground were collected over sidewalks, green spaces, and parking lots in high density commercial and residential areas. Panel autoregression (PAR) analysis was then used to assess significant contributors, and prediction equations were developed. These explained over 90% of the total observed variation. The prediction equations were then used with a geographic information system (GIS) to create a cartographic map of hot and cool areas for a particular study site. The results indicate that planting trees can reduce ground ambient temperatures. Moreover, a cartographic map is effective tool for identifying heat vulnerable areas. This study offers a more comprehensive spatial scale analysis and most explicit prediction map than other studies to date.

Introduction

- Today's cities are drawing people in increasing numbers. Although urban areas occupy only about 4% of the Earth's land mass, they contain nearly half the world's population. Moreover, it is projected that more than 60% of that population will be living in urban areas by 2030 (United Nations (UN), 2004; World Resource Institute, 2000). It is also projected that the Earth's temperature will increase by 1.4 to 5.8 °C over the next century (Intergovernmental Panel on Climate Change (IPCC), 2001a). Since the potential risk of damage to a wide range of ecological and human systems is known to be associated with these projected climate changes, interest in the influence of weather on human health has grown considerably in recent years. The major impacts of climate change on human health are likely to occur via changes in the magnitude and frequency of extreme events that trigger natural disasters (IPCC, 2001b). As a result, the impact of a variable climate on human health and well-being has been the subject of numerous studies, with the majority of the work being performed by medical specialists and a small group of climatologists (Kalkstein, 1991).

- Global warming is predicted to increase the frequency, duration, and magnitude of heat waves (IPCC, 2001a, 2001b). In the recent years, heat-related mortality and morbidity in the United States has already indicated a high vulnerability of urban populations to extreme heat (McGeehin & Mirabelli, 2001; National Weather Service (NWS), 2004). Indeed, heat waves are now the largest cause of human fatalities among all meteorological hazards (such as floods, hurricanes, and tornadoes). As temperature of urban air increases with city growth, the urban heat island (UHI) effect is believed to be a key factor that aggravates more heat wave impacts on urban dwellers (IPCC, 2001a; Wilhelmi, Purvis, & Harriss, 2004).

- In the US, the impact of UHI on human health has been a concern since the 1750s (Meyer, 1991), and excessive heat-related deaths have been correlated with urban density (Buechley, Van Bruggen, & Truppi, 1972). Thus, global urbanization, the UHI effect, and a potential increase of heat waves raise a series of interrelated questions regarding health risks to sensitive urban populations (Landsberg, 1970a; McMichael, 2000). While episodic events causing heat-related fatalities always draw the greatest public notice, heat-related illnesses, are of equal concern equally endangering athletes, children, the elderly, and ill individuals (Barrow & Clark, 1998; Wexler, 2002). The best prevention for heat-related corollaries is to avoid the hot environment (Barrow & Clark, 1998; Jones et al., 1982; Kilbourne, Choi, & Jones, 1982; Wexler, 2002). Thus, it is necessary to identify such environment for those vulnerable populations and develop mitigation strategies to alleviate those casualties.

- Recent applications of geospatial technologies involinh other natural hazards suggests that efforts to mitigate and/or manage heat wave impacts can be improved through spatial and temporal modeling of UHI dynamics (Wilhelmi et al., 2004). The aim of this study is to identify causal relationships between observed levels of pedestrian comfort and characteristics of a city's physical environment. Its goal is to identify areas within a city that are vulnerable to summer heat associated with UHI. This was done by [1] collecting field data on ground-level air temperature at selected sites, [2] relating field measurements to the nearby weather station record, [3] assessing physical comfort using a physiological heat index (HI), [4] determining the influence of selected urban characteristics on UHI by using regression analysis, and [5] using these results to construct a GIS-based cartographic model that identifies relatively hotter and cooler areas at the scale of city blocks. The result of this study will enable planners to better identify critical areas for tree planting in the City of Philadelphia.

Urban Heat Islands (UHI)

•   An UHI is defined as a local urban area of high air temperature in relation to its surroundings. This phenomenon is unique to cities, and is now well documented (Arnfield, 2003; Oke, 1974, 1979, 1987).[1] Its magnitude is typically proportional to the size and/or density of the urban area involved (Oke, 1973). However, it is also affected by a variety of human activities including fuel combustion and metabolism of living beings (Fan & Sailor, 2005). The reduction of ventilation and air exchange inside urban areas also affects evaporation processes and heat exchange (Britter & Hanna, 2003; Oke, 1973).

•   The most dominant factor affecting UHI is the change in the solar radiation balance (Oke, 1987). This is caused by several components of the radiation budget. Albedo, measurement of a surface reflectivity, decreases as natural landscapes succumb to urban construction. Indeed, urban buildings are very good heat conductors; they store considerably more energy than bare soil, grass or tree leaves. As a consequence, they act as reservoirs of the radiation received heat during the day and slowly re-emit its heat during the late afternoon and night.

•   The displacement of vegetation and soils further enhances heat retention by limiting the effective natural cooling effects of evapotranspiration. This is the process by which intercepted radiation energy is utilized by plant, soils, and water bodies to convert water to water vapor. In urbanized areas, precipitation rapidly drains from impervious surfaces of roofs and streets so that when the rain ceases, only a thin film remains to be evaporated. In contrast, soil and areas covered by vegetation have a large storage capacity for water, which therefore evaporates more gradually and thus consumes substantial amounts of heat. The excess heat energy absorbed by urban constructions is large enough to raise the average temperature of the urban area by several degrees relative to the surrounding nonurban areas (Oke, 1987) .

- The form and size of UHI varies over time and space. Though it occurs throughout both day and night, the night-time effect is much greater. At night, urban air temperatures are in fact often 5-11 ºC (9-19.8 ºF) greater than nearby rural areas (Chandler, 1976). This difference is greatest under a clear sky and calm wind conditions just after sunset. The UHI effect is generally attributed to the formation of an urban boundary layer that 'domes' up over the city, induced by the local slowing of the air flow (Britter & Hanna, 2003; Oke, 1987). It involves three atmospheric layers: an urban surface layer (USL) at ground level, an urban canopy layer (UCL), roughly from ground to roof level, and an urban boundary layer (UBL) from roof up and beyond. Each layer displays different characteristics depending on spatial and temporal variations controlled by various assemblages of energy exchange processes (Arnfield, 2003).

Implications of High Temperature

- Heat-related fatalities associated with extreme heat wave events in the US indicate a continuing vulnerability of urban populations. Although heat-related mortality is one of the most underestimated causes of death in the US (Kalkstein, 1991), the National Weather Service (NWS) has estimated that a total of 2,590 people in the US lost their lives due to extreme heat between 1986 and 2003 (NWS, 2004). Exposure to extreme heat waves, which are defined as 3 or more consecutive days of temperatures over 32.2 ºC (90 ºF), can have a number of negative health effects due to vital fluid and mineral loss in the body. Indeed, the effect of heat waves can be been seen in increased mortality as early as the day after such high temperature occurs (CDC, 1995). During the severe event, when body temperature rises over 40.6 ºC (105 ºF), heat-related illness and death are likely to increase (NWS, 2004). This was evident in early June 1994, when several US cities experienced a severe heat wave that took 1,021 lives (Wilhelmi et al., 2004).[2]

- A high number of deaths are primarily associated with high daytime and nighttime temperatures that last for 48 hours (Kalkstein, 1995). The geographic locations of the cities also play an important role. Recent estimates indicate that, in very large cities like Shanghai and New York, several thousand additional heat-related deaths can be expected annually by the middle of the 21st century. The impact will be greatest in mid-latitude cities, where heat events are less frequent but extreme when they occur (Kalkstein, 1995).[3]

- The factors that most affect rates of heat-related mortality are the duration and timing of a heat wave and the geographical location of the vulnerable population (Clarke & Bach, 1971; Nieuwolt, 1966). One reason for this phenomenon is that people living in warmer regions are likely to acclimate to high temperature more easily than those who live in cooler regions. Another is the difference of building design. In high and mid-latitude regions, buildings are designed to protect against cold more so than heat. According to the 25 years of analyzed mortality data, most of excess summer mortality in the US has occurred in northern cities (Kalkstein, 1995). There was little or no mortality response to high apparent temperatures in southern cities, regardless of the severity of the extreme heat event (Kalkstein, 1995). Susceptibility also appears to be greater early in the summer season, primarily because the human body has not yet acclimated to the inclement climate (Wilhelmi et al., 2004).

Heat Warning Systems

- With future global climate change, the impact of extreme heat on human health is expected to be exacerbated, and heat-related illnesses and deaths associated with it are expected to be a significant health concern in human settlements (IPCC, 2001a, 2001b). Accordingly,

there has been an increasing interest in the development of heat warning systems that could enable authorities to issue public health advisories when hazardous heat waves are imminent.

- The benefits of alerting heat-vulnerable populations in urbanized areas are already apparent from development and deployment of existing heat warning systems. In large cities around the world and several cities in the US including Philadelphia (Kalkstein, 2000). Philadelphia's system identifies potentially oppressive air masses that may elevate mortality in the summer (Kalkstein, Jamason, Greene, Libby, & Robinson, 1996). It employs a synoptic climatological approach by grouping days with homogeneous meteorological conditions (such as temperature, humidity, cloud coverage, wind speed, and other variables) and comparing past heat wave episodes that caused high mortality rates. A similar system was also developed by Guest *et al.* (1999). Moreover, Chan *et al.* (2001) developed a mechanistic framework based on environmental conditions and behavioral responses linked to a physiological model in order to achieve more accurate mortality rates.

- Even though these systems are currently operating and have the ability to reduce risks associated with heat, it remains to generate information that will lead to better understanding of heat impacts and to produce spatially explicit mitigation strategies (Chan et al., 2001; Patz et al., 2000; Wilhelmi et al., 2004). Indeed, existing heat warning systems clearly point to the need for a better understanding of the finer-scale geospatial conditions that affect heat-vulnerable populations.

Various Observation Techniques

- Previous studies of UHI have used three methods to observe air temperature in urban settings: placing instruments at selected locations (Clarke & Bach, 1971; Nieuwolt, 1966),

mounting instruments on vehicles that traverse the study site (Preston-Whyte, 1970; Sundborg, 1950), and the use of remote sensing (Adams, 1999; Aniello, Morgan, Busbey, & Newland, 1995; Hafner & Kidder, 1999; Iino & Hoyano, 1996; Voogt & Oke, 2003; Wilhelmi et al., 2004). Although each technique captures the trend, they all have certain disadvantages.

• The disadvantage of placing instruments at set location is that the parameters obtained from observation instruments are relatively unreliable if measurement errors are greater than ± 0.5 ºC (Sundborg, 1950). These samples are also spatially limited. Measurements made from instruments on moving vehicles, the second method, can provide insight into average conditions but do not provide simultaneous data collection from separate points (Sundborg, 1950) though it appears that beginning and end traverse observations seldom differ significantly (Preston-Whyte, 1970). Advanced remote sensing technology can quantify UHI, but roofs, treetops, roads and open horizontal areas are oversampled, while vertical surfaces (such as building walls) and areas below tree crowns tend to be ignored (Arnfield, 2003; Stone & Rodgers, 2001; Wilhelmi et al., 2004). Furthermore, most remote sensing information is at a coarse spatial resolution.

• Because the goal of this study is to evaluate the influence of physical features on local ambient temperatures, measurements were made using a set of portable air-temperature and moisture probes. The accuracy of utilized instruments was determined in a preliminary testing to overcome the limitation of instrumental error (data not shown).

Urban Characteristics

• Stresses are imposed on the body by meteorological conditions including temperature, moisture content of the air, wind speed, and radiant heat (Clarke & Bach, 1971; Wexler, 2002; Wilhelmi et al., 2004). These conditions are also affected by the materials and morphology of

urban environments, where heat storage is greater than in undeveloped or agricultural sites (Grimmond & Oke, 1999). Indeed, Landsberg (1970b) found that the warmest air occurred over the pavement in front of a high-rise apartment, in a parking lot in the center of the city, the parking lot in a garden apartment development, and a protected small square surrounded by a store and small shops and/or parking lots. Conversely, a tree-shaded playground in the city showed insignificant temperature rise compared to the surrounding rural area.

- These differences can be explained by the differences in the shape and materials of the urban surface. The climate of city streets is typically examined by considering the properties of symmetrical 'canyons' characterized by its width and length, building height, and orientation (Grimmond, Cleugh, & Oke, 1991; Grimmond & Oke, 1999; Kondo & Yamazawa, 1986; Oke, Kalanda, & Steyn, 1980/1981; Yersel & Goble, 1986). Façade materials also contribute to the phenomenon by increasing solar radiation absorption during the daytime (Oke, 1987). Consequently, previous studies have categorized urban microclimatic environments by vegetation (trees, grass, etc.), impervious surface (concrete, asphalt, etc.) and the three dimensional surface area of the buildings, subdivided into the area of roofs and walls (Grimmond & Oke, 1999; Grimmond & Souch, 1994).

Methodology

- The methodology employed in this study encompassed five major tasks of study area, physiological index and human comfort, field HI measurements, weather station HI records, urban characteristics, and prediction map.

- *Study Area*: In order to capture a variety of urban site characteristics, two adjacent zip code areas were chosen in Philadelphia, PA: 19103 (West Center City) and 19104 (University City) (Figure 1). The former is a business districts, and the latter is a mixed residential-institutional neighborhood. In general, University City has more pervious surfaces and planted trees, while West Center City contains more high-rise buildings (Figure 2).

- *Physiological Index and Human Comfort*: The heat index (HI) is one of the most familiar physiological indices used to quantify the impact of heat on human beings (Rothfusz, 1990). This has been utilized by NWS and the popular media to reveal how hot the human body feels when temperature and humidity are combined. This relation is

$$HI = -42.379 + 2.049015323T + 10.14333127R - 0.22475541TR - 6.83783*10^{-3}T^2$$

$$- 5.481717*10^{-2}R^2 + 1.22874*10^{-3}T^2R + 8.5282*10^{-4} - 1.99*10^{-6}T^2R$$

where T = ambient temperature (ºF) and R = relative humidity (%).

This equation is based on the parameters from Steadman (1979) that uses more conventional independent variables. The equation is only valid for temperatures 80 ºF or higher, and relative humidities of 40% or greater. Those conditions were always met in this study.

- *Field HI Measurements*: Field measurements were carried out between mid-June and early September of 2005. HOBO H8 Pro RH/Temp loggers (H08-032-08, Onset Computer Corp.) were used to record temperature (ºF) and relative humidity (%). After preliminary testing[4], instruments were mounted on a wooden box covered with white tape to reduce direct solar

energy absorption. Each instrument was placed horizontally 1m above the ground surface on a wooden tripod. To be freely exposed to the environment, these instruments were placed at least 2 m away from nearby buildings, obstructions, and artificially-generated heat sources such as air-conditioning exhaust. Instruments were programmed to record at 10-minute intervals. These measurements were then averaged on an hourly basis. Since the storage heat flux is typically greatest at noon, and the most intense UHI effects occur several hours after sunset, field HI measurements were conducted at 13:00 (daytime) and 22:00 (nighttime). These measurements were conducted for two consecutive days at the each location to eliminate measurement errors. The observed temperature and relative humidity were then used to compute HI as described above and the results in Fahrenheit were converted into Celsius.

- *Weather Station HI Records*: HI announcements by the popular media are based on records of weather stations that are located in open spaces and on roof-tops, and thus do not capture the pedestrian level conditions within the urban settings. In order to predict the spatial distribution of pedestrian level HI, above-canopy HI recorded at a nearby roof-top weather station was incorporated. The weather station is one of a network of more than dozen stations in the City of Philadelphia. It is equipped with a standard AirWatch system that is operated and maintained by the Automated Weather Source's AirWatch system (http://achieve.weatherbug.com/) and the Department of Earth and Environmental Science of the University of Pennsylvania. The station is situated 2.75 m (9 feet) above the top of a four story building near the center of the study area. The station measured temperature and relative humidity every 5 minutes. These measures were averaged on an hourly basis and then used to calculate the average hourly above-canopy HI that corresponded to the ground level measurements.

- *Urban Characteristics*: Following previous studies, the amount of shade (tree coverage), street width (including sidewalks), distance to nearest building, and building height (number of stories) were used to determine the urban street characteristics. The percent of shade above each sample point was measured by an AccuPAR (model LP-80, Decagon Devices, Inc.). The AccuPAR measures intercepted photosynthetically-active radiation under any type of canopy. These measurements indicate the amount of shade within a horizontal circle of 2 m in diameter directly over the field measuring instrument. Measurements were also made in full sunlight and used to calculate the shade covering upon the measuring instrument. This includes shade from tree coverage and buildings. The numbers of building stories adjacent to the sampling areas were counted visually during the field measurement. Two other indices, street width (feet) and distance to building (feet) were determined by the use of GIS data obtained from Pennsylvania Spatial Data Access (PASDA: http://www.pasda.psu.edu/).

- *Prediction Map*: Data on the residential building stories was acquired from the Cartographic Modeling Laboratory (CML: http://cml.upenn.edu/) at University of Pennsylvania. The information on high rise building stories data was provided from the Mayor's office of Philadelphia City. Utilizing the linear regression equation derived from the OLS model, cartographic models were created by way of map algebra (Tomlin, 1990) using the ArcGIS geographic information system (ESRI). Note that shade generated by buildings and/or other obstructions was not included in this map. Building roofs were also excluded thus indicated as white color. These maps were constructed at a raster resolution of 10×10 feet.

Analysis

- *Verifying Underlying Assumptions for Regression Analysis*: Four basic underlying assumptions were checked under the ordinary least squares (OLS) statistical model in JMP-IN (SAS Institute, Inc.). These four basic conditions are: [1] relationship between independent and dependent variables by Pearson product-moment correlation matrix, [2] higher order of colinearity by the variance influence factor (VIF), [3] normality of residuals by normal quantile plot, and [4] linearity assumption by regressing residuals on explanatory variables.

- *Stepwise Regression Analysis*: Variables that are ineffective under OLS model is unlikely to be effective under autoregressive model. This was also carried out in JMP-IN and omission of variables that indicated over the significant level of 0.25 was done under OLS statistical model.

- *Panel Autoregression (PAR) Analysis*: Field HI measurements were carried out for two consecutive days at the same location and under different urban environments. Accordingly, it is likely that spatial and temporal autocorrelation could occur. Spatial autocorrelation was present, but its influence was not evident and results were similar relative to the OLS statistical model. Thus, temporal autocorrelation was only considered in the analysis. To take into account for this, PAR model was created on a basis of autoregressive model (Bailey & Gatrell, 1995). The model is $y = X\beta + u$, $u = \rho Wu + \varepsilon$, $\varepsilon \sim N(0, \sigma^2 I)$ where W is a temporal weight matrix that directs second day field HI measurement to depend on the first day measurement, u is the prediction errors, ρ is an autoregressive parameter, and I is the Moran's I. The analysis was conducted in MATLAB (The Math Works, Inc.).

- *Goodness-of-fit Measurement*: Relative to R^2 in OLS statistical model, four alternative indices (Pseudo R^2, squared correlation, log likelihood value, and Akaike's Information Criterion (AIC)) were used (Anselin, 1988). These calculations were also conducted in MATLAB.

Results

- All independent variables (weather station HI records = SHI, amount of shade = Sh, street width = SW, distance to building = DB, and building stories = BS) had linear relations to the dependent variable (field HI measurement = FHI). The strength of the correlations changed depending on the surface materials and time (Table 1B). Indeed, for the daytime measurements over the impervious surfaces, Sh, SW, and BS were negatively correlated while SHI and DB had positive correlations. Over pervious surfaces during the daytime, only SHI had a positive correlation. Similarly, for the nighttime measurements over the impervious surface, all explanatory variables entailed positive correlation. Nevertheless, over pervious surfaces during the nighttime, SHI and BS exhibited positive correlation while SW and DB revealed negative correlation. Here, strong correlation was only apparent between FHI and SHI, over 0.88, and others were relatively weakly correlated.

- Although models that include all explanatory variables can be effective in prediction, stepwise regression analyses under OLS model were conducted to reveal the most important variables (data not shown). From this, SHI, Sh, and BS were significant for both surface materials at daytime. Nevertheless, all variables were correlated with both types of surface materials at nighttime. As variables that are ineffective under OLS model are unlikely to be effective under autoregressive model, only the variables derived from stepwise regression analyses were incorporated into the autoregression analysis. Although there were skewed distributions of some variables, there were no reasons to reject the underlying assumption for regression analysis (data not shown).

- Since same field HI measurements were conducted for two consecutive days at the same location, temporal autocorrelation was determined to be present. The violation of independence

result the estimates obtained from the OLS estimator to be biased and lead to indicate some

coefficients to be significant, when in fact they are not. Accordingly, PAR analysis was utilized

to capture the true occurrence of the event (Table 2A). Similar to the correlation of variables,

parameter estimates revealed that the effect of independent variables changed over different

surface materials and time, except for SHI that was strongly significant in all cases. Certainly, at

daytime regardless of surface material, both Sh and BS indicated strong significant effect. On the

other hand, at nighttime over the impervious surface, SW and DB entailed significant level and

BS to be weakly significant. Nonetheless, over the pervious surface, both DB and BS exhibited

strong coefficient, but SW revealed no significant effect. The final models explained over 90%

of the total variation (Table 2B). In both timeframes, impervious surfaces indicated slightly poor

goodness-of-fit measurements.[5]

- The models prediction precision was evaluated using OLS model (Table 3A) by way of

calculating 95% prediction intervals (PI) on conditional means (Table 3B). Similar to the PAR

models' goodness-of-fit measurements, adjusted R^2 for impervious surface indicated slightly

lower value in both time periods. Additionally, it indicated that over 90% of the total variations

were explained. Based on these significant models, 95% PI did not exceed $\pm$ 2.62 ºC ($\pm$ 9.45 ºF)

and $\pm$ 2.08 ºC ($\pm$ 7.51 ºF) at daytime and nighttime, respectively (Table 3B). The high

performance of the model can also be determined by the root mean square error (RMSE) that

they were less than 1.5. Again, pervious surface materials had lower RMSE than impervious

surface where they were even less than 1.0.

- These results indicate that the prediction models are sufficient to identify the pedestrian

level HI once SHI is recorded. Thus, prediction models in Table 3A were applied in ArcGIS for

creating an explicit cartographic prediction map for the study site (Figure 3). This was simulated

under the SHI of 32 and 28 ℃ (89.6 and 82.4 ℉) for daytime and nighttime, respectively (Figure

3 A and C). The cool and hot areas within this study site were the lower and upper 10% bounds

of the predictions (Figure 3 B and D).[6] Comparing these maps to those of tree coverage (Figure

2D) indicates that the cool and hot areas corresponds to the amount of trees that are covering the

area. Obviously, tree-shaded areas are much cooler than those without trees.

- During the daytime, non-shaded impervious surfaces with low BS are as much as 3.91 ℃

(7.04 ℉) higher HI than SHI. Conversely, shaded pervious surface that are related with high BS

at same time were as much as 0.75 ℃ (1.35 ℉) lower HI than SHI. Grouping the nighttime

under- and overestimated areas indicated that impervious surface that are associated with wide

streets, adjacent to buildings and few building stories can have a HI as 3.74 ℃ (6.73 ℉) higher

HI than SHI. On the contrary, pervious surfaces that are situated with narrow streets, far from

nearby building, and low building stories indicated as much as 0.63 ℃ (1.13 ℉) lower HI than

SHI. Cool areas are essentially large tree planted green spaces and hot areas are in opposition

large open parking lots. The maximum HI difference of cool and hot areas are approximately

4.66 ℃ (8.39 ℉) and 4.37 ℃ (7.86 ℉) at daytime and nighttime, respectively.

Discussion

- This study demonstrated that the physical characteristics of urban streets and parking lots can have a large influence on the local HI. Moreover, these influences can cause the HI to vary over 4 ºC between nearby areas within a city. The techniques used in this study are useful in identifying locally hot areas within a city and can be used to focus education and assistance during heat waves. Indeed, the prediction derived here explicitly indicates where mitigation strategies should be implemented.

- Pedestrian-level HI, and thus level of discomfort and stress is dependent upon the thermal radiation and thermal properties of the site. This study indicates that hotter areas during the day and night are typically non-shaded impervious areas exposed to the direct sun. Cooler areas are typically on pervious ground and are well shaded by trees or building. This study also suggests that the thermal bulk properties (including heat capacity and thermal conductivity) and the radiative properties (albedo and emissivity) of buildings and streets are the main factors responsible for differences in heat in urban environments.

- The study also demonstrates that Sh, SW and DB can influence nighttime HI. Since non-shaded areas absorb more heat for longer periods of time, especially in the case of impervious surfaces, the heat emitted by such areas is significant after sunset. Certainly, streets and building façades on treeless blocks are likely to absorb more heat than shaded ones. Therefore, heat emitted from those surfaces increases pedestrian discomfort.

- These results also suggest that more trees should be planted at areas of open parking lots and along wide streets with heavy traffic (both pedestrian and vehicles). This is especially true in areas that do not receive artificial shade from surrounding tall structures. In the processes of tree

planting, appropriate orientation should also be considered. It is ideal to cover roofs and south-, east-, and west-facing walls.

- Alleviating the impact of heat during the summer by way of planting trees in a community is often suggested as one of UHI mitigation strategies (Rosenfeld et al., 1995). Large open parks in particular are known to reduce ambient air temperature within the urban setting at microclimate (Jauregui, 1990/91). Along with heat reduction, the presence of urban trees and/or forests is known to provide numerous additional benefits. Among these are a more pleasant, healthy, and comfortable environments to live, work and play in, savings in the costs of providing a wide range of urban services, substantial improvements in individual and community well-being, increase in real estate values, reduced energy use during the summer, and improved air quality (Akbari, Pomerantz, & Taha, 2001; Dwyer, McPherson, Schroeder, & Rowntree, 1992; Rosenfeld, Akbari, Romm, & Pomerantz, 1998; Wachter, 2004; Wagrowski & Hites, 1997).

- Taking these benefits into account, efforts to cool communities via tree plantings (Semrau, 1992) and proactive local activities - such as those of the Philadelphia Horticulture Society and University City Green (both in Philadelphia area) - are encouraged. However, many tree species are reported to emit highly photochemically reactive hydrocarbons that may potentially adversely affect air quality (Benjamin, Sudol, Bloch, & Winter, 1996). Hence, appropriate species selection and orientation of trees are highly recommended.

- If a program of tree plantings were to be put into place, urban pedestrian heat discomfort would be alleviated during the heat events and throughout the summer. This might then reduce the incidence and severity of heat-related illnesses among vulnerable populations. Considering these benefits, city planners and authorities should advocate plantings in the hotter areas.

Acknowledgements

References

Adams, E. (1999). Urban heat. *Architecture, 88*(1), 134-135.

Akbari, H., Pomerantz, M., & Taha, H. (2001). Cool surfaces and shade trees to reduce energy use and improve air quality in urban areas. *Solar Energy, 70*(3), 295-310.

Aniello, C., Morgan, K., Busbey, A., & Newland, L. (1995). Mapping micro-urban heat island using landsat tm and a gis. *Computers & Geosciences, 21*(8), 965-969.

Anselin, L. (1988). *Spatial econometrics: Methods and models*:Kluwer Academic, Dordrecht.

Arnfield, A. J. (2003). Two decades of urban climate research: A review of turbulence, exchanges of energy and water, and the urban heat island. *International Journal of Climatology, 23*, 1-26.

Bailey, T. C., & Gatrell, A. C. (1995). *Interactive spatial data analysis*.Harlow: Longman.

Barrow, M. W., & Clark, K. A. (1998). Heat-related illnesses. *American Family Physician, 58*(3), 749-756.

Benjamin, M. T., Sudol, M., Bloch, L., & Winter, A. M. (1996). Low-emitting urban forests: A taxonomic methodology for assigning isoprene and monoterpene emission rates. *Atmospheric Environment, 30*(9), 1437-1452.

Britter, R. E., & Hanna, S. R. (2003). Flow and dispersion in urban areas. *Annual Review of Fluid Mechanics, 35*, 469-496.

Buechley, R. W., Van Bruggen, J., & Truppi, L. E. (1972). Heat island = death island? *Environmental Research, 5*, 85-92.

Center for Disease Control (CDC). (1984). Heat-associated mortality - new york city. *Morbidity and Mortality Weekly Report (MMWR), 33*(29), 430-432.

Center for Disease Control (CDC). (1994). Heat-related deaths - philadelphia and united states, 1993-1994. *Morbidity and Mortality Weekly Report (MMWR), 43*(25), 453-455.

Center for Disease Control (CDC). (1995). Heat-related illnesses and deaths - united states, 1994-1995. *Morbidity and Mortality Weekly Report (MMWR), 44*(25), 465-468.

Chan, N. Y., Stacey, M. T., Smith, A. E., Ebi, K. L., & Wilson, T. F. (2001). An empirical mechanistic framework for heat-related illness. *Climate Research, 16*, 133-143.

Chandler, T. J. (1976). *Urban climatology and its relevance to urban design*.Geneva, Switzerland: World Meteorological Organization (WMO).

Clarke, J. F., & Bach, W. (1971). Comparison of the comfort conditions in different urban and suburban microenvironments. *International Journal of Biometeorology, 15*(1), 41-54.

Dwyer, J. F., McPherson, E. G., Schroeder, H. W., & Rowntree, R. A. (1992). Assessing the benefits and costs of the urban forest. *Journal of Arboriculture, 18*(5), 227-234.

Fan, H., & Sailor, D. J. (2005). Modeling the impacts of anthropogenic heating on the urban climate of philadelphia: A comparison of implementations in two pbl schemes. *Atmospheric Environment, 39*, 73-84.

Grimmond, C. S. B., Cleugh, H. A., & Oke, T. R. (1991). An objective urban heat storage model and its comparison with other schemes. *Atmospheric Environment, 25B*(3), 311-326.

Grimmond, C. S. B., & Oke, T. R. (1999). Heat storage in urban area: Local-scale observations and evaluation of a simple model. *Journal of Applied Meteorology, 38*, 922-940.

Grimmond, C. S. B., & Souch, C. (1994). Surface description for urban climate studies: A gis based methodology. *Geocarto International, 1*, 47-59.

Guest, C. S., Willson, K., Woodward, A. J., Hennessy, K., Kalkstein, L. S., Skinner, C., et al. (1999). Climate and mortality in australia: Retrospective study, 1970-1990, and predicted impact in five major cities in 2030. *Climate Research, 13*, 1-15.

Hafner, J., & Kidder, S. Q. (1999). Urban heat island modeling in conjunction with satellite-drived surface/soil parameters. *Journal of Applied Meteorology, 38*, 448-465.

Howard, L. (1818). *The climate of london / deduced from meteorological observation*.London: W. Phillips.

Iino, A., & Hoyano, A. (1996). Development of a method to predict the heat island potential using remote sensing and gis data. *Energy and Buildings, 23*, 199-205.

Intergovernmental Panel on Climate Change (IPCC). (2001a). *Climate change 2001: Impacts, adaptation, and vulnerability*.UK: Cambridge University Press.

Intergovernmental Panel on Climate Change (IPCC). (2001b). *Climate change 2001: Scientific basis*.UK: University of Cambridge Press.

Jauregui, E. (1990/91). Influence of large urban park on temperature and convective precipitation in a tropical city. *Energy and Buildings, 15-16*, 457-463.

Jones, T. S., Liang, A. P., Kilbourne, E. M., Griffin, M. R., Patriarca, P. A., Fite Wassilak, S. G., et al. (1982). Morbidity and mortality associated with the july 1980 heat wave in st. Louis and kansas city, mo. *Journal of the American Medical Association, 247*(24), 3327-3331.

Kalkstein, L. S. (1991). A new approach to evaluate the impact of climate on human mortality. *Environmental Health Perspectives, 96*, 145-150.

Kalkstein, L. S. (1995). Lesson from a very hot summer. *The Lancet, 346*, 857-859.

Kalkstein, L. S. (2000). Saving lives during extreme weather in summer. *British Medical Journal, 321*, 650-651.

Kalkstein, L. S., Jamason, P. F., Greene, J. S., Libby, J., & Robinson, L. (1996). The philadelphia hot weather-health watch/warning system: Development and application, summer 1995. *Bulletin of the American Meteorological Society, 77*(7), 1519-1528.

Kilbourne, E. M., Choi, K., & Jones, T. S. (1982). Risk factor for heatstroke: A case-control study. *The Journal of the American Medical Association, 247*(24), 3332-3336.

Kondo, J., & Yamazawa, H. (1986). Aerodynamic roughness over an inhomogeneous ground surface. *Boundary-Layer Meteorology, 35*, 331-348.

Landsberg, H. E. (1970a). Man-made climatic change. *Science, 170*(3964), 1265-1274.

Landsberg, H. E. (1970b). *Urban climate*.Geneva, Switzerland: World Meteorological Organization (WMO).

McGeehin, M. A., & Mirabelli, M. (2001). The potential impact of climate variability and change on temperature-related morbidity and mortality in the united states. *Environmental Health Perspectives, 109*(2), 185-189.

McMichael, A. J. (2000). The urban environment and health in a world of increasing globalization: Issues for developing countries. *Bulletin of the World Health Organization, 78*(9), 1117-1126.

Meyer, W. B. (1991). Urban heat island and urban health: Early american perspectives. *Professional Geographer, 43*(1), 38-48.

National Weather Service (NWS). (2004). *Natural hazard statistics*:Office of Climate, Water and Weather Services.

Nieuwolt, S. (1966). The urban microclimate of singapore. *The Journal of Tropical Geography, 22*, 30-37.

Oke, T. R. (1973). City size and the urban heat island. *Atmospheric Environment, 7*, 769-779.

Oke, T. R. (1974). *Review of urban climatology 1968-1973*.Geneva, Switzerland: World
      Meteorological Organization (WMO).
Oke, T. R. (1979). *Review of urban climatology 1973-1976*.Geneva, Switzerland: World
      Meteorological Organization (WMO).
Oke, T. R. (1987). *Boundary layer climates, 2nd edition*:Routledge.
Oke, T. R., Kalanda, B. D., & Steyn, D. G. (1980/1981). Parameterization of heat storage in
      urban areas. *Urban Ecology, 5*, 45-54.
Patz, J. A., McGeehin, M. A., Bernard, S. M., Ebi, K. L., Epstein, P. R., Grambsch, A., et al.
      (2000). The potential health impacts of climate variability and change for the united
      states: Executive summary of the report of the health sector of the u.S. National
      assessment. *Environmental Health Perspectives, 108*(4), 367-376.
Preston-Whyte, R. A. (1970). A spatial model of an urban heat island. *Journal of Applied
      Meteorology, 9*, 571-573.
Rosenfeld, A. H., Akbari, H., Bretz, S., Fishman, B. L., Kurn, D. M., Sailor, D., et al. (1995).
      Mitigation of urban heat islands: Mateirals, utility programs, updates. *Energy and
      Buildings, 22*, 255-265.
Rosenfeld, A. H., Akbari, H., Romm, J. J., & Pomerantz, M. (1998). Cool communities:
      Strategies for heat island mitigation and smog reduction. *Energy and Buildings, 28*(1),
      51-62.
Rothfusz, L. P. (1990). *The heat index equation (or, more than you wanted to know about heat
      index)*. Fort Worth, TX.
Semrau, A. (1992). Introducing cool communities. *American Forests, 98*(July/August), 49-53.
Steadman, R. G. (1979). The assessment of sultriness. Part i: A temperature-humidity index
      based on human physiology and clothing science. *Journal of Applied Meteorology, 18*,
      861-873.
Stone, B., Jr., & Rodgers, M. O. (2001). Urban form and thermal efficiency: How the design of
      cities influences the urban heat island effect. *Journal of American Planning Association,
      67*(2), 186-198.
Sundborg, A. (1950). Local climatological studies of the temperature conditions in an urban area.
      Tellus, 2, 221-231.
Tomlin, C. D. (1990). *Geographic information systems and cartographic modeling*.Englewood
      Cliffs, NJ: Prentice Hall.
United Nations (UN). (2004). *Urban and rural areas 2003.* Department of Economic and Social
      Affairs, Population Division.
Voogt, J. A., & Oke, T. R. (2003). Thermal remote sensing of urban climates. *Remote Sensing of
      Environment, 86*, 370-384.
Wachter, S. (2004). The determinants of neighborhood transformations in philadelphia -
      identification and analysis: The new kensington pilot study. *Unpublished Manuscript*,
      The Wharton School, University of Pennsylvania.
Wagrowski, D. M., & Hites, R. A. (1997). Polycyclic aromatic hydrocarbon accumulation in
      urban, suburban, and rural vegetation. *Environmental Science and Technology, 31*(1),
      279-282.
Wexler, R. K. (2002). Evaluation and treatment of heat-related illnesses. *American Family
      Physician, 65*(11), 2307-2314.

Wilhelmi, O. V., Purvis, K. L., & Harriss, R. C. (2004). Designing a geospatial information infrastructure for mitigation of heat wave hazards in urban area. *Natural Hazards Review, 5*(3), 147-158.

World Resource Institute. (2000). *World resource 2000-2001*.New York: Oxford University Press.

Yersel, M., & Goble, R. (1986). Roughness effects on urban turbulence parameters. *Boundary-Layer Meteorology, 37*, 271-284.

Author Note

Department of Earth and Environmental Science

University of Pennsylvania, University City, PA 19104, USA

Email address: moka@sas.upenn.edu

Footnotes

- 1. The identification of UHI was first documented by Luke Howard's pioneering examination of London's climate (1818). It is typically presented as a temperature difference between the air within the urban settlement and that measured in a rural area immediately outside the settlement (ΔT_{u-r}). This ΔT_{u-r} is used to detect the UHI intensity where maximum degree is depicted at the urban core (Oke, 1987).

- 2. Temperature was initially thought to be the single predictive meteorological variable for increasing mortality during the heat wave (Clarke & Bach, 1971; Wexler, 2002). It is now known that various meteorological variables contribute to the cause. These additional variables include relative humidity, wind speed, and fluxes in both short- and long-wave radiation (Buechley et al., 1972). Heat-related incidents are a greater problem in cities than in suburban or rural areas due to the combined effect of high temperature and high humidity. Indeed, it is already evident from the July 1966 that hot spell impacted several metropolitan regions of the US where higher mortality ratios were found in the center of cities than in surrounding suburban/rural areas where positive correlation between higher temperature and population density are evident during the heat wave (Wilhelmi et al., 2004).

- 3. These are areas which exhibit the greatest number of heat-related deaths, and include large cities in eastern and Midwestern North America, western Europe, northern India, and China (CDC, 1984, 1994). In the US, increased mortality due to heat waves has been linked to high and mid-latitude regions such as New York City and Philadelphia (Wilhelmi et al., 2004). During the episode, 118 deaths (11.56% of total death toll) were determined to be associated with the heat wave in Philadelphia, PA, where the condition was with high temperatures of 33.9-38.3 ℃ (93-101 ℉) and high humidity of 36-58% (CDC, 1994).

- 4. These instruments were first tested in various conditions such as in a refrigerator and an incubator. These tests showed that the standard deviations between instruments were less than 0.3 ℃ and less than 1.9 % for temperature and relative humidity, respectively (data not shown). They were then placed over two different surface materials, impervious and pervious. Impervious surfaces include asphalt, concrete, and brick. Pervious surface were limited to grass growing areas and excluded bare soil. The reason impervious surfaces include three materials is that during the preliminary testing temperature above concrete and brick were not significantly different (data not shown). Differences between asphalt and concrete/brick can be explained by the variables of street width and distance to buildings.

- 5. The reason that impervious surfaces have a lower goodness-of-fit measurements and larger errors can be understood from previous studies. Indeed, surface roughness elements cause complex flows around them thus three-dimensional effects are strongly dependent on the characteristics of the elements including their shape, plan density, flexibility, etc. (Oke, 1987). Voogt and Oke (2003) also support this notion that overall urban surface structure have impacts of structural features such as: roof geometry, variable building height and vegetation geometry. Therefore, impervious surfaces are regarded to have rougher property than pervious surfaces.

- 6. In the nighttime prediction map, inaccuracy due to the over- and underestimation became evident. Indeed, from the data sampled analysis (Table 1), the range of HI prediction was determined to be 27.37-31.74 ℃ (81.27-89.13 ℉). Therefore, areas that are beyond this range are extrapolated regions. The maximum SW and DB within the study site were 440 and 848, respectively. As a result, impervious surfaces that are related to wider SW beyond the collected range can be overestimated. Likewise, pervious surface that are associated with DB beyond the collected range can be underestimated.

Tables

Table 1. Summary of the Datasets.

Note: n = sample points, FHI = field HI measurement, SHI = weather station HI record, Sh = amount of shade, SW = street width, DB = distance to building, BS = building stories, Std Dev = standard deviation, and Std Err Mean = standard error mean.

(A) descriptions of datasets, and (B) Pearson product-moment correlation matrices.

(A)		Descriptions	FHI (C)	SHI (C)	Sh (%)	SW (ft)	DB (ft)	BS (#)
Day (13:00)	**Impervious Surface** (n = 102)	Maximum	45.22	40.07	96.93	42.00	73.17	41.00
		Minimum	25.00	25.05	0.00	8.20	1.56	1.50
		Mean	33.07	30.89	41.76	19.77	13.32	8.84
		Std Dev	4.21	3.39	42.45	6.72	16.37	12.02
		Std Err Mean	0.42	0.34	4.20	0.67	1.62	1.19
	Pervious Surface (n = 58)	Maximum	42.55	40.07	97.78	42.00	60.20	41.00
		Minimum	25.12	25.05	0.00	11.66	5.65	2.25
		Mean	30.79	29.87	42.00	23.17	31.18	8.89
		Std Dev	4.09	3.82	40.16	9.25	16.12	10.17
		Std Err Mean	0.54	0.50	5.27	1.21	2.12	1.34
Night (22:00)	**Impervious Surface** (n= 106)	Maximum	36.61	32.90	.	42.00	73.17	45.00
		Minimum	23.51	21.62	.	7.64	1.56	1.50
		Mean	28.67	26.43	.	19.74	12.67	11.55
		Std Dev	3.39	3.15	.	7.26	16.28	14.29
		Std Err Mean	0.33	0.31	.	0.70	1.58	1.39
	Pervious Surface (n = 52)	Maximum	35.13	32.90	.	42.00	60.20	41.00
		Minimum	23.98	23.76	.	11.66	5.66	2.25
		Mean	27.62	26.93	.	24.07	32.95	9.54
		Std Dev	3.35	2.84	.	9.36	16.03	10.56
		Std Err Mean	0.46	0.39	.	1.30	2.22	1.46

(B)		Impervious Surface						Pervious Surface					
	Term	FHI	SHI	Sh	SW	DB	BS	FHI	SHI	Sh	SW	DB	BS
Day (13:00)	FHI	1	0.8861	-0.3762	-0.0738	-0.0886	0.1190	1	0.9490	-0.3998	-0.3544	-0.3603	0.0112
	SHI	0.8861	1	-0.0556	-0.0258	-0.1348	0.2549	0.9490	1	-0.2268	-0.3860	-0.3106	0.0757
	Sh	-0.3762	-0.0556	1	0.0884	-0.0676	-0.0200	-0.3998	-0.2268	1	0.0685	0.1760	-0.1450
	SD	-0.0738	-0.0258	0.0884	1	0.3855	0.3786	-0.3544	-0.3860	0.0685	1	0.7420	0.1239
	DB	-0.0886	-0.1348	-0.0676	0.3855	1	-0.2047	-0.3603	-0.3106	0.1760	0.7420	1	0.1964
	BS	0.1190	0.2549	-0.0200	0.3786	-0.2047	1	0.0112	0.0757	-0.1450	0.1239	0.1964	1
Night (22:00)	FHI	1	0.9445	.	0.1783	-0.0788	0.2195	1	0.9800	.	-0.5132	-0.5096	0.1669
	SHI	0.9445	1	.	0.1654	0.0188	0.2318	0.9800	1	.	-0.5320	-0.4882	0.1234
	SW	0.1783	0.1654	.	1	0.3597	0.2839	-0.5132	-0.5320	.	1	0.7190	0.0735
	DB	-0.0788	0.0188	.	0.3597	1	-0.2645	-0.5096	-0.4882	.	0.7190	1	0.1454
	BS	0.2195	0.2318	.	0.2839	-0.2645	1	0.1669	0.1234	.	0.0735	0.1454	1

Table 2. Assessment for predicting the pedestrian heat comfort level.

Note: AIC = Akaike's Information Criterion.

(A) PAR analysis results, and (B) goodness-of-fit measurements of the PAR model.

(A)		Impervious Surface			Pervious Surface		
	Term	Coefficient	Z-value	Probability	Coefficient	Z-value	Probability
Day (13:00)	Constant	0.8974	0.7995	0.4240	2.8066	3.1731	0.0015
	SHI	1.0990	30.6484	0.0000	0.9858	36.0555	0.0000
	Sh	-0.0330	-9.3193	0.0000	-0.0218	-5.8766	0.0000
	BS	-0.0435	-3.3984	0.0007	-0.0559	-3.5854	0.0003
Night (22:00)	Constant	1.5605	1.7264	0.0843	-2.8859	-2.4892	0.0128
	SHI	1.0143	29.8300	0.0000	1.1312	30.5245	0.0000
	SW	0.0438	2.5499	0.0108	0.0211	1.5326	0.1254
	DB	-0.0306	-4.0310	0.0001	-0.0194	-2.4395	0.0147
	BS	-0.0152	-1.7768	0.0756	0.0183	2.1773	0.0295

(B)	Day (13:00)		Night (22:00)	
Surface	Impervious	Pervious	Impervious	Pervious
Pseudo R^2	0.9856	0.9973	0.9276	0.9667
Adjusted Pseudo R^2	0.9852	0.9971	0.9247	0.9638
Squared Correlation	0.9048	0.9417	0.9083	0.9665
Log Likelihood Value	-164.1677	-71.9462	-152.3540	-47.8776
AIC	340.3355	155.8924	318.7080	109.7552
Corrected AIC	341.2197	157.5394	319.8508	112.3006

Table 3. Predicting the pedestrian heat comfort level.

Note: RMSE = root-mean-square error, SE Pred = standard error of predicted, and PI =

prediction interval

(A) prediction models derived from OLS model, and (B) 95% prediction intervals on conditional

mean under OLS model.

(A)	Surface	Model	Adjusted R^2
Day **(13:00)**	**Impervious**	0.44 + 1.11(SHI) - 0.03(Sh) - 0.04(BS)	0.9021
	Pervious	2.93 + 0.97(SHI) - 0.02(Sh) - 0.04(BS)	0.9410
Night **(22:00)**	**Impervious**	1.42 + 1.02(SHI) + 0.04(SW) - 0.03(DB) - 0.02(BS)	0.9047
	Pervious	-2.93 + 1.13(SHI) + 0.02(SW) - 0.02(DB) + 0.02(BS)	0.9636

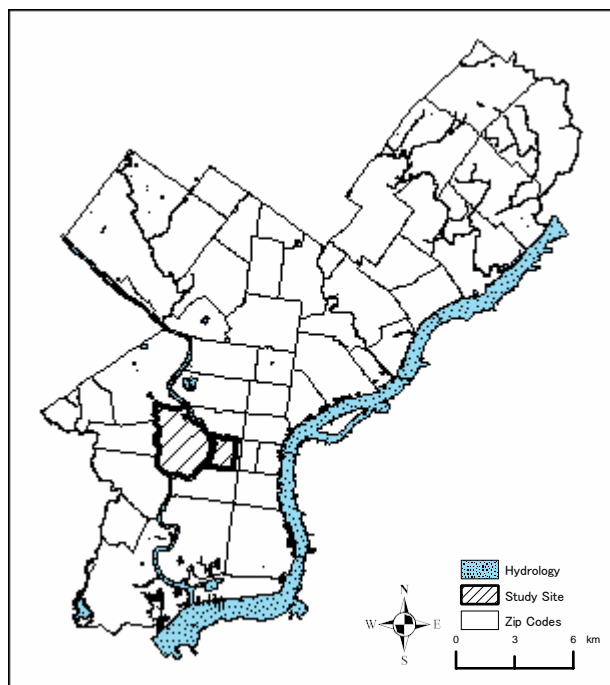| (B)	Surface	Mean Response	RMSE	SE Pred	Upper 95% PI	Lower 95% PI	Range
Day **(13:00)**	**Impervious**	33.07	1.3162	0.1303	35.69	30.44	± 2.62
	Pervious	30.79	0.9927	0.1303	32.80	28.78	± 2.01
Night **(22:00)**	**Impervious**	28.67	1.0460	0.1016	30.76	26.59	± 2.08
	Pervious	27.62	0.6391	0.0886	28.92	26.32	± 1.30

Figures

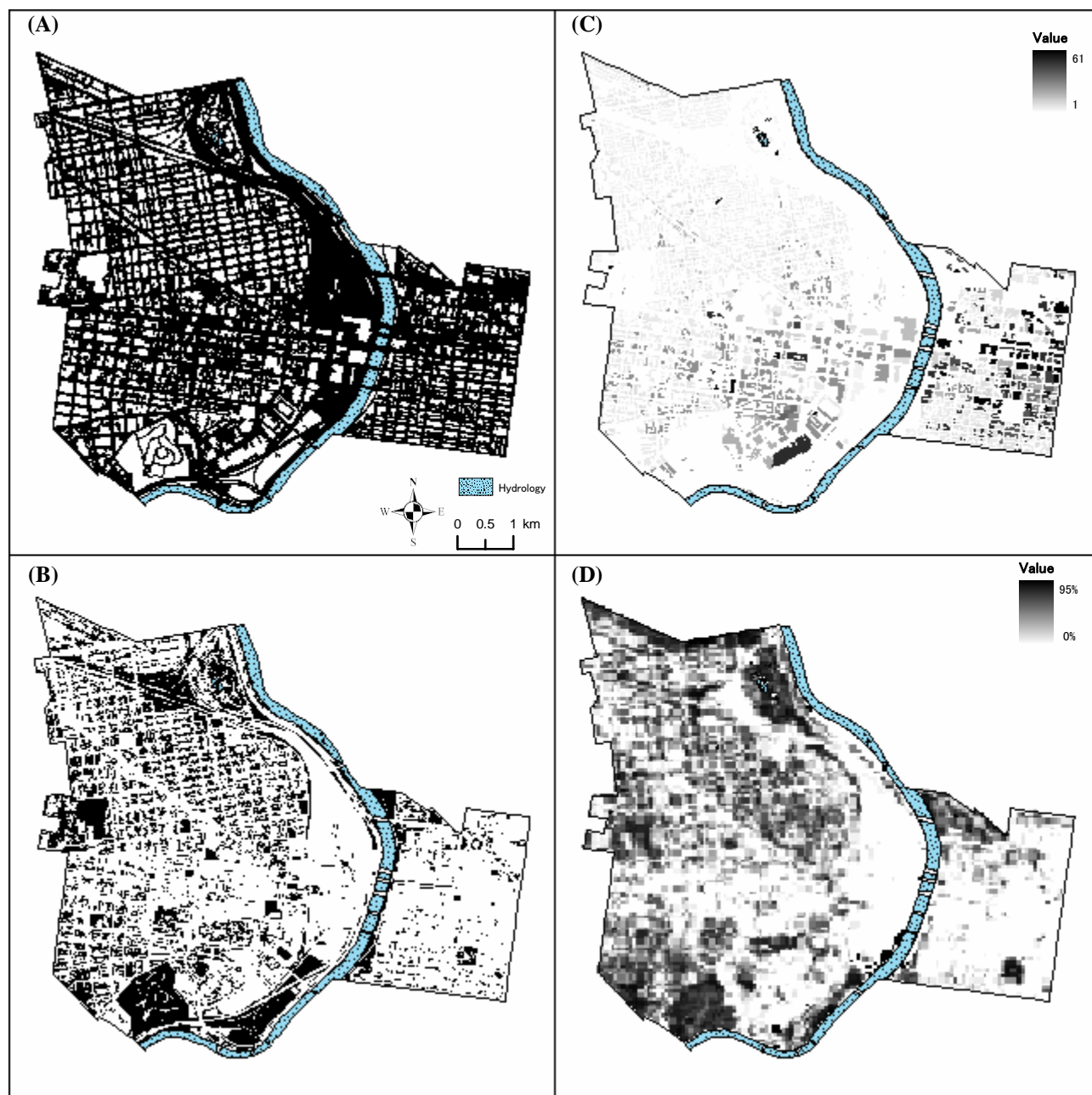Figure 1. Map of Philadelphia and selected study site.

Figure 2. Urban characteristics of the study site.

(A) impervious surface, (B) pervious surface, (C) building stories, and (D) tree coverage.

Figure 3. Cartographic map of the pedestrian heat comfort level.

(A) prediction map for daytime, (B) hot and cool areas at daytime, (C) prediction map for

nighttime, and (D) hot and cool areas at nighttime.

The Influence of Urban Street Characteristics on Pedestrian Heat Comfort Levels

in Philadelphia

<u>CONTEXT</u>

Masayoshi Oka, M.S.

Master of Environmental Studies

Department of Earth and Environmental Science

University of Pennsylvania

August, 2006

Capstone Project

Advisors

Frederick N. Scatena, Ph.D.   (Department of Earth and Environmental Science)

C. Dana Tomlin, Ph.D.   (Department of Landscape Architecture and Regional Planning)

Background Information

<u>Necessity of the Warning System</u>

In recent years, heat-related mortality and morbidity records in the United States have indicated a high vulnerability of urban populations to extreme heat. This is, in fact, the major cause of fatalities among natural disasters (NWS, 2004). Appendix 1-1 summarizes the fatalities and injuries associated with a variety of hazards that occurred in the United States between 1995 and 2003. As climate change is expected to raise humidity and nighttime minimum temperature (more than daytime highs), heat-related illnesses and deaths associated with heat events are anticipated to be a significant health concern in human settlements (IPCC, 2001a; 2001b). Accordingly, there has been a growing impetus to develop warning systems that would allow authorities to issue advisories to the public when hazardous heat waves are imminent.

Such systems are already evident in Rome, Shangahi, Toronto, and several American cities including Philadelphia (Kalkstein, 2000). The Philadelphia Hot Weather-Health Watch/Warning System (PWWS) identifies potential-oppressive air masses that may elevate heat mortality in the summer (Kalkstein *et al.*, 1996). It employs a synoptic climatological approach that operates by grouping days with homogeneous meteorological conditions (such as temperature, humidity, cloud coverage, wind speed, and other variables) and comparing these to the past heat waves that caused high mortality rates. A similar system was also developed in Australia, where correlations between temporal synoptic indices and past heat-related mortality data were utilized to identify dangerous air masses (Guest *et al.*, 1999). Chan *et al.* (2001) also developed a mechanistic framework based on environmental conditions and behavioral responses linked to a physiological model in order to achieve more accurate mortality predictions.

Although these systems are capable of predicting upcoming heat events and thus reducing mortality rates, Wihelmi *et al.* (2004) argue that there is inadequate understanding of the geospatial nature of vulnerable populations and their surroundings, which limits the ability to design and develop effective strategies for reducing human health threats. Likewise, Chan *et al.* (2001) state that finer distinctions among physiological conditions are warranted when more data become available, including varying degrees of compromised health and varying levels of heat acclimatization. Although these warning systems are currently in operation, it has been suggested that further interdisciplinary research is needed: to develop and integrate improved weather forecasting capabilities for extreme heat events, to generate more sophisticated vulnerability assessments, and to produce innovations in warning and response systems (Patz *et al.*, 2000). Considering these implications, the generation of information that will lead to better understanding of these impacts and to produce more effective mitigation strategies are crucial.

In order to meet these needs, finer scales of temporal, geographic, and demographic resolution are needed. Furthermore, such studies must incorporate physiological factors, including core body temperature and adverse health impacts. Since heat-related illnesses are mostly treatable and preventable (CDC, 1995; 1994; Barrow and Clark, 1998), an bility to anticipate conditions that warrant prompt treatment would likely reduce the mortality rate associated with extreme heat. Accordingly, it is anticipated that modeling relationships among physical characteristics of the urban environment, social characteristics of that environment, and observed levels of fatalities associated with the urban heat will produce the foundation for an explicit system of UHI analysis and prediction.

Taking into to account the necessity of further development and deployment of heat reduction strategies aimed at heat vulnerable population, a collaborative research project was established involving various peers across the Penn campus and from Philadelphia Department of Public Health. The initiative was designed to examine the causes and effects of UHI in Philadelphia where causal relationships between observed levels of heat-induced morbidity and characteristics of this city's physical and social environment that are associated with UHI effects can be established. This research project was designed to synthesize five major principals: [1] compiling data on urban heat [2] modeling urban heat [3] assessing data on heat-related morality, [4] relating morbidity to urban environment, and [5] recommending heat reduction strategies.

The main objective of this study is to compile a collection of data, create a spatially-explicit model of urban heat, and to develop a set of heat mitigation strategies. These are the first, second, and part of fifth research principal. Therefore, further studies (third, fourth, and additional fifth principals) were not discussed here. However, prospective principals could be conducted by assessing of data on heat-related fatalities and them to the urban environment.

Data on heat-related fatalities could be done by identifying and evaluating information from available sources of current data on heat-related records in Philadelphia. As source or combination of sources would yield reliability, comprehensive and geographically-detailed information should be applied. Four primary sources includes 911 calls (available at the census tract level and containing demographic information such as age and gender of the ill patients), emergency room records indicating heat-related illness as the chief complaint (providing demographic information such as age and gender at the zip code level from the Temple University Hospital, the Presbyterian Medical Center, the Hospital of the University of

Pennsylvania, the Methodist Hospital, and the Episcopal Hospital), hospital discharge and admission billing data (containing detailed information on diagnosis at the zip code level), and Philadelphia Health Center data (available at level of individual street addresses). Additional sources of morbidity data may be sought as well, and barriers to obtaining address-level 911, emergency room, and hospital discharge data should also be assessed.

For relating morbidity data to the urban environment, exploring at finest scale achievable should be considered. Then, utilization of spatial analysis techniques is recommended for assessment. Since previous studies have suggested social factors and physical conditions can exacerbate the cause of heat-related fatalities, this process should aim to reveal the correlation of those factors to actual records. The intent could be to look for a relationship between heat-related morbidity (as dependent variable) and selected characteristics of the both the social and physical characteristics (as independent variables). The selection of social and/or physical characteristics should reflect those previous studies (such as from Appendix 1-2 to 1-6). Spatial autoregression and spatial lag models are suggested to be used for assessment that will take into account a spatial autocorrelation. Ultimately, the results should be able to generate a map depicting the relative risk for heat morbidity throughout the City of Philadelphia.

After these were conducted, examination on existing UHI mitigation strategies and determination on remediation measures in reducing heat-related mortality (for example, addressed by the current heat/health warning system of the NOAA/National Weather Service and the Philadelphia Department of Public Health.) should be considered. If those were not feasibly implemented by the City of Philadelphia, an essential task should be to make location-specific recommendations on their use in appropriate urban settings. It should advocate policies that would encourage community intervention in the built environment.

<u>Heat- illnesses and Vulnerable Populations</u>

Common heat-related illnesses include (in order to severity) heat edema, heat cramp, heat syncope, heat exhaustion, and heat stroke (Barrow and Clark, 1998). These illnesses are likely to be deadly if not adequately treated or prevented. All are believed to be triggered by pre-existing illness, certain medical conditions (Wexler, 2002), and environmental conditions (Wexler, 2002; Barrow and Clark, 1998). A vulnerable population is generally defined as a group of individuals based on epidemiological and statistical analyses (Chan *et al.*, 2001; Wilhelmi *et al.*, 2004).

According to these criteria, the main causal factors are characteristics of the environment, social and behavioral attributes, and biological and medical conditions (Kilbourne *et al.*, 1982). In addition, females, children (particularly infants), elderly individuals (over the age of 65), persons under certain drugs treatments (e.g., neuroleptics, anticholinergics, and tranquilizers), and individuals with excessive alcohol consumption have been determined to be at a higher risk for heat-related illness and mortality (CDC, 1994; 1995). Appendices 1-2 to 1-4 summarize the those potential risk factors (Kilbourne *et al.*, 1982; CDC, 1984; Barrow and Clark, 1998).

The body's ability to regulate temperature decreases for those who are elderly and/or obese, have heart disease, are under certain medications, and/or live in areas of poor air circulation. Under these conditions, people actually lose some of their ability to thermoregulate their bodies through radiation and evaporative heat loss when exposed to high temperatures and elevated humidity (Wilhelmi *et al.*, 2004). Additionally, they often do not have the ability to leave a hot residence for cooler alternatives. Living conditions and social networks also contribute to the overall vulnerability to extreme heat (McGeehin and Mirabelli, 2001). Significantly higher deaths occurred among people living in nursing homes without air conditioning during the heat events in New York City in 1972 and 1973 (Wilhelmi *et al.*, 2004).

Moreover, the elderly, the poor, and African Americans were found to be highly vulnerable groups during the extreme heat episode of July 1980 in St. Louis and Kansas City, MO (Jones *et al.*, 1982).

The elderly were the most vulnerable age group during the extensive heat waves in New York City during June of 1984 (CDC, 1984). A study of the Chicago heat wave in July of 1995 revealed that the elderly and infirmed are more likely to be at risk as they may be confined to a bed, unable to care for themselves, living alone, and/or incapable of leaving home each day (Wilhelmi *et al.*, 2004). This risk decreases if they have a social network of friends or family in the neighborhood, air conditioning, and/or access to transportation (Wilhelmi *et al.*, 2004). The poor are another vulnerable group, as they often do not own an air conditioner, lack means of transportation to cooler location, and/or often live in highly dense neighborhoods (Wilhelmi *et al.*, 2004).

During extended heat waves, deficient nocturnal cooling can have a particularly devastating impact on morbidity and mortality, especially in urban high-rise buildings. Urban settings often include high-rise apartment buildings, and people residing in the top floors of such buildings are at a greater risk as well (Barrow and Clark, 1998). Homes located in high crime rate areas are also more vulnerable because people are often afraid to leave their windows open at night thereby obstructing indoor air circulation (Wilhelmi *et al.*, 2004). With the changing demographics in the US, there has been increased attention to natural hazards and to the vulnerability of racial and ethnic communities (Wilhelmi *et al.*, 2004). A lower preparedness level, language barriers, and socio-economic factors such as income, housing issues, and availability of quality health care, may also contribute to increased vulnerability of racial and ethnic communities (Wilhelmi *et al.*, 2004).

Substitute Descriptions

Observation

For the purpose obtaining temperature and humidity data, HOBO H8 Pro RH/Temp loggers (Appendix 2A; H08-032-08, Onset Computer Corp.) were mounted on a wooden box (Appendix 2B), which was covered with white tape to protect from the precipitation and to reduce direct solar radiation. They were place horizontally (Appendix 2C) above 1m from the ground surface on a wooden tripod (Appendix 2D) for the field observations.

This logger has a feature for temperature measurement range of -30 to 50 ºC (-22 to 122 ºF) by accuracy of $\pm$ 0.2 at 21 ºC (0.33 at 70 ºF) and relative humidity measurement range of 0 to 100% by accuracy of $\pm$ 3% ($\pm$ 4% in condensing environment). During the preliminary testing, the accuracy was tested in three stable conditions: incubator, refrigerating room, and closed office space. In all cases, they indicated sufficient precision (data not shown) that are thought to eliminate a concern toward error generated by instruments during the observations. Consequently, these instruments were used to record two meteorological parameters in the field measurements.

Physiological Index

Conduction, convection, radiation, and evaporation are four processes involved in removing excess heat from human body (Barrow and Clark, 1998). Conduction occurs when the body comes in contact with something cold, allowing heat to be transferred to the cooler object. Convection takes place when air passes over the body, lifting heat away, as occurs on a windy day or through the use of fans. Radiation is the infrared dissipation by which the body leases heat into the environment. Evaporation, the primary thermoregulatory mechanism, is the process where a sweat from the skin plays a major role in heat dissipation. However, these systems can

be overwhelmed during periods of heat load and when the metabolic heat load exceeds the body's capability for heat dissipation. As ambient temperature and humidity increase, heat dissipation is less efficient. Elevated humidity also decreases the evaporation of sweat. Also, high ambient temperatures can cause heat gain through radiation.

Heat-related fatalities are induced by multiple environmental factors such as temperature, humidity, sun exposure, and wind (Barrow and Clark, 1998). Previous study has examined that when the core body temperature is higher than 104ºF (40ºC), heat-related illnesses and deaths occurs (Jones *et al.*, 1982; Kilbourne *et al.*, 1982; CDC, 1995; 1994; Barrow and Clark, 1998; Wexler, 2002). Although core body temperature is known to be increased through work-related activities and athletic performance that increase metabolic rate, elevated ambient temperature also play a role in this process. In fact, the basic mechanism that leads to heat-related illness is the body's inability to dissipate heat produced by metabolic activity, often as a result of increased ambient temperature (Barrow and Clark, 1998).

As ambient temperature and humidity increase, heat dissipation is less efficient, and elevated humidity decreases the evaporation of sweat. Also, high ambient temperatures can cause heat gain through radiation (Barrow and Clark, 1998). Therefore, reasonable physiological index that can be utilized in this study is the estimation of the core body temperature. However, limitation of individual deviations from the average response, physiological, emotional, and/or anthropometric characteristics raises difficulties for calculating the core temperature (Givoni and Goldman, 1972). Thus, heat index (HI) was chosen as physiological indicator in this paper.

HI is a combination of several factors and is used to evaluate heat stress on the human body. It is considered as index of how hot the actual body feels when temperature and humidity are combined. The HI values are derived from a collection of empirical equations that comprise a

model. Rothfusz (1990) developed the HI equation by calculating the parameters from Steadman (1979), which uses more conventional independent variables. Each of those parameters is given by assumed magnitudes, in parentheses, in order to simplify the model (Appendix 1-7). This equation is utilized by NWS to more effectively alert the general public and appropriate authorities to the hazardous and prolonged excessive heat episodes (NWS, 2005).

Note that HI equation is based upon shady and light wind condition. Exposure to direct sunlight can increase the HI values by up to 15 ℉. Also, strong winds, particularly with very hot and dry air can be extremely hazardous. Additionally, The there is an error of $\pm$ 1.3 ℉ as it is obtained by multiple regression analysis. The equation is only valid for temperatures higher than 80 ℉ and relative humidities greater than 40%. Kalkstein (1995) suggest that HI is not sufficient to be utilized for accurate indicator. Moreover, it is possible that identification of core body temperature (Givoni and Goldman, 1972) would be a better estimation. Considering these, it is likely that HI may not be an optimal indicator that should be considered.

Despite the fact that HI have certain limitations, it can be derived from two observable meteorological parameters and effectively represent the variations of the study area. Hence, above limitations were ignored and it was utilized to designate pedestrian level comfort.

Urban Characteristics

In order to characterize the study area, simpler but adequate environmental indices to Grimmond and Souch (1994; Appenddix 1-5) and Grimmond & Oke (1999; Appendix 1-6) were implemented to determine the environmental conditions. Since observations were done at very local scale, four indices were believed to capture the general urban condition. Here, however, the direction of the street (north-south and east-west) employed by Kondo and Yamazawa (1986)

was not implemented due to the complexity that may rise. Orientation of streets may effect the ventilation and length to sun exposure, but this was ignored due to the fact that observation period was relatively short and difference within the observation periods were likely to be insignificant for consideration.

Regression Analysis

After compiling field measurements, they were aggregated into hourly base measurements (Appendix 3) and regression analyses were conducted. Results of analyses are shown in Appendix 4. It consist of 6 procedures: (A) Distribution of Variables, (B) Pearson Product Moment Correlation Matrix, (C) Stepwise Regression, (D) OLS Regression, (E) Distribution of Residuals derived from OLS Regression, and (F) Regressing Residuals on Explanatory Variables were conducted separately for different surface type and time periods.

In multiple regression analysis, a linear model should satisfy the condition of errors to have no correlation, expectation of residual to be zero, and each explanatory variable to have equal variances. Therefore, colinearity of independent variables should be avoided. Additionally, normality of residual and linearity assumption should be fulfilled. Accordingly, these basic three underlying assumptions were confirmed under OLS statistical model in JMP-IN.

After three basic procedures (A through C), firstly, by way of the variance influence factor (denoted as VIF), colinearity of variables were determined under OLS regression analysis (D). VIF is one of the measurements that are used to detect the impact of colinearity among the explanatory variables in a regression model on the precision of estimation. If any of VIF value is significantly different from others, it indicates the existence of colinearity. Considering this, however, all results suggested no existence of colinearity among the variables.

Multiple regression analysis also assumes that the residuals are normally distributed. Thus, this was verified by normal quantile plots. Normal quantile plot is a sctterplot of the percentiles of the data versus the percentiles of a population in fact having the normal distribution. If the data comes from a normal population, the resulting point should fall closely along the straight line. Accordingly, there were no reasons to reject the normality of the residuals under the OLS regression for each dataset.

Lastly, multiple regression analysis also requires the variances to be the same for all explanatory variables, linearity assumption. So, this condition was determined by bivariate scatterplot where residuals were plotted against each explanatory variable. If all variables in the sequence or vector have the same finite variance, it is expected to have no increasing or decreasing condition, zero. As a result, there were no evidences to violate the condition in all cases. Consequently, skewed distributions of variables were left untransformed and further analysis was conducted from the original values.

Panel Autoregression (PAR) Analysis

The linear model of autocorrelation is understood to be $u_i = \sum_{j \neq i} \rho W_{ij} u_j + \varepsilon_i$. W is the weight matrix, $\sum_{j \neq i} W_{ij} u_j$ summarizes the spatial influence of other residuals on u_i, and ε_i is the internal effect at i being identically and independently distributed ($\varepsilon_i \sim N(0, \sigma^2)$, $i = 1, \ldots, n$). Here, $\sum_j W_{ij} u_j$ is a simple weighted average of the u_j's reflecting the dependency on u_i. The scale of these influence is reintroduced by parameter, ρ, which is assumed to be common to all residuals that satisfies the condition of $|\rho| < 1$. Thus, autocorrelation model could then be written as $u_i = \rho \sum_j W_{ij} u_j + \varepsilon_i$, $i = 1, \ldots, n$.

Only temporal autocorrelation was considered in this study as spatial autocorrelation had no influence and results were similar relative to the OLS statistical model. (data not shown). In order to take into account for the temporal autocorrelation, panel autoregressive (PAR) model was created on a basis of spatial autoregressive (SAR) model (Bailey and Gatrell, 1995). The autoregressive model provides a foundation for general autocorrelation analysis. A linear model of this is expressed by: $y_i = \beta_0 + \sum_{i=1}^{k} \beta_i x_{ij} + u_j$, $j = 1,\ldots,n$ of data ($y_j, x_{1j},\ldots,x_{kj}$) for units, $j = 1,\ldots,n$. Spatial effects is to postulated that the residuals ($u_i : j = 1,\ldots,n$) follow a spatial autoregressive model: $u_j = \rho \sum_{h=1}^{n} W_{jh} u_h + \varepsilon_h$, $\varepsilon_h \sim N(0,\sigma^2)$. Therefore, SAR model is given by: $y = X\beta + u$, $u = \rho W u + \varepsilon$, $\varepsilon \sim N(0,\sigma^2 I)$ where W is the spatial weight matrix, ρ is the spatial dependency parameter (residual dependency), and I is the Moran's I.

In the PAR model, W is the temporal weight matrix that directs second day field HI measurement to depend on the first day measurement. The weight matrix takes the condition of

$$u_t \begin{cases} \varepsilon_i & , \quad t = 1 \\ \rho u_{t-1} + \varepsilon_i & , \quad t = 2 \end{cases}$$ and $|\rho| < 1$ where t denotes the observation day. Thus, it is expressed as:

$$\rho W u = \rho \begin{pmatrix} 1 & 0 \\ 0 & 1 \end{pmatrix} \begin{pmatrix} u_{t_1} \\ u_{t_2} \end{pmatrix} = \rho \begin{pmatrix} u_{t_1} & 0 \\ 0 & u_{t_1} \end{pmatrix} \text{ where } u_t = \begin{bmatrix} u_{t,1,1} & \cdots & u_{t,1,k} \\ \vdots & \ddots & \vdots \\ u_{t,n,1} & \cdots & u_{t,n,k} \end{bmatrix}, k \text{ is number of parameter}$$

estimates, and n is the number of sample points. As seen in Appendix 3 (observing the column "Date/Time"), datasets were arranged in such a way that first day field measurements were organized at the upper table followed by the second day field measurements. The PAR analysis with its procedure commands and OLS regression analysis conducted in MATLAB are shown in Appendix 5.

In this model, unknown parameters are essentially β, ρ, and σ^2. Therefore, maximum likelihood estimation (MLE) was used to estimate these unknown parameters capturing the influences of the underlying probability distribution of a given dataset. The idea behind MLE is to determine the parameters that maximize the likelihood (probability) of the sample data. This leads to the notion that the likelihood of a set of data is the probability of obtaining that particular set of data, given the chosen probability distribution model.

Goodness-of-fit Measurements

The indication of R^2 (or adjusted R^2 depending on the model) is best known for measuring the goodness of fit of the model where errors are assumed to be identically and independently distributed, $\varepsilon \sim N(0, \sigma^2 I)$. As this condition is violated under the presence of spatial autocorrelation, four alternative measurements (Pseudo R^2, squared correlation, Log likelihood value, and Akaike's Information Criterion [AIC]) were applied to reveal more meaningful indication and comparable to the R^2 measurement in OLS regression.

Observe first that both PAR model could be reduced into $y_\rho = X_\rho \beta + \varepsilon$ where it satisfies all conditions of the linear model, $\varepsilon \sim N(0, \sigma^2 I)$. Accordingly, first of all, since MLE procedure provides a consistent estimate ($\hat{\rho}$) of ρ, under $y_{\hat{\rho}} = X_{\hat{\rho}} \beta + \varepsilon$ analogous measurement to R^2 could be obtained by $\hat{R}^2 = \dfrac{\hat{y}' B_{\hat{\rho}}' D B_{\hat{\rho}} \hat{y}}{y' B_{\hat{\rho}}' D B_{\hat{\rho}} y}$. Here, $D = (I - \dfrac{1}{n} 11')$ denotes the deviation vector, and predicted value is given by $B_{\hat{\rho}} \hat{y} = B_{\hat{\rho}} (X' B_{\hat{\rho}}' B_{\hat{\rho}} X)^{-1} X' B_{\hat{\rho}}' B_{\hat{\rho}} y$ where $B_{\hat{\rho}} = I - \rho W$. This alternative measurement is called the Pseudo R^2, which is an interpretation similar to the R^2 where its maximum is 1. Similar to the adjusted R^2, adjusted

Pseudo R^2 modifies both the numerator and the denominator by their respective degrees of freedom that is more meaningful for the case in multiple regression analysis. Secondly, the squared correlation is the method for measuring how closely related the variances are. The expression focus on the degree, parameter θ (maximum likelihood), relationship between y and $\hat{y}$, by $R^2 = corr(y, \hat{y})^2$ where $corr(y, \hat{y}) = \cos[\theta(D_y, D_{\hat{y}})] = \dfrac{y'\hat{y}}{\|y\| \cdot \|\hat{y}\|}$. For both Pseudo R^2 and squared correlation, higher value to 1 suggests better fit of the model. Thirdly, Log likelihood is a function of the parameter θ with actual observed data that is derived from MLE, $L(\hat{\theta})$. This calculates the ratio of the maximum value of the likelihood function under the constraint of the null hypothesis ($\rho = 0$) to the maximum with constraining the value by (-2)* Log($\cdot$) where smaller value suggests a better model. And finally, AIC also utilizes $L(\hat{\theta})$ to compute $2(L(\hat{\theta}) + k)$. Again the model that yields lower value of AIC is considered to be better.

References

Bailey, T. C. and Gatrell, A. C. (1995) Interactive Spatial Data Analysis, Longman, Harlow.

Barrow, M. W. and Clark, K. A. (1998) Heat-Related Illnesses. American Family Physician, 58, 749-756.

Center for Disease Control (CDC) (1984) Heat-Associated Mortality - New York City. Morbidity and Mortality Weekly Report (MMWR), 33, 430-432.

Center for Disease Control (CDC) (1994) Heat-Related Deaths - Philadelphia and United States, 1993-1994. Morbidity and Mortality Weekly Report (MMWR), 43, 453-455.

Center for Disease Control (CDC) (1995) Heat-Related Illnesses and Deaths - United States, 1994-1995. Morbidity and Mortality Weekly Report (MMWR), 44, 465-468.

Chan, N. Y., Stacey, M. T., Smith, A. E., Ebi, K. L. and Wilson, T. F. (2001) An Empirical Mechanistic Framework for Heat-Related Illness. Climate Research, 16, 133-143.

Givoni, B. and Goldman, R. F. (1972) Predicting Rectal Temperature Response to Work, Environment, and Clothing. Journal of Applied Physiology, 32, 812-822.

Grimmond, C. S. B. and Oke, T. R. (1999) Heat Storage in Urban Area: Local-Scale Observations and Evaluation of a Simple Model. Journal of Applied Meteorology, 38, 922-940.

Grimmond, C. S. B. and Souch, C. (1994) Surface Description for Urban Climate Studies: A GIS Based Methodology. Geocarto International, 1, 47-59.

Guest, C. S., Willson, K., Woodward, A. J., Hennessy, K., Kalkstein, L. S., Skinner, C. and McMichael, A. J. (1999) Climate and Mortality in Australia: Retrospective Study, 1970-1990, and Predicted Impact in Five Major Cities in 2030. Climate Research, 13, 1-15.

Intergovernmental Panel on Climate Change (IPCC) (2001a) Climate Change 2001: Impacts, Adaptation, and Vulnerability, Cambridge University Press, UK.

Intergovernmental Panel on Climate Change (IPCC) (2001b) Climate Change 2001: Scientific Basis, University of Cambridge Press, UK.

Jones, T. S., Liang, A. P., Kilbourne, E. M., Griffin, M. R., Patriarca, P. A., Fite Wassilak, S. G., Mullan, R. J., Herrick, R. F., Donnell, H. D., Choi, K. and Thacher, S. B. (1982) Morbidity and Mortality Associated with the July 1980 Heat Wave in St. Louis and Kansas City, MO. Journal of the American Medical Association, 247, 3327-3331.

Kalkstein, L. S. (1995) Lesson from a Very Hot Summer. The Lancet, 346, 857-859.

Kalkstein, L. S. (2000) Saving Lives During Extreme Weather in Summer. British Medical Journal, 321, 650-651.

Kalkstein, L. S., Jamason, P. F., Greene, J. S., Libby, J. and Robinson, L. (1996) The Philadelphia Hot Weather-Health Watch/Warning System: Development and Application, Summer 1995. Bulletin of the American Meteorological Society, 77, 1519-1528.

Kilbourne, E. M., Choi, K. and Jones, T. S. (1982) Risk Factor for Heatstroke: A Case-Control Study. The Journal of the American Medical Association, 247, 3332-3336.

Kondo, J. and Yamazawa, H. (1986) Aerodynamic Roughness over an Inhomogeneous Ground Surface. Boundary-Layer Meteorology, 35, 331-348.

McGeehin, M. A. and Mirabelli, M. (2001) The Potential Impact of Climate Variability and Change on Temperature-Related Morbidity and Mortality in the United States. Environmental Health Perspectives, 109, 185-189.

National Weather Service (NWS) (2004) Natural Hazard Statistics. Office of Climate, Water and Weather Services.

National Weather Service (NWS) (2005) Heat Wave - Major Summer Killer. Forecast Office.

Patz, J. A., McGeehin, M. A., Bernard, S. M., Ebi, K. L., Epstein, P. R., Grambsch, A., Gubler, D. J., Romieu, I., Rose, J. B., Samet, J. M. and Trtanj, J. (2000) The Potential Health Impacts of Climate Variability and Change for the United States: Executive Summary of the Report of the Health Sector of the U.S. National Assessment. Environmental Health Perspectives, 108, 367-376.

Rothfusz, L. P. (1990) The Heat Index Equation (or, more than you wanted to know about heat index). In NWS South Region Technical Attachment, Vol. SR/SSD 90-23 Fort Worth, TX.

Steadman, R. G. (1979) The Assessment of Sultriness. Part I: A Temperature-Humidity Index Based on Human Physiology and Clothing Science. Journal of Applied Meteorology, 18, 861-873.

Wexler, R. K. (2002) Evaluation and Treatment of Heat-Related Illnesses. American Family Physician, 65, 2307-2314.

Wilhelmi, O. V., Purvis, K. L. and Harriss, R. C. (2004) Designing a Geospatial Information Infrastructure for Mitigation of Heat Wave Hazards in Urban Area. Natural Hazards Review, 5, 147-158.

Appendix 1-1. Natural Fatalities and Injuries in the US from 1995-2003 (NWS, 2004).

Year	Lightning		Tornado		Flood		Hurricane		Heat		Cold	
	Fatalities	Injuries	Fatalities	Injuries	Fatalities	Injuries	Fatalities	Injuries	Fatalities	Injuries	Fatalities	Injuries
1995	85	433	30	650	80	57	17	112	1,021	1,549	22	0
1996	52	309	25	705	131	95	37	22	36	129	62	31
1997	42	306	67	1,033	118	525	1	32	81	530	51	9
1998	44	283	130	1,868	136	6,440	9	77	173	633	11	27
1999	46	243	94	1,842	68	301	19	10	502	1,477	7	32
2000	51	364	41	882	38	47	0	1	158	469	26	0
2001	44	371	40	743	48	277	24	7	166	445	4	0
2002	51	256	55	968	49	88	51	346	167	378	11	0
2003	43	236	54	1,087	86	70	14	233	36	174	20	14
Total	**458**	**2,801**	**536**	**9,778**	**754**	**7,900**	**172**	**840**	**2,340**	**5,784**	**214**	**113**

Appendix 1-2. Risk Factors to Heat Illnesses (CDC, 1984; Kilbourne, Choi, & Jones, 1982).

Environmental	Social and Behavioral	Biological and Medical	
No home air conditioning	Race (black)	Heat disease	Arthritis
Less home fan use	Gender (female)	Lung disease	Hypertension
Less windows open	Low educational attainment	Liver disease	Cancer
Less trees and shrubbery	Not warned about heat danger	Kidney disease	Diabetes
Low ceiling height	Unemployed	Thyroid disease	Depression
High number of living units	Living alone	Able to care for self	Use of drugs
High home floor	Less contact with others	Smoking	
Facade of brick, stone, or concrete	High activity during heat	Obesity	
Surface of concrete or asphalt	Wearing thick clothing	Alcohol consumption	
High buildings within 300ft	Less time in cool places	Alcoholism	
Home near to buildings	No extra cool baths or showers	Characteristic activity level	
	No extra liquids	Mental illness	
	No use of heat wave shelter	Previous heatstroke	

Appendix 1-3.Vulnerable Conditions to the Risk of Heat Illness (Barro & Clark, 1998).

Physical Conditions	**Increased Body Mass**
Fever	More heat generated for same level of activity
Dehydration	Less efficient heat dissipation
Medication	Fewer heat-activated sweat glands in skin overlying adipose tissue
Prolonged exertion	Decreased cardiac output per unit of body weight
Chronic Illnesses	**Younger age**
Cardiac conditions	Decreased ability to sweat
Cystic fibrosis	Decreased cardiac output at a given metabolic rate
Uncontrolled diabetes	Greater core temperature required to initiate sweating
Uncontrolled hypertension	Slower acclimatization
Eating disorders	More heat produced for the same level of activity
Malignant hyperthermia	**Additional Factor**
Peripheral vascular disease	Lack of access to air conditionings
Extensive skin disease or damage, or both	Residing in upper floors in tall building
Autonomic nervous system disorders	Sleep deprivation (decreases skin blood flow and rate of sweating)
Psychiatric conditions	Use of equipment or heavy clothing (football player's pads, etc.)
Hyperthyroidism	Previous heat stroke
Older Age	Recent move from a temperate to hot climate
Decreased vasodilatory response	Urban setting
Decreased thirst response	
Decreased fitness level	
Decreased maximum heat rate, resulting in decreased maximum cardiac output	
Decreased mobility resulting in increased difficulty of easily obtaining fluids	

Appendix 1-4. Medical Conditions to the Risk of Heat Illnesses (Barro & Clark, 1998).

Alpha agonists	Heroin
Amphetamines	Inhaled anesthetics
Anticholinergic medications	Laxatives
Antihistamines	Lysergic acid diethylamide
Anti-parkinsonian agents	Monoamine oxidase inhibitors
Beta-adrenergic blockers	Phencyclidine hydrochloride
Calcium channel blockers	Phenothiazines
Cocaine	Sympathomimetic medications
Diuretics	Thyroid agonists
Ethanol	Tricyclic antidepressants

Appendix 1-5. Attributes Determined for Each Land-Use Category (Grimmond & Souch, 1994).

Densities	Percent areal cover			
Buildings	Buildings	Trees/shrubs	Water	Sand
Trees	Garages	Parking lot	Dirt	Scruff
Roads	Grass	Main road	Pavement (non-parking lot)	

Appendix 1-6. General Land-Use Categories (Grimmond & Souch, 1994).

General Land-Use		Categories and Description
Residential	A	Housing density and shape (whether attached or not).
	B	Moderated density housing, small houses with trees
	C	Moderate density housing, size of houses and yards (trees/extensive landscaping)
	D	Large houses, small grass yards with some trees and shrubs
	E	Large houses, large yards, yards landscaped with shrubs and trees
	EA	Mixture of "A" and "E" type housing
	F	Houses equally spaced, large grass yards, few trees (with housing density)
	MH	Mobile homes
Apartments	AA	5-6 stories, U-shaped (arrangement of parking around the building)
	AB	Square shaped buildings
	AL	L-shaped buildings, 7 stories tall, no trees
	AL1	Rectangular shaped buildings
	AR1	Duplexes
	AR2	Mixture of "AR1" and "A" type houses
	AR3	Highly mixed
	BB	Low-level apartments (2 stories), rectangular shape, and height and size
Commercial	CB	Large commercial buildings - less than 6 stories
or Industrial	CC	Very tall commercial buildings - at least 15 stories
	CS	Small commercial buildings
	I	Industrial - either large low level buildings or many small buildings
Institutional	HS	High school: Large building, few trees, medium size parking lot
	S	Elementary/Junior High school: Much smaller building than HS
	U	University: Large buildings, parking lot, vegetated grounds
Transportation	MRI	Major roads (e.g. interstates)
	RR	Rail road tracks or side-yards
Vacant/Wild	DI	"Dirt"
Vegetated	VG	Golf course
	VGR	100% grass
	VM	50% grass/ 50% tree and shrub
	VPC	Cemetery
	VT	Trees and shrubs
Impervious	CN	Concrete
surfaces	IP	Parking lot (impervious)
	IS	Tennis court
Water	WL	Lake
	WR	River

Appendix 1-7. Assumed Parameters of Magnitudes for HI Equation (Rothfusz, 1990).

Vapor pressure. Ambient vapor pressure of the atmosphere. [1.6 kPa]

Dimensions of a human. Determines the skin's surface area. [5'7'' tall, 147 pounds]

Effective radiation area of skin. A ratio that depends upon skin surface area. [0.8]

Significant diameter of a human. Based on the body's volume and density. [15.3cm]

Clothing cover. Long trouser and short-sleeved shirt is assumed. [84% coverage]

Core temperature. Internal body temperature. [98.6 F]

Core vapor pressure. Depends upon body's core temperature and salinity. [5.65 kPa]

Surface temperature and vapor pressures of skin and clothing. Affects heat transfer from the skin's surface either by radiation or convection. These values are determined by an iterative process.

Activity. Determines metabolic output. [180 W m-2 of skin area for the model person walking outdoors at a speed of 3.1 mph]

Effective wind speed. Vector sum of the body's movement and an average wind speed. Angle between vectors influences convection from skin surface (below). [5 kts]

Clothing resistance to heat transfer. The magnitude of this value is based on the assumption that the clothing is 20% fiber and 80% air.

Clothing resistance to moisture transfer. Since clothing is mostly air, pure vapor diffusion is used.

Radiation from the surface of the skin. A radioactive heat-transfer coefficient determined from previous studies.

Convection from the surface of the skin. A convection coefficient also determined from previous studies. Influenced by kinematic viscosity of air and angle of wind.

Sweating rate. Assumes that sweat is uniform and not dripping from the body.

Ventilation rate. The amount of heat lost via exhaling.

Skin resistance to heat transfer. A function of activity, skin temperature, among others. [2-12%, depending upon humidity]

Skin resistance to moisture transfer. A function of the vapor-pressure difference across the skin (and, therefore, relative humidity). It decreases with increasing activity.

Surface resistance to heat transfer. As radiation and convection from the skin increases, this value decreases.

Surface resistance to moisture transfer. Similar to heat transfer resistance but also depends upon conditions in the boundary layer just above skin's surface.

Appendix 2. HOBO H8 Pro RH/Temp loggers Images

(A)

(B)

(C)

(D)
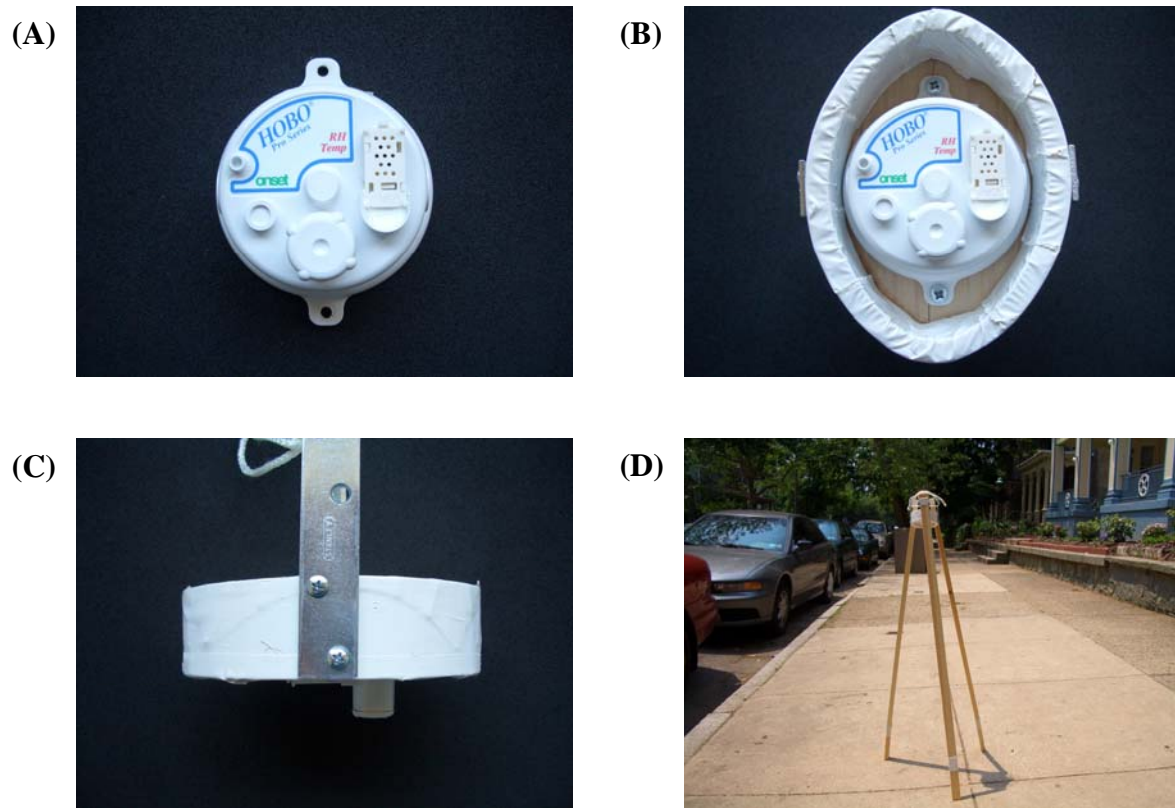
(A) H08-032-08., Onset Computer Corp., (B) the HOBO instrument mounted on a wooden box covered with white tape, (C) horizontal image of (B), and (D) the HOBO instrument placed above 1m from the surface on a wooden tripod.

Appendix 3-1. Dataset of Impervious Surface at Daytime (13:00).

	Date/Time	Address (Street Name)	Surface Material	FHI (C)	SHI (C)	Sh (%)	SW (m)	DB (m)	BS (#)
1	2005/6/6 13:00	Between 34th & 35th Race Street	Brick	32.68	31.80	96.93	18.61	5.79	3.25
2	2005/6/6 13:00	Between 34th & 35th Race Street	Brick	36.61	31.80	0.00	18.61	8.46	3.25
3	2005/6/6 13:00	Between 34th & 35th Race Street	Concrete	32.48	31.80	96.06	18.61	5.45	3.25
4	2005/6/6 13:00	Between 34th & 35th Race Street	Concrete	36.02	31.80	0.00	18.61	5.00	3.25
5	2005/6/13 13:00	35th between Race and Powelton	Concrete	35.03	32.52	90.58	15.58	8.80	3.25
6	2005/6/13 13:00	35th between Race and Powelton	Concrete	37.27	32.52	0.00	15.58	4.72	3.25
7	2005/6/13 13:00	Between 34th & 35th Race Street	Concrete	32.85	32.52	95.64	18.61	8.88	3.25
8	2005/6/13 13:00	Between 34th & 35th Race Street	Brick	36.41	32.52	0.00	18.61	7.17	3.25
9	2005/6/16 13:00	35th between Pearl & Baring St.	Concrete	29.39	27.57	0.00	15.96	8.39	3.50
10	2005/6/16 13:00	35th between Pearl & Baring St.	Concrete	28.27	27.57	86.66	15.96	8.80	3.25
11	2005/6/16 13:00	35th between Pearl & Baring St.	Concrete	28.08	27.57	95.33	15.96	8.31	3.25
12	2005/6/28 13:00	Between 43rd & 44th Walnut St	Asphalt	41.28	33.47	0.00	22.13	20.14	1.50
13	2005/6/28 13:00	Between 43rd & 44th Walnut St	Asphalt	40.35	33.47	0.00	22.13	20.26	3.50
14	2005/6/28 13:00	Between 43rd & 44th Walnut St	Concrete	37.23	33.47	76.48	22.13	22.19	3.25
15	2005/6/28 13:00	Between 43rd & 44th Walnut St	Concrete	40.04	33.47	0.00	22.13	23.89	3.25
16	2005/6/28 13:00	44th between Walnut and Locust St	Concrete	37.00	33.47	81.02	18.19	3.06	3.75
17	2005/6/28 13:00	44th between Walnut and Locust St	Concrete	39.92	33.47	0.00	18.19	3.19	3.75
18	2005/7/1 13:00	Between 44th & 45th Walnut St	Concrete	32.33	31.11	90.83	23.24	3.83	3.50
19	2005/7/1 13:00	Between 44th & 45th Walnut St	Concrete	34.16	31.11	0.00	23.24	4.52	3.50
20	2005/7/1 13:00	Buckingham PL	Concrete	30.95	31.11	91.73	12.20	2.23	3.25
21	2005/7/1 13:00	Buckingham PL	Concrete	33.81	31.11	0.00	12.20	2.32	3.25
22	2005/7/1 13:00	Between 44th & 45th Locust St	Concrete	30.78	31.11	96.40	19.67	3.19	3.25
23	2005/7/1 13:00	Between 44th & 45th Locust St	Concrete	34.35	31.11	0.00	19.67	5.99	3.25
24	2005/7/9 13:00	Corner of Holden St & Powelton Ave	Asphalt	28.34	28.40	83.70	24.57	45.05	2.25
25	2005/7/9 13:00	Corner of Holden St & Powelton Ave	Asphalt	30.54	28.40	0.00	24.57	73.17	2.25
26	2005/7/21 13:00	43rd between Locust St & Spruce St	Asphalt	33.81	33.12	66.18	16.97	30.22	1.50
27	2005/7/21 13:00	43rd between Locust St & Spruce St	Asphalt	38.17	33.12	0.00	16.97	17.98	1.50
28	2005/7/23 13:00	37th Waren St	Asphalt	32.03	29.00	72.32	17.13	13.16	2.00
29	2005/7/23 13:00	37th Waren St	Asphalt	35.22	29.00	0.00	17.13	16.17	2.00
30	2005/7/25 13:00	Between Hutchinson Gym & Franklin Field	Asphalt	35.69	33.16	60.39	11.66	21.64	2.00
31	2005/7/25 13:00	Between Hutchinson Gym & Franklin Field	Asphalt	37.99	33.16	0.00	11.66	18.06	2.00
32	2005/7/27 13:00	43rd between Walnut & Sansom St	Asphalt	43.01	40.07	12.20	15.33	6.83	1.50
33	2005/7/27 13:00	43rd between Walnut & Sansom St	Asphalt	45.22	40.07	0.00	15.33	16.93	1.50
34	2005/8/2 13:00	20th between Market & Commerce St	Concrete	36.97	35.14	72.80	34.75	4.07	41.00
35	2005/8/2 12:00	Between 20th & 21st Market St	Concrete	33.91	34.45	95.65	27.01	4.04	41.00
36	2005/8/2 12:00	Between 20th & 21st Market St	Concrete	36.25	34.45	0.00	27.01	3.86	41.00
37	2005/8/4 13:00	Between 19th & 20th JFK	Concrete	35.15	36.42	96.58	32.40	4.30	20.00
38	2005/8/4 13:00	Between 19th & 20th JFK	Brick	36.96	36.42	73.80	32.40	2.82	30.00
39	2005/8/4 13:00	Between 19th & 20th JFK	Concrete	37.59	36.42	0.00	32.40	6.74	30.00
40	2005/8/21 13:00	Between 18th & 29th Ludlow St	Concrete	38.61	35.35	0.00	8.20	1.83	37.00
41	2005/8/21 13:00	Between 18th & 29th Ludlow St	Concrete	34.39	35.35	88.83	8.20	1.56	5.00
42	2005/8/21 13:00	19th between Ludlow & Ranstead St	Concrete	37.92	35.35	0.00	15.54	3.92	30.00
43	2005/8/21 13:00	19th between Ludlow & Ranstead St	Concrete	35.75	35.35	38.20	15.54	3.59	30.00
44	2005/8/23 13:00	Northwest Corner of Rittenhouse Square	Concrete	29.93	27.61	0.00	21.60	35.10	20.00
45	2005/8/26 13:00	Between 20th & 21st Chestnut St	Concrete	28.72	26.81	0.00	18.07	3.28	2.50
46	2005/8/26 13:00	Between 20th & 21st Chestnut St	Concrete	28.02	26.81	92.69	18.07	1.71	4.00
47	2005/8/26 13:00	20th between Chestnut & Sansom St	Concrete	28.56	26.81	0.00	15.54	3.19	4.25
48	2005/8/26 13:00	20th between Chestnut & Sansom St	Concrete	27.33	26.81	78.72	15.54	3.72	4.25
49	2005/8/29 13:00	Corner of Ben Franklin Parkway & Race Street at 18th	Concrete	31.90	31.19	87.46	16.42	14.73	3.50
50	2005/9/2 13:00	Corner of 20th & Race Street	Concrete	30.97	30.10	81.00	30.71	70.15	7.00
51	2005/9/4 13:00	North Corner of Logan Circle @ 19th	Concrete	28.21	26.37	31.40	42.00	56.85	7.00
52	2005/6/9 13:00	Between 34th & 35th Race Street	Brick	33.23	32.38	96.93	18.61	5.79	3.25
53	2005/6/9 13:00	Between 34th & 35th Race Street	Brick	37.90	32.38	0.00	18.61	8.46	3.25
54	2005/6/9 13:00	Between 34th & 35th Race Street	Concrete	32.52	32.38	96.06	18.61	5.45	3.25
55	2005/6/9 13:00	Between 34th & 35th Race Street	Concrete	36.49	32.38	0.00	18.61	5.00	3.25
56	2005/6/14 13:00	35th between Race and Powelton	Concrete	35.30	33.75	90.58	15.58	8.80	3.25
57	2005/6/14 13:00	35th between Race and Powelton	Concrete	37.96	33.75	0.00	15.58	4.72	3.25
58	2005/6/14 13:00	Between 34th & 35th Race Street	Concrete	33.73	33.75	95.64	18.61	8.88	3.25
59	2005/6/14 13:00	Between 34th & 35th Race Street	Brick	37.07	33.75	0.00	18.61	7.17	3.25
60	2005/6/20 13:00	35th between Pearl & Baring St.	Concrete	25.41	25.05	0.00	15.96	8.39	3.50
61	2005/6/20 13:00	35th between Pearl & Baring St.	Concrete	25.15	25.05	86.66	15.96	8.80	3.25
62	2005/6/20 13:00	35th between Pearl & Baring St.	Concrete	25.00	25.05	95.33	15.96	8.31	3.25
63	2005/6/29 13:00	Between 43rd & 44th Walnut St	Asphalt	34.17	29.32	0.00	22.13	20.14	1.50
64	2005/6/29 13:00	Between 43rd & 44th Walnut St	Asphalt	33.56	29.32	0.00	22.13	20.26	3.50
65	2005/6/29 13:00	Between 43rd & 44th Walnut St	Concrete	33.49	29.32	76.48	22.13	22.19	3.25
66	2005/6/29 13:00	Between 43rd & 44th Walnut St	Concrete	32.67	29.32	0.00	22.13	23.89	3.25
67	2005/6/29 13:00	44th between Walnut and Locust St	Concrete	31.70	29.32	81.02	18.19	3.06	3.75
68	2005/6/29 13:00	44th between Walnut and Locust St	Concrete	32.19	29.32	0.00	18.19	3.19	3.75
69	2005/7/3 13:00	Between 44th & 45th Walnut St	Concrete	26.80	26.73	90.83	23.24	3.83	3.50
70	2005/7/3 13:00	Between 44th & 45th Walnut St	Concrete	29.12	26.73	0.00	23.24	4.52	3.50
71	2005/7/3 13:00	Buckingham PL	Concrete	26.74	26.73	91.73	12.20	2.23	3.25
72	2005/7/3 13:00	Buckingham PL	Concrete	28.13	26.73	0.00	12.20	2.32	3.25
73	2005/7/3 13:00	Between 44th & 45th Locust St	Concrete	26.98	26.73	96.40	19.67	3.19	3.25

74	2005/7/3 13:00	Between 44th & 45th Locust St	Concrete	30.13	26.73	0.00	19.67	5.99	3.25
75	2005/7/10 13:00	Corner of Holden St & Powelton Ave	Asphalt	30.38	31.80	83.70	24.57	45.05	2.25
76	2005/7/10 13:00	Corner of Holden St & Powelton Ave	Asphalt	33.95	31.80	0.00	24.57	73.17	2.25
77	2005/7/22 13:00	43rd between Locust St & Spruce St	Asphalt	35.51	34.07	66.18	16.97	30.22	1.50
78	2005/7/22 13:00	43rd between Locust St & Spruce St	Asphalt	39.09	34.07	0.00	16.97	17.98	1.50
79	2005/7/24 13:00	37th Waren St	Asphalt	31.13	29.13	72.32	17.13	13.16	2.00
80	2005/7/24 13:00	37th Waren St	Asphalt	33.73	29.13	0.00	17.13	16.17	2.00
81	2005/7/26 13:00	Between Hutchinson Gym & Franklin Field	Asphalt	36.70	37.16	60.39	11.66	21.64	2.00
82	2005/7/26 13:00	Between Hutchinson Gym & Franklin Field	Asphalt	39.92	37.16	0.00	11.66	18.06	2.00
83	2005/7/28 13:00	43rd between Walnut & Sansom St	Asphalt	29.14	27.19	12.20	15.33	6.83	1.50
84	2005/7/28 13:00	43rd between Walnut & Sansom St	Asphalt	30.65	27.19	0.00	15.33	16.93	1.50
85	2005/8/3 13:00	20th between Market & Commerce St	Concrete	36.24	34.30	72.80	34.75	4.07	41.00
86	2005/8/3 12:00	Between 20th & 21st Market St	Concrete	33.32	33.54	95.65	27.01	4.04	41.00
87	2005/8/3 12:00	Between 20th & 21st Market St	Concrete	36.73	33.54	0.00	27.01	3.86	41.00
88	2005/8/6 13:00	Between 19th & 20th JFK	Concrete	28.58	29.18	96.58	32.40	4.30	20.00
89	2005/8/6 13:00	Between 19th & 20th JFK	Brick	29.63	29.18	73.80	32.40	2.82	30.00
90	2005/8/6 13:00	Between 19th & 20th JFK	Concrete	30.18	29.18	0.00	32.40	6.74	30.00
91	2005/8/22 13:00	Between 18th & 29th Ludlow St	Concrete	33.70	29.63	0.00	8.20	1.83	37.00
92	2005/8/22 13:00	Between 18th & 29th Ludlow St	Concrete	28.90	29.63	88.83	8.20	1.56	5.00
93	2005/8/22 13:00	19th between Ludlow & Ranstead St	Concrete	32.26	29.63	0.00	15.54	3.92	30.00
94	2005/8/22 13:00	19th between Ludlow & Ranstead St	Concrete	30.78	29.63	38.20	15.54	3.59	30.00
95	2005/8/24 13:00	Northwest Corner of Rittenhouse Square	Concrete	28.57	26.04	0.00	21.60	35.10	20.00
96	2005/8/27 13:00	Between 20th & 21st Chestnut St	Concrete	32.08	27.66	0.00	18.07	3.28	2.50
97	2005/8/27 13:00	Between 20th & 21st Chestnut St	Concrete	29.50	27.66	92.69	18.07	1.71	4.00
98	2005/8/27 13:00	20th between Chestnut & Sansom St	Concrete	29.92	27.66	0.00	15.54	3.19	4.25
99	2005/8/27 13:00	20th between Chestnut & Sansom St	Concrete	28.75	27.66	78.72	15.54	3.72	4.25
100	2005/9/1 13:00	Corner of Ben Franklin Parkway & Race Street at 18th	Concrete	27.99	27.82	87.46	16.42	14.73	3.50
101	2005/9/3 13:00	Corner of 20th & Race Street	Concrete	27.20	26.02	81.00	30.71	70.15	7.00
102	2005/9/5 13:00	North Corner of Logan Circle @ 19th	Concrete	28.55	26.48	31.40	42.00	56.85	7.00

Appendix 3-2. Dataset of Pervious Surface at Daytime (13:00).

|	Date/Time	Address (Street Name)	Surface Material	FHI (C)	SHI (C)	Sh (%)	SW (m)	DB (m)	BS (#)
1	2005/6/13 13:00	35th between Race and Powelton	Grass	33.92	32.52	94.25	15.58	5.66	3.25
2	2005/6/13 13:00	35th between Race and Powelton	Grass	36.30	32.52	0.00	15.58	10.03	3.25
3	2005/6/16 13:00	35th between Powelton & Pearl St.	Grass	28.07	27.57	0.00	15.39	9.48	3.25
4	2005/6/16 13:00	35th between Powelton & Pearl St.	Grass	27.87	27.57	73.13	15.39	18.39	3.25
5	2005/6/16 13:00	35th between Powelton & Pearl St.	Grass	28.02	27.57	92.75	15.39	19.45	3.25
6	2005/7/9 13:00	Corner of Holden St & Powelton Ave	Grass	27.74	28.40	94.69	24.57	51.51	2.25
7	2005/7/9 13:00	Corner of Holden St & Powelton Ave	Grass	29.36	28.40	0.00	24.57	48.18	2.25
8	2005/7/21 13:00	43rd between Locust St & Spruce St	Grass	34.81	33.12	0.00	16.97	35.20	4.00
9	2005/7/21 13:00	43rd between Locust St & Spruce St	Grass	33.18	33.12	59.89	16.97	35.88	4.00
10	2005/7/23 13:00	37th Waren St	Grass	29.31	29.00	35.75	17.13	8.86	4.00
11	2005/7/23 13:00	37th Waren St	Grass	30.51	29.00	0.00	17.13	25.98	4.00
12	2005/7/25 13:00	Between Hutchinson Gym & Franklin Field	Grass	34.17	33.16	34.39	11.66	11.33	10.00
13	2005/7/25 13:00	Between Hutchinson Gym & Franklin Field	Grass	35.20	33.16	0.00	11.66	13.32	10.00
14	2005/7/27 13:00	43rd between Walnut & Sansom St	Grass	40.93	40.07	72.25	15.33	17.14	3.25
15	2005/7/27 13:00	43rd between Walnut & Sansom St	Grass	42.55	40.07	0.00	15.33	26.45	3.25
16	2005/8/4 13:00	Between 20th & 21st JFK	Grass	34.97	36.42	23.36	26.97	37.72	41.00
17	2005/8/4 13:00	Between 20th & 21st JFK	Grass	36.26	36.42	0.00	26.97	36.62	41.00
18	2005/8/23 13:00	Northwest Corner of Rittenhouse Square	Grass	29.19	27.61	0.00	21.60	31.60	20.00
19	2005/8/23 13:00	Northwest Corner of Rittenhouse Square	Grass	28.76	27.61	68.45	21.60	29.09	20.00
20	2005/8/23 13:00	Northwest Corner of Rittenhouse Square	Grass	26.56	27.61	95.98	21.60	52.59	20.00
21	2005/8/29 13:00	Corner of Ben Franklin Parkway & Race Street at 18th	Grass	33.83	31.19	0.00	35.06	29.70	3.50
22	2005/8/29 13:00	Corner of Ben Franklin Parkway & Race Street at 18th	Grass	33.17	31.19	38.51	35.06	24.04	3.50
23	2005/8/29 13:00	Corner of Ben Franklin Parkway & Race Street at 18th	Grass	31.64	31.19	87.46	16.42	19.88	3.50
24	2005/9/2 13:00	Corner of 20th & Race Street	Grass	32.91	30.10	0.00	30.71	39.01	7.00
25	2005/9/2 13:00	Corner of 20th & Race Street	Grass	30.67	30.10	86.57	30.71	47.23	7.00
26	2005/9/2 13:00	Corner of 20th & Race Street	Grass	29.34	30.10	97.78	30.71	54.69	7.00
27	2005/9/4 13:00	North Corner of Logan Circle @ 19th	Grass	29.25	26.37	0.00	42.00	60.19	7.00
28	2005/9/4 13:00	North Corner of Logan Circle @ 19th	Grass	27.15	26.37	71.85	42.00	50.91	7.00
29	2005/9/4 13:00	North Corner of Logan Circle @ 19th	Grass	26.29	26.37	90.88	42.00	54.03	7.00
30	2005/6/14 13:00	35th between Race and Powelton	Grass	34.85	33.75	94.25	15.58	5.66	3.25
31	2005/6/14 13:00	35th between Race and Powelton	Grass	37.68	33.75	0.00	15.58	10.03	3.25
32	2005/6/20 13:00	35th between Powelton & Pearl St.	Grass	26.02	25.05	0.00	15.39	9.48	3.25
33	2005/6/20 13:00	35th between Powelton & Pearl St.	Grass	25.33	25.05	73.13	15.39	18.39	3.25
34	2005/6/20 13:00	35th between Powelton & Pearl St.	Grass	25.12	25.05	92.75	15.39	19.45	3.25
35	2005/7/10 13:00	Corner of Holden St & Powelton Ave	Grass	28.39	31.80	94.69	24.57	51.51	2.25
36	2005/7/10 13:00	Corner of Holden St & Powelton Ave	Grass	32.21	31.80	0.00	24.57	48.18	2.25
37	2005/7/22 13:00	43rd between Locust St & Spruce St	Grass	34.46	34.07	59.89	16.97	35.20	4.00
38	2005/7/22 13:00	43rd between Locust St & Spruce St	Grass	36.14	34.07	0.00	16.97	35.88	4.00
39	2005/7/24 13:00	37th Waren St	Grass	29.59	29.13	35.75	17.13	8.86	4.00
40	2005/7/24 13:00	37th Waren St	Grass	30.11	29.13	0.00	17.13	25.98	4.00
41	2005/7/26 13:00	Between Hutchinson Gym & Franklin Field	Grass	37.03	37.16	34.39	11.66	11.33	10.00
42	2005/7/26 13:00	Between Hutchinson Gym & Franklin Field	Grass	38.78	37.16	0.00	11.66	13.32	10.00
43	2005/7/28 13:00	43rd between Walnut & Sansom St	Grass	27.16	27.19	72.25	15.33	17.14	3.25
44	2005/7/28 13:00	43rd between Walnut & Sansom St	Grass	29.39	27.19	0.00	15.33	26.45	3.25
45	2005/8/6 13:00	Between 20th & 21st JFK	Grass	29.30	29.18	23.36	26.97	37.72	41.00
46	2005/8/6 13:00	Between 20th & 21st JFK	Grass	29.99	29.18	0.00	26.97	36.62	41.00
47	2005/8/24 13:00	Northwest Corner of Rittenhouse Square	Grass	28.11	26.04	0.00	21.60	31.60	20.00
48	2005/8/24 13:00	Northwest Corner of Rittenhouse Square	Grass	27.90	26.04	68.45	21.60	29.09	20.00
49	2005/8/24 13:00	Northwest Corner of Rittenhouse Square	Grass	25.85	26.04	95.98	21.60	52.59	20.00
50	2005/9/1 13:00	Corner of Ben Franklin Parkway & Race Street at 18th	Grass	28.61	27.82	0.00	35.06	29.70	3.50
51	2005/9/1 13:00	Corner of Ben Franklin Parkway & Race Street at 18th	Grass	28.60	27.82	38.51	35.06	24.04	3.50
52	2005/9/1 13:00	Corner of Ben Franklin Parkway & Race Street at 18th	Grass	27.71	27.82	87.46	16.42	19.88	3.50
53	2005/9/3 13:00	Corner of 20th & Race Street	Grass	28.92	26.02	0.00	30.71	39.01	7.00
54	2005/9/3 13:00	Corner of 20th & Race Street	Grass	26.97	26.02	86.57	30.71	47.23	7.00
55	2005/9/3 13:00	Corner of 20th & Race Street	Grass	26.13	26.02	97.78	30.71	54.69	7.00
56	2005/9/5 13:00	North Corner of Logan Circle @ 19th	Grass	29.54	26.48	0.00	42.00	60.19	7.00
57	2005/9/5 13:00	North Corner of Logan Circle @ 19th	Grass	27.60	26.48	71.85	42.00	50.91	7.00
58	2005/9/5 13:00	North Corner of Logan Circle @ 19th	Grass	26.49	26.48	90.88	42.00	54.03	7.00

Appendix 3-3. Dataset of Impervious Surface at Nighttime (22:00).

	Date/Time	Address (Street Name)	Surface Material	FHI (C)	SHI (C)	SW (m)	DB (m)	BS (#)
1	2005/6/7 22:00	Between 34th & 35th Race Street	Brick	28.20	27.50	18.61	5.79	3.25
2	2005/6/7 22:00	Between 34th & 35th Race Street	Brick	28.31	27.50	18.61	8.46	3.25
3	2005/6/7 22:00	Between 34th & 35th Race Street	Concrete	28.76	27.50	18.61	5.45	3.25
4	2005/6/7 22:00	Between 34th & 35th Race Street	Concrete	29.53	27.50	18.61	5.00	3.25
5	2005/6/13 22:00	35th between Race and Powelton	Concrete	32.15	30.12	15.58	8.80	3.25
6	2005/6/13 22:00	35th between Race and Powelton	Concrete	32.68	30.12	15.58	4.72	3.25
7	2005/6/13 22:00	Between 34th & 35th Race Street	Concrete	32.19	30.12	18.61	8.88	3.25
8	2005/6/13 22:00	Between 34th & 35th Race Street	Brick	32.08	30.12	18.61	7.17	3.25
9	2005/6/28 22:00	Between 43rd & 44th Walnut St	Asphalt	30.15	26.24	22.13	20.14	1.50
10	2005/6/28 22:00	Between 43rd & 44th Walnut St	Asphalt	29.72	26.24	22.13	20.26	3.50
11	2005/6/28 22:00	Between 43rd & 44th Walnut St	Concrete	29.63	26.24	22.13	22.19	3.25
12	2005/6/28 22:00	Between 43rd & 44th Walnut St	Concrete	29.76	26.24	22.13	23.89	3.25
13	2005/6/28 22:00	44th between Walnut and Locust St	Concrete	29.63	26.24	18.19	3.06	3.75
14	2005/6/28 22:00	44th between Walnut and Locust St	Concrete	29.66	26.24	18.19	3.19	3.75
15	2005/7/1 22:00	Between 44th & 45th Walnut St	Concrete	25.40	22.74	23.24	3.83	3.50
16	2005/7/1 22:00	Between 44th & 45th Walnut St	Concrete	25.29	22.74	23.24	4.52	3.50
17	2005/7/1 22:00	Buckingham PL	Concrete	23.90	22.74	12.20	2.23	3.25
18	2005/7/1 22:00	Buckingham PL	Concrete	24.74	22.74	12.20	2.32	3.25
19	2005/7/1 22:00	Between 44th & 45th Locust St	Concrete	23.93	22.74	19.67	3.19	3.25
20	2005/7/1 22:00	Between 44th & 45th Locust St	Concrete	24.28	22.74	19.67	5.99	3.25
21	2005/7/9 22:00	Corner of Holden St & Powelton Ave	Asphalt	25.44	25.21	24.57	45.05	2.25
22	2005/7/9 22:00	Corner of Holden St & Powelton Ave	Asphalt	25.27	25.21	24.57	73.17	2.25
23	2005/7/21 22:00	43rd between Locust St & Spruce St	Asphalt	31.45	29.36	16.97	30.22	1.50
24	2005/7/21 22:00	43rd between Locust St & Spruce St	Asphalt	32.49	29.36	16.97	17.98	1.50
25	2005/7/23 22:00	37th Waren St	Asphalt	26.86	26.00	17.13	13.16	2.00
26	2005/7/23 22:00	37th Waren St	Asphalt	27.20	26.00	17.13	16.17	2.00
27	2005/7/25 22:00	Between Hutchinson Gym & Franklin Field	Asphalt	35.85	32.86	11.66	21.64	2.00
28	2005/7/25 22:00	Between Hutchinson Gym & Franklin Field	Asphalt	36.61	32.86	11.66	18.06	2.00
29	2005/7/28 22:00	43rd between Walnut & Sansom St	Asphalt	26.35	25.09	15.33	6.83	1.50
30	2005/7/28 22:00	43rd between Walnut & Sansom St	Asphalt	26.62	25.09	15.33	16.93	1.50
31	2005/8/2 22:00	20th between Market & Commerce St	Concrete	33.28	30.95	34.75	4.07	41.00
32	2005/8/2 22:00	20th between Market & Commerce St	Concrete	33.32	30.95	34.75	3.78	41.00
33	2005/8/2 22:00	Between 20th & 21st Market St	Concrete	32.85	30.95	27.01	4.04	41.00
34	2005/8/2 22:00	Between 20th & 21st Market St	Concrete	33.24	30.95	27.01	3.86	41.00
35	2005/8/4 22:00	Between 19th & 20th JFK	Concrete	35.41	32.29	32.40	4.30	20.00
36	2005/8/4 22:00	Between 19th & 20th JFK	Brick	35.68	32.29	32.40	2.82	30.00
37	2005/8/4 22:00	Between 19th & 20th JFK	Concrete	35.74	32.29	32.40	6.74	30.00
38	2005/8/17 22:00	Between 19th & 20th Commerce St	Concrete	27.63	26.03	7.64	2.41	20.00
39	2005/8/17 22:00	Between 19th & 20th Commerce St	Concrete	27.48	26.03	7.64	3.66	20.00
40	2005/8/17 22:00	19th between Market & Commerce St	Brick	27.58	26.03	17.66	3.98	45.00
41	2005/8/17 22:00	19th between Market & Commerce St	Brick	27.54	26.03	17.66	4.03	45.00
42	2005/8/21 22:00	Between 18th & 29th Ludlow St	Concrete	29.04	27.36	8.20	1.83	37.00
43	2005/8/21 22:00	Between 18th & 29th Ludlow St	Concrete	28.67	27.36	8.20	1.56	5.00
44	2005/8/21 22:00	19th between Ludlow & Ranstead St	Concrete	29.12	27.36	15.54	3.92	30.00
45	2005/8/21 22:00	19th between Ludlow & Ranstead St	Concrete	28.91	27.36	15.54	3.59	30.00
46	2005/8/23 22:00	Northwest Corner of Rittenhouse Square	Concrete	25.98	25.06	21.60	35.10	20.00
47	2005/8/26 22:00	Between 20th & 21st Chestnut St	Concrete	25.89	24.44	18.07	3.28	2.50
48	2005/8/26 22:00	Between 20th & 21st Chestnut St	Concrete	25.64	24.44	18.07	1.71	4.00
49	2005/8/26 22:00	20th between Chestnut & Sansom St	Concrete	25.77	24.44	15.54	3.19	4.25
50	2005/8/26 22:00	20th between Chestnut & Sansom St	Concrete	25.73	24.44	15.54	3.72	4.25
51	2005/8/29 22:00	Corner of Ben Franklin Parkway & Race Street at 18th	Concrete	27.36	25.33	16.42	14.73	3.50
52	2005/9/2 22:00	Corner of 20th & Race Street	Concrete	27.26	26.56	30.71	70.15	7.00
53	2005/9/4 22:00	North Corner of Logan Circle @ 19th	Concrete	25.81	25.12	42.00	56.85	7.00
54	2005/6/9 22:00	Between 34th & 35th Race Street	Brick	26.68	24.89	18.61	5.79	3.25
55	2005/6/9 22:00	Between 34th & 35th Race Street	Brick	27.48	24.89	18.61	8.46	3.25
56	2005/6/9 22:00	Between 34th & 35th Race Street	Concrete	26.88	24.89	18.61	5.45	3.25
57	2005/6/9 22:00	Between 34th & 35th Race Street	Concrete	27.87	24.89	18.61	5.00	3.25
58	2005/6/14 22:00	35th between Race and Powelton	Concrete	33.06	31.37	15.58	8.80	3.25
59	2005/6/14 22:00	35th between Race and Powelton	Concrete	33.57	31.37	15.58	4.72	3.25
60	2005/6/14 22:00	Between 34th & 35th Race Street	Concrete	33.11	31.37	18.61	8.88	3.25
61	2005/6/14 22:00	Between 34th & 35th Race Street	Brick	33.39	31.37	18.61	7.17	3.25
62	2005/6/29 22:00	Between 43rd & 44th Walnut St	Asphalt	27.15	24.18	22.13	20.14	1.50
63	2005/6/29 22:00	Between 43rd & 44th Walnut St	Asphalt	27.36	24.18	22.13	20.26	3.50
64	2005/6/29 22:00	Between 43rd & 44th Walnut St	Concrete	27.14	24.18	22.13	22.19	3.25
65	2005/6/29 22:00	Between 43rd & 44th Walnut St	Concrete	27.23	24.18	22.13	23.89	3.25
66	2005/6/29 22:00	44th between Walnut and Locust St	Concrete	26.04	24.18	18.19	3.06	3.75
67	2005/6/29 22:00	44th between Walnut and Locust St	Concrete	26.17	24.18	18.19	3.19	3.75
68	2005/7/5 22:00	Between 44th & 45th Walnut St	Concrete	25.28	21.62	23.24	3.83	3.50
69	2005/7/5 22:00	Between 44th & 45th Walnut St	Concrete	26.11	21.62	23.24	4.52	3.50
70	2005/7/5 22:00	Buckingham PL	Concrete	23.76	21.62	12.20	2.23	3.25
71	2005/7/5 22:00	Buckingham PL	Concrete	24.92	21.62	12.20	2.32	3.25
72	2005/7/5 22:00	Between 44th & 45th Locust St	Concrete	23.51	21.62	19.67	3.19	3.25
73	2005/7/5 22:00	Between 44th & 45th Locust St	Concrete	24.31	21.62	19.67	5.99	3.25

74	2005/7/10 22:00	Corner of Holden St & Powelton Ave	Asphalt	32.49	26.81	24.57	45.05	2.25
75	2005/7/10 22:00	Corner of Holden St & Powelton Ave	Asphalt	27.52	26.81	24.57	73.17	2.25
76	2005/7/22 22:00	43rd between Locust St & Spruce St	Asphalt	32.61	30.19	16.97	30.22	1.50
77	2005/7/22 22:00	43rd between Locust St & Spruce St	Asphalt	32.38	30.19	16.97	17.98	1.50
78	2005/7/24 22:00	37th Waren St	Asphalt	27.09	25.96	17.13	13.16	2.00
79	2005/7/24 22:00	37th Waren St	Asphalt	27.32	25.96	17.13	16.17	2.00
80	2005/7/26 22:00	Between Hutchinson Gym & Franklin Field	Asphalt	36.13	32.90	11.66	21.64	2.00
81	2005/7/26 22:00	Between Hutchinson Gym & Franklin Field	Asphalt	36.47	32.90	11.66	18.06	2.00
82	2005/7/29 22:00	43rd between Walnut & Sansom St	Asphalt	27.54	24.79	15.33	6.83	1.50
83	2005/7/29 22:00	43rd between Walnut & Sansom St	Asphalt	27.83	24.79	15.33	16.93	1.50
84	2005/8/3 22:00	20th between Market & Commerce St	Concrete	33.40	30.80	34.75	4.07	41.00
85	2005/8/3 22:00	20th between Market & Commerce St	Concrete	33.49	30.80	34.75	3.78	41.00
86	2005/8/3 22:00	Between 20th & 21st Market St	Concrete	33.34	30.80	27.01	4.04	41.00
87	2005/8/3 22:00	Between 20th & 21st Market St	Concrete	33.05	30.80	27.01	3.86	41.00
88	2005/8/7 22:00	Between 19th & 20th JFK	Concrete	29.49	25.47	32.40	4.30	20.00
89	2005/8/7 22:00	Between 19th & 20th JFK	Brick	29.80	25.47	32.40	2.82	30.00
90	2005/8/7 22:00	Between 19th & 20th JFK	Concrete	29.57	25.47	32.40	6.74	30.00
91	2005/8/18 22:00	Between 19th & 20th Commerce St	Concrete	25.98	22.80	7.64	2.41	20.00
92	2005/8/18 22:00	Between 19th & 20th Commerce St	Concrete	25.99	22.80	7.64	3.66	20.00
93	2005/8/18 22:00	19th between Market & Commerce St	Brick	25.60	22.80	17.66	3.98	45.00
94	2005/8/18 22:00	19th between Market & Commerce St	Brick	25.51	22.80	17.66	4.03	45.00
95	2005/8/22 22:00	Between 18th & 29th Ludlow St	Concrete	27.14	25.51	8.20	1.83	37.00
96	2005/8/22 22:00	Between 18th & 29th Ludlow St	Concrete	26.62	25.51	8.20	1.56	5.00
97	2005/8/22 22:00	19th between Ludlow & Ranstead St	Concrete	26.60	25.51	15.54	3.92	30.00
98	2005/8/22 22:00	19th between Ludlow & Ranstead St	Concrete	26.52	25.51	15.54	3.59	30.00
99	2005/8/24 22:00	Northwest Corner of Rittenhouse Square	Concrete	25.21	24.99	21.60	35.10	20.00
100	2005/8/28 22:00	Between 20th & 21st Chestnut St	Concrete	28.14	23.31	18.07	3.28	2.50
101	2005/8/28 22:00	Between 20th & 21st Chestnut St	Concrete	26.84	23.31	18.07	1.71	4.00
102	2005/8/28 22:00	20th between Chestnut & Sansom St	Concrete	27.07	23.31	15.54	3.19	4.25
103	2005/8/28 22:00	20th between Chestnut & Sansom St	Concrete	26.84	23.31	15.54	3.72	4.25
104	2005/9/1 22:00	Corner of Ben Franklin Parkway & Race Street at 18th	Concrete	26.19	25.42	16.42	14.73	3.50
105	2005/9/3 22:00	Corner of 20th & Race Street	Concrete	24.79	24.90	30.71	70.15	7.00
106	2005/9/5 22:00	North Corner of Logan Circle @ 19th	Concrete	24.52	23.76	42.00	56.85	7.00

Appendix 3-4. Dataset of Pervious Surface at Nighttime (22:00).

	Date/Time	Address (Street Name)	Surface Material	FHI (C)	SHI (C)	SW (m)	DB (m)	BS (#)
1	2005/6/13 22:00	35th between Race and Powelton	Grass	31.81	30.12	15.58	5.66	3.25
2	2005/6/13 22:00	35th between Race and Powelton	Grass	31.44	30.12	15.58	10.03	3.25
3	2005/7/9 22:00	Corner of Holden St & Powelton Ave	Grass	24.91	25.21	24.57	51.51	2.25
4	2005/7/9 22:00	Corner of Holden St & Powelton Ave	Grass	24.85	25.21	24.57	48.18	2.25
5	2005/7/21 22:00	43rd between Locust St & Spruce St	Grass	30.74	29.36	16.97	35.20	4.00
6	2005/7/21 22:00	43rd between Locust St & Spruce St	Grass	30.47	29.36	16.97	35.88	4.00
7	2005/7/23 22:00	37th Waren St	Grass	25.62	26.00	17.13	8.86	4.00
8	2005/7/23 22:00	37th Waren St	Grass	25.37	26.00	17.13	25.98	4.00
9	2005/7/25 22:00	Between Hutchinson Gym & Franklin Field	Grass	34.95	32.86	11.66	11.33	10.00
10	2005/7/25 22:00	Between Hutchinson Gym & Franklin Field	Grass	34.84	32.86	11.66	13.32	10.00
11	2005/7/28 22:00	43rd between Walnut & Sansom St	Grass	25.17	25.09	15.33	17.14	3.25
12	2005/7/28 22:00	43rd between Walnut & Sansom St	Grass	25.09	25.09	15.33	26.45	3.25
13	2005/8/4 22:00	Between 20th & 21st JFK	Grass	33.17	32.29	26.97	37.72	41.00
14	2005/8/4 22:00	Between 20th & 21st JFK	Grass	33.45	32.29	26.97	36.62	41.00
15	2005/8/23 22:00	Northwest Corner of Rittenhouse Square	Grass	25.62	25.06	21.60	31.60	20.00
16	2005/8/23 22:00	Northwest Corner of Rittenhouse Square	Grass	25.69	25.06	21.60	29.09	20.00
17	2005/8/23 22:00	Northwest Corner of Rittenhouse Square	Grass	25.54	25.06	21.60	52.59	20.00
18	2005/8/29 22:00	Corner of Ben Franklin Parkway & Race Street at 18th	Grass	27.02	25.33	35.06	29.70	3.50
19	2005/8/29 22:00	Corner of Ben Franklin Parkway & Race Street at 18th	Grass	27.14	25.33	35.06	24.04	3.50
20	2005/8/29 22:00	Corner of Ben Franklin Parkway & Race Street at 18th	Grass	27.01	25.33	16.42	19.88	3.50
21	2005/9/2 22:00	Corner of 20th & Race Street	Grass	27.06	26.56	30.71	39.01	7.00
22	2005/9/2 22:00	Corner of 20th & Race Street	Grass	27.16	26.56	30.71	47.23	7.00
23	2005/9/2 22:00	Corner of 20th & Race Street	Grass	27.38	26.56	30.71	54.69	7.00
24	2005/9/4 22:00	North Corner of Logan Circle @ 19th	Grass	25.64	25.12	42.00	60.19	7.00
25	2005/9/4 22:00	North Corner of Logan Circle @ 19th	Grass	25.48	25.12	42.00	50.91	7.00
26	2005/9/4 22:00	North Corner of Logan Circle @ 19th	Grass	25.51	25.12	42.00	54.03	7.00
27	2005/6/14 22:00	35th between Race and Powelton	Grass	32.60	31.37	15.58	5.66	3.25
28	2005/6/14 22:00	35th between Race and Powelton	Grass	31.85	31.37	15.58	10.03	3.25
29	2005/7/10 22:00	Corner of Holden St & Powelton Ave	Grass	26.74	26.81	24.57	51.51	2.25
30	2005/7/10 22:00	Corner of Holden St & Powelton Ave	Grass	26.75	26.81	24.57	48.18	2.25
31	2005/7/22 22:00	43rd between Locust St & Spruce St	Grass	31.30	30.19	16.97	35.20	4.00
32	2005/7/22 22:00	43rd between Locust St & Spruce St	Grass	31.22	30.19	16.97	35.88	4.00
33	2005/7/24 22:00	37th Waren St	Grass	25.56	25.96	17.13	8.86	4.00
34	2005/7/24 22:00	37th Waren St	Grass	25.77	25.96	17.13	25.98	4.00
35	2005/7/26 22:00	Between Hutchinson Gym & Franklin Field	Grass	35.12	32.90	11.66	11.33	10.00
36	2005/7/26 22:00	Between Hutchinson Gym & Franklin Field	Grass	35.04	32.90	11.66	13.32	10.00
37	2005/7/29 22:00	43rd between Walnut & Sansom St	Grass	26.06	24.79	15.33	17.14	3.25
38	2005/7/29 22:00	43rd between Walnut & Sansom St	Grass	25.96	24.79	15.33	26.45	3.25
39	2005/8/7 22:00	Between 20th & 21st JFK	Grass	27.41	25.47	26.97	37.72	41.00
40	2005/8/7 22:00	Between 20th & 21st JFK	Grass	27.67	25.47	26.97	36.62	41.00
41	2005/8/24 22:00	Northwest Corner of Rittenhouse Square	Grass	25.07	24.99	21.60	31.60	20.00
42	2005/8/24 22:00	Northwest Corner of Rittenhouse Square	Grass	25.12	24.99	21.60	29.09	20.00
43	2005/8/24 22:00	Northwest Corner of Rittenhouse Square	Grass	25.04	24.99	21.60	52.59	20.00
44	2005/9/1 22:00	Corner of Ben Franklin Parkway & Race Street at 18th	Grass	25.77	25.42	35.06	29.70	3.50
45	2005/9/1 22:00	Corner of Ben Franklin Parkway & Race Street at 18th	Grass	26.09	25.42	35.06	24.04	3.50
46	2005/9/1 22:00	Corner of Ben Franklin Parkway & Race Street at 18th	Grass	26.09	25.42	16.42	19.88	3.50
47	2005/9/3 22:00	Corner of 20th & Race Street	Grass	24.57	24.90	30.71	39.01	7.00
48	2005/9/3 22:00	Corner of 20th & Race Street	Grass	24.49	24.90	30.71	47.23	7.00
49	2005/9/3 22:00	Corner of 20th & Race Street	Grass	24.68	24.90	30.71	54.69	7.00
50	2005/9/5 22:00	North Corner of Logan Circle @ 19th	Grass	24.14	23.76	42.00	60.19	7.00
51	2005/9/5 22:00	North Corner of Logan Circle @ 19th	Grass	23.98	23.76	42.00	50.91	7.00
52	2005/9/5 22:00	North Corner of Logan Circle @ 19th	Grass	24.03	23.76	42.00	54.03	7.00

Appendix 4-1. Result of Preliminary Testing for Impervious Surface at Daytime (13:00).

(A) Distribution of Variables

FHI (C)
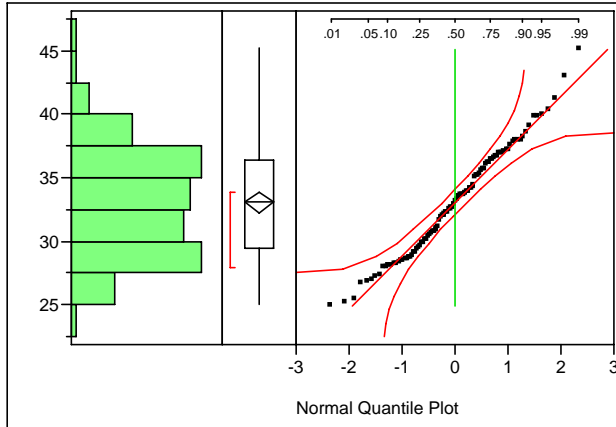
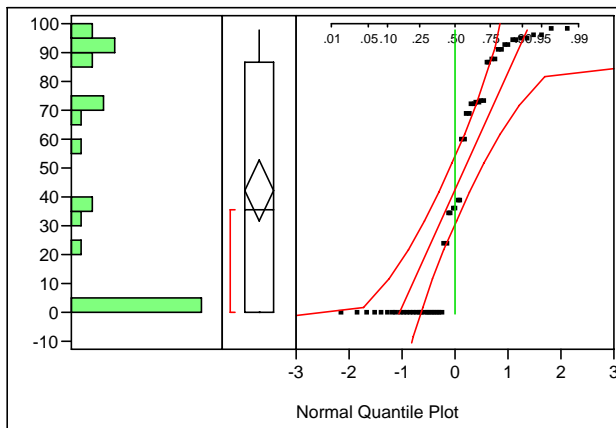| Quantiles		
100.0%	maximum	45.223
99.5%		45.223
97.5%		42.016
90.0%		38.116
75.0%	quartile	36.432
50.0%	median	33.043
25.0%	quartile	29.472
10.0%		28.036
2.5%		25.298
0.5%		24.999
0.0%	minimum	24.999

Moments	
Mean	33.067897
Std Dev	4.2054392
Std Err Mean	0.4164005
upper 95% Mean	33.893923
lower 95% Mean	32.24187
N	102

SHI (C)
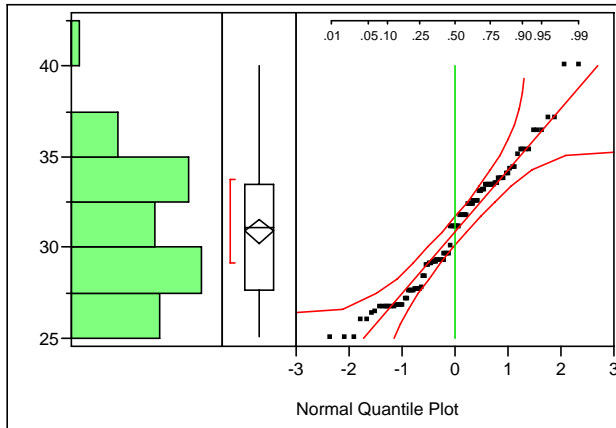
Quantiles		
100.0%	maximum	40.065
99.5%		40.065
97.5%		38.396
90.0%		35.348
75.0%	quartile	33.467
50.0%	median	31.114
25.0%	quartile	27.659
10.0%		26.727
2.5%		25.047
0.5%		25.047
0.0%	minimum	25.047

Moments	
Mean	30.89429
Std Dev	3.3947263
Std Err Mean	0.336128
upper 95% Mean	31.561078
lower 95% Mean	30.227503
N	102

Sh (%)
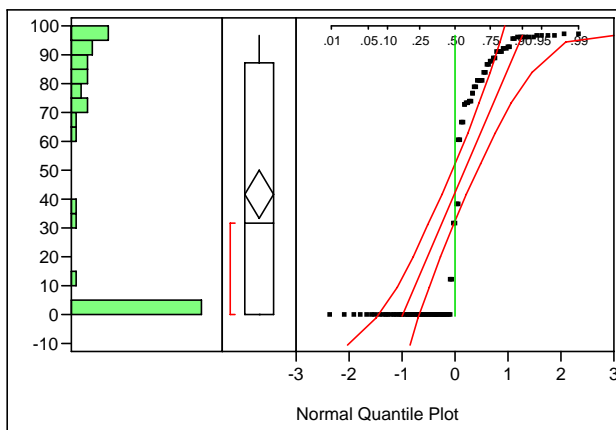
Quantiles		
100.0%	maximum	96.930
99.5%		96.930
97.5%		96.729
90.0%		95.647
75.0%	quartile	87.460
50.0%	median	31.400
25.0%	quartile	0.000
10.0%		0.000
2.5%		0.000
0.5%		0.000
0.0%	minimum	0.000

Moments	
Mean	41.756471
Std Dev	42.44704
Std Err Mean	4.2028833
upper 95% Mean	50.09386
lower 95% Mean	33.419081
N	102

SW (m)
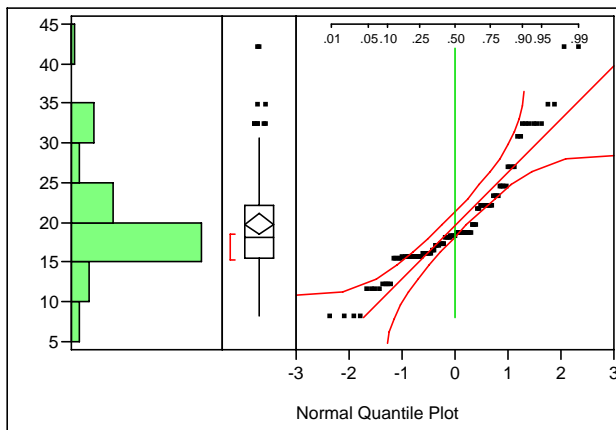
Quantiles

100.0%	maximum	41.998
99.5%		41.998
97.5%		37.832
90.0%		31.892
75.0%	quartile	22.128
50.0%	median	18.190
25.0%	quartile	15.584
10.0%		12.195
2.5%		8.199
0.5%		8.199
0.0%	minimum	8.199

Moments

Mean	19.774528
Std Dev	6.7205714
Std Err Mean	0.6654357
upper 95% Mean	21.094573
lower 95% Mean	18.454482
N	102

DB (m)
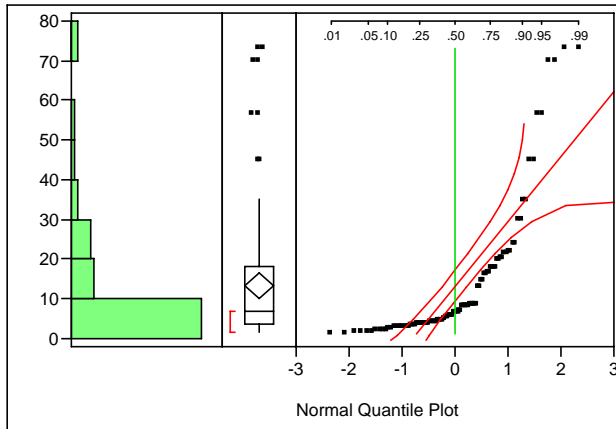
Quantiles

100.0%	maximum	73.173
99.5%		73.173
97.5%		71.437
90.0%		33.636
75.0%	quartile	17.983
50.0%	median	6.736
25.0%	quartile	3.725
10.0%		2.468
2.5%		1.645
0.5%		1.561
0.0%	minimum	1.561

Moments

Mean	13.318983
Std Dev	16.366483
Std Err Mean	1.6205233
upper 95% Mean	16.533665
lower 95% Mean	10.104301
N	102

BS (#)
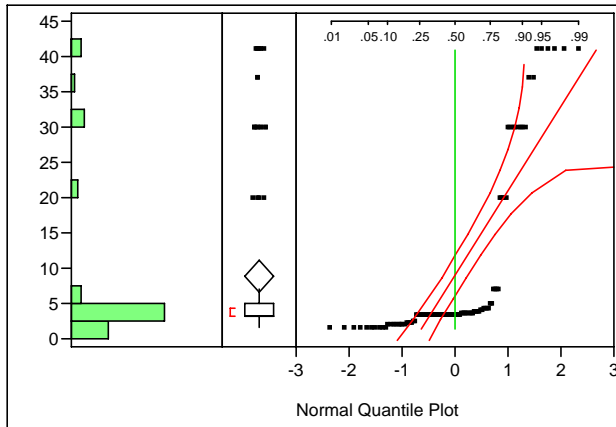
Quantiles

100.0%	maximum	41.000
99.5%		41.000
97.5%		41.000
90.0%		30.000
75.0%	quartile	5.000
50.0%	median	3.250
25.0%	quartile	3.250
10.0%		1.650
2.5%		1.500
0.5%		1.500
0.0%	minimum	1.500

Moments

Mean	8.8431373
Std Dev	12.023797
Std Err Mean	1.1905333
upper 95% Mean	11.204835
lower 95% Mean	6.4814395
N	102

(B) Pearson Product Moment Correlation Matrix

Multivariate Correlations

	FHI (C)	SHI (C)	Sh (%)	SW (m)	DB (m)	BS (#)
FHI (C)	1.0000	0.8861	-0.3762	-0.0738	-0.0886	0.1190
SHI (C)	0.8861	1.0000	-0.0556	-0.0258	-0.1348	0.2549
Sh (%)	-0.3762	-0.0556	1.0000	0.0884	-0.0676	-0.0200
SW (m)	-0.0738	-0.0258	0.0884	1.0000	0.3855	0.3786
DB (m)	-0.0886	-0.1348	-0.0676	0.3855	1.0000	-0.2047
BS (#)	0.1190	0.2549	-0.0200	0.3786	-0.2047	1.0000

Scatterplot Matrix
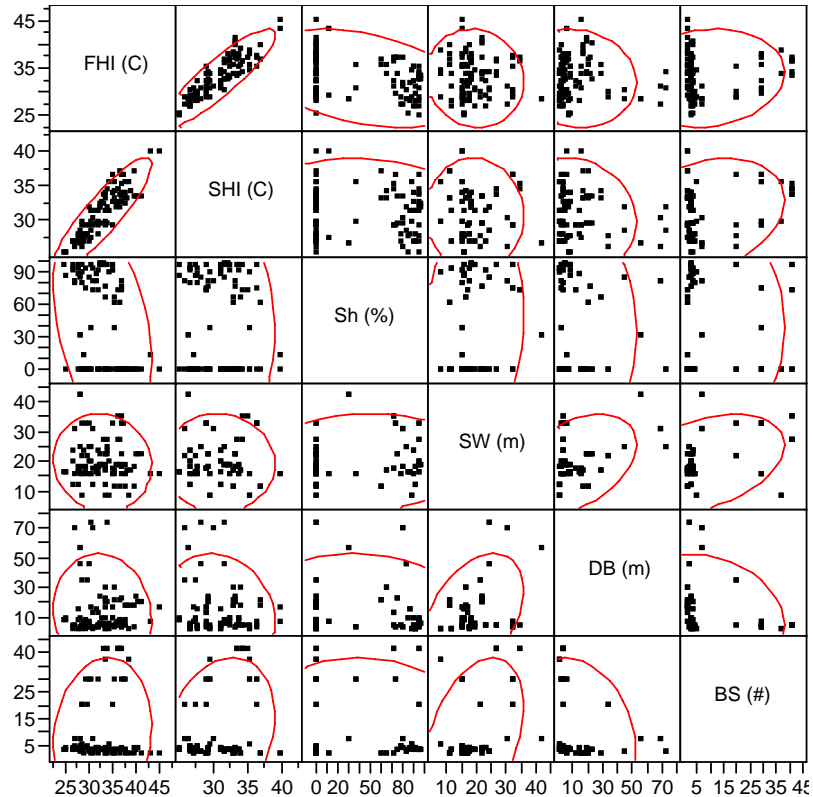
(C) Stepwise Regression

Stepwise Fit
Response: FHI (C)

Current Estimates

SSE	DFE	MSE	RSquare	RSquare Adj	Cp	AIC
169.76388	98	1.7322845	0.9050	0.9021	3.6271435	59.96244

Stepwise Regression Control

Lock	Entered	Parameter	Estimate	nDF	SS	F Ratio	Prob>F
X	X	Intercept	0.44038649	1	0	0.000	1.0000
	X	SHI (C)	1.11174027	1	1341.471	774.394	0.0000
	X	Sh (%)	-0.0325553	1	192.2642	110.989	0.0000
		SW (m)	0	1	1.078294	0.620	0.4329
		DB (m)	0	1	0.354044	0.203	0.6535
	X	BS (#)	-0.0406554	1	22.56613	13.027	0.0005

Prob to Enter 0.250
Prob to Leave 0.250

Direction: Mixed

Step History

Step	Parameter	Action	"Sig Prob"	Seq SS	RSquare	Cp	p
1	SHI (C)	Entered	0.0000	1402.447	0.7851	122.72	2
2	Sh (%)	Entered	0.0000	191.481	0.8923	14.604	3
3	BS (#)	Entered	0.0005	22.56613	0.9050	3.6271	4

(D) OLS Regression

Response FHI (C)
Whole Model
Actual by Predicted Plot

FHI (C) Predicted P<.0001 RSq=0.90
RMSE=1.3162
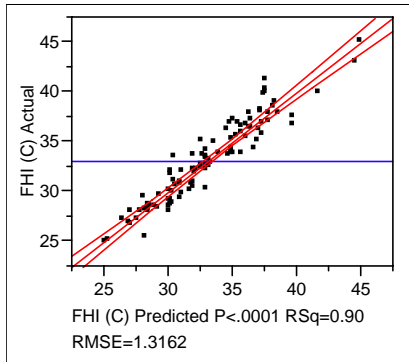
Summary of Fit

RSquare	0.904961
RSquare Adj	0.902052
Root Mean Square Error	1.316163
Mean of Response	33.0679
Observations (or Sum Wgts)	102

Analysis of Variance

Source	DF	Sum of Squares	Mean Square	F Ratio
Model	3	1616.4937	538.831	311.0524
Error	98	169.7639	1.732	Prob > F
C. Total	101	1786.2576		<.0001

Residual by Predicted Plot

FHI (C) Predicted
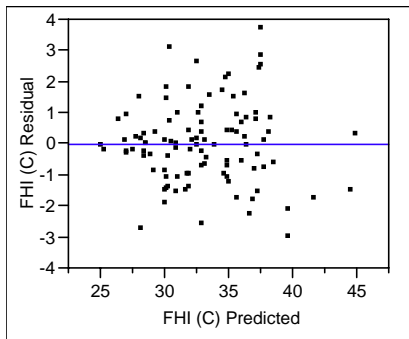
Parameter Estimates

Term	Estimate	Std Error	t Ratio	Prob>|t|	VIF
Intercept	0.4403865	1.233374	0.36	0.7218	.
SHI (C)	1.1117403	0.039951	27.83	<.0001	1.0723986
Sh (%)	-0.032555	0.00309	-10.54	<.0001	1.0031403
BS (#)	-0.040655	0.011264	-3.61	0.0005	1.0695067

Effect Tests

Source	Nparm	DF	Sum of Squares	F Ratio	Prob > F
SHI (C)	1	1	1341.4712	774.3943	<.0001
Sh (%)	1	1	192.2642	110.9888	<.0001
BS (#)	1	1	22.5661	13.0268	0.0005

Leverage Plot
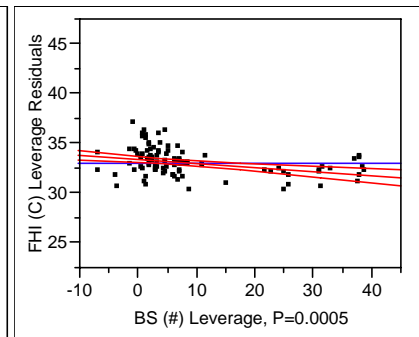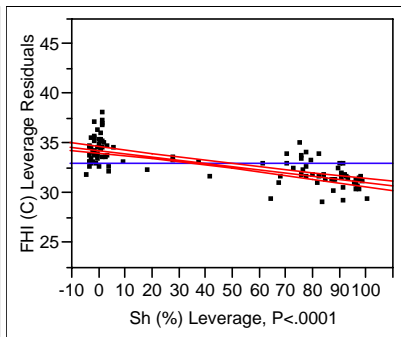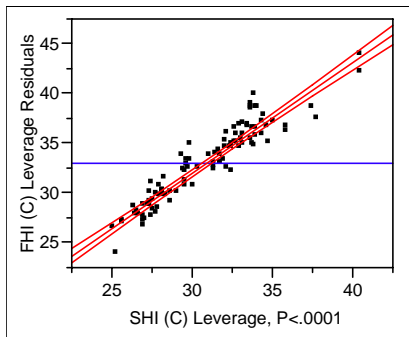
SHI (C) Leverage, P<.0001

Sh (%) Leverage, P<.0001

BS (#) Leverage, P=0.0005

(E) Distribution of Residuals derived from OLS Regression

Residual FHI (C) Distributions

Quantiles		
100.0%	maximum	3.692
99.5%		3.692
97.5%		2.939
90.0%		1.760
75.0%	quartile	0.757
50.0%	median	-0.031
25.0%	quartile	-0.863
10.0%		-1.546
2.5%		-2.654
0.5%		-3.007
0.0%	minimum	-3.007

Moments	
Mean	2.257e-14
Std Dev	1.2964685
Std Err Mean	0.1283695
upper 95% Mean	0.2546506
lower 95% Mean	-0.254651
N	102

Normal(2.3e-14,1.29647)
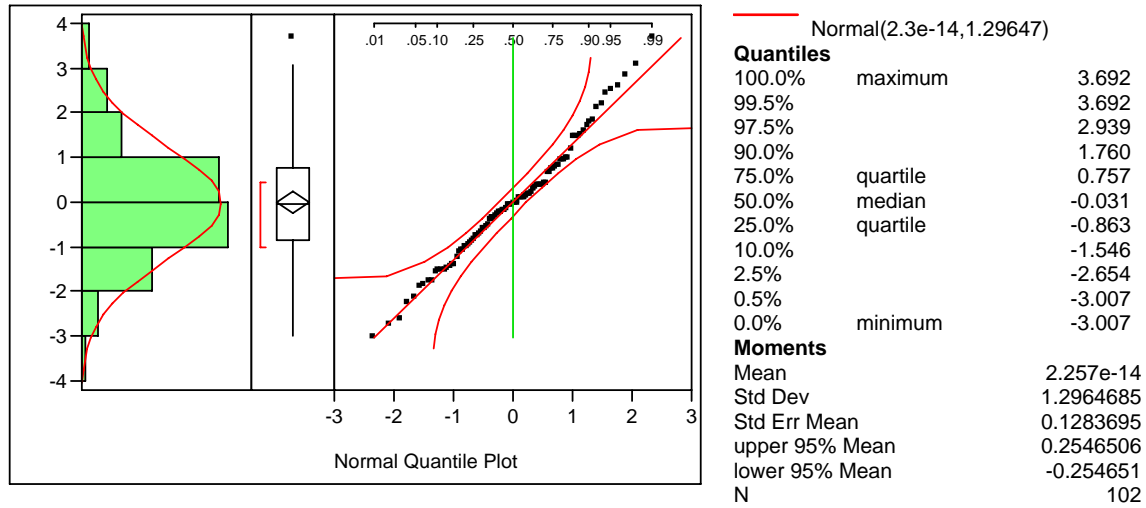
Fitted Normal
Parameter Estimates

Type	Parameter	Estimate	Lower 95%	Upper 95%
Location	Mu	2.257e-14	-0.25465	0.254651
Dispersion	Sigma	1.296468	1.13969	1.503663

(F) Regressing Residuals on Explanatory Variables

Bivariate Fit of Residual FHI (C) By SHI (C)

Linear Fit

Linear Fit
Residual FHI (C) = -5.17e-14 + 2.403e-15 SHI (C)

Summary of Fit

RSquare	0
RSquare Adj	-0.01
Root Mean Square Error	1.302935
Mean of Response	2.26e-14
Observations (or Sum Wgts)	102

Analysis of Variance

Source	DF	Sum of Squares	Mean Square	F Ratio
Model	1	0.00000	0.00000	0.0000
Error	100	169.76388	1.69764	Prob > F
C. Total	101	169.76388		1.0000

Parameter Estimates

Term	Estimate	Std Error	t Ratio	Prob>|t|
Intercept	-5.17e-14	1.186906	-0.00	1.0000
SHI (C)	2.403e-15	0.038191	0.00	1.0000
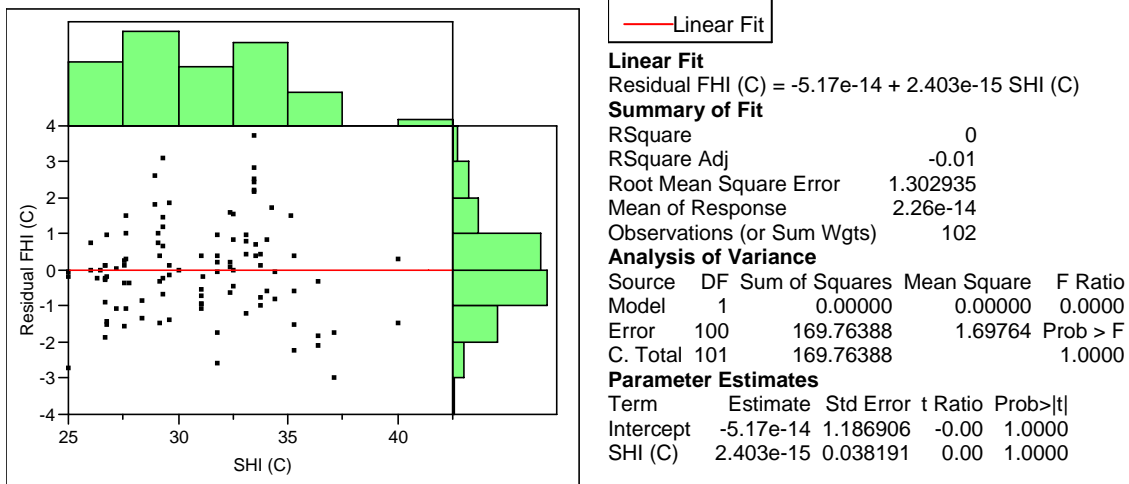
Bivariate Fit of Residual FHI (C) By Sh (%)
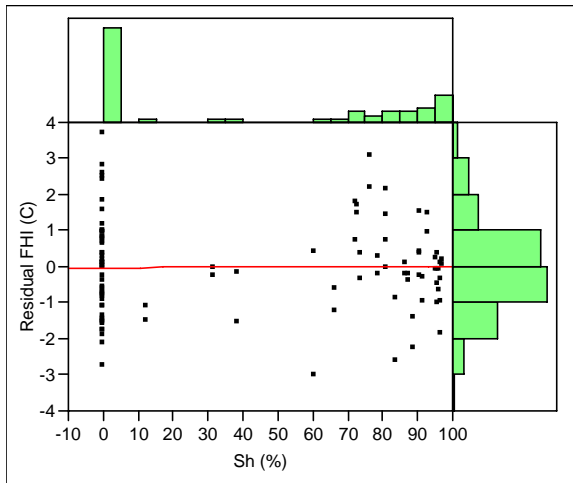
———Linear Fit

Linear Fit
Residual FHI (C) = -1.04e-14 + 7.907e-16 Sh (%)
Summary of Fit

RSquare	0
RSquare Adj	-0.01
Root Mean Square Error	1.302935
Mean of Response	2.26e-14
Observations (or Sum Wgts)	102

Analysis of Variance

Source	DF	Sum of Squares	Mean Square	F Ratio
Model	1	0.00000	0.00000	0.0000
Error	100	169.76388	1.69764	Prob > F
C. Total	101	169.76388		1.0000

Parameter Estimates

Term	Estimate	Std Error	t Ratio	Prob>|t|
Intercept	-1.04e-14	0.181409	-0.00	1.0000
Sh (%)	7.907e-16	0.003054	0.00	1.0000

Bivariate Fit of Residual FHI (C) By BS (#)
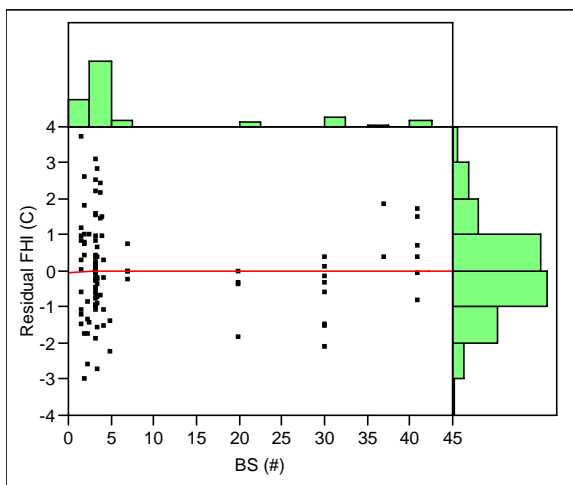
———Linear Fit

Linear Fit
Residual FHI (C) = -8.44e-15 + 3.506e-15 BS (#)
Summary of Fit

RSquare	0
RSquare Adj	-0.01
Root Mean Square Error	1.302935
Mean of Response	2.26e-14
Observations (or Sum Wgts)	102

Analysis of Variance

Source	DF	Sum of Squares	Mean Square	F Ratio
Model	1	0.00000	0.00000	0.0000
Error	100	169.76388	1.69764	Prob > F
C. Total	101	169.76388		1.0000

Parameter Estimates

Term	Estimate	Std Error	t Ratio	Prob>|t|
Intercept	-8.44e-15	0.160423	-0.00	1.0000
BS (#)	3.506e-15	0.010783	0.00	1.0000

67

Appendix 4-2. Result of Preliminary Testing for Pervious Surface at Daytime (13:00).

(A) Distribution of Variables

FHI (C)

Normal Quantile Plot
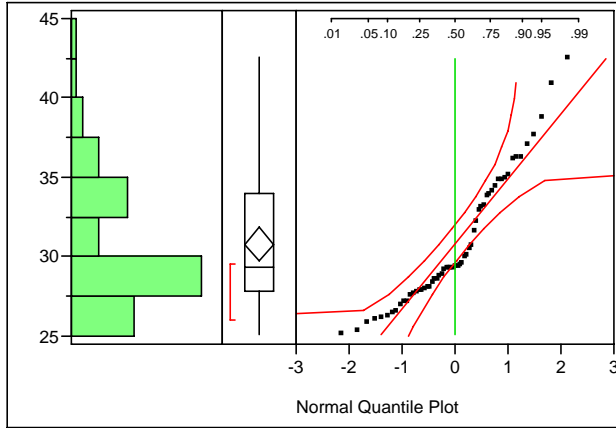
Quantiles		
100.0%	maximum	42.549
99.5%		42.549
97.5%		41.781
90.0%		36.377
75.0%	quartile	33.984
50.0%	median	29.349
25.0%	quartile	27.834
10.0%		26.279
2.5%		25.218
0.5%		25.121
0.0%	minimum	25.121

Moments	
Mean	30.791563
Std Dev	4.0860873
Std Err Mean	0.5365295
upper 95% Mean	31.865944
lower 95% Mean	29.717181
N	58

SHI (C)

Normal Quantile Plot
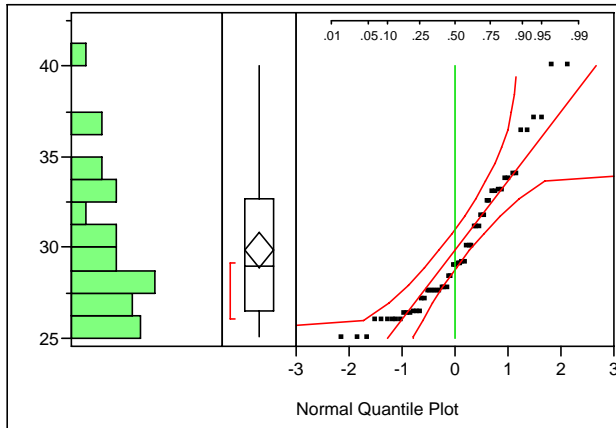
Quantiles		
100.0%	maximum	40.065
99.5%		40.065
97.5%		40.065
90.0%		36.424
75.0%	quartile	32.667
50.0%	median	29.003
25.0%	quartile	26.478
10.0%		26.023
2.5%		25.047
0.5%		25.047
0.0%	minimum	25.047

Moments	
Mean	29.872877
Std Dev	3.8173994
Std Err Mean	0.5012491
upper 95% Mean	30.876611
lower 95% Mean	28.869143
N	58

Sh (%)

Normal Quantile Plot

Quantiles		
100.0%	maximum	97.780
99.5%		97.780
97.5%		97.780
90.0%		94.690
75.0%	quartile	86.793
50.0%	median	35.750
25.0%	quartile	0.000
10.0%		0.000
2.5%		0.000
0.5%		0.000
0.0%	minimum	0.000

Moments	
Mean	41.997931
Std Dev	40.161464
Std Err Mean	5.2734586
upper 95% Mean	52.55785
lower 95% Mean	31.438012
N	58

SW (m)
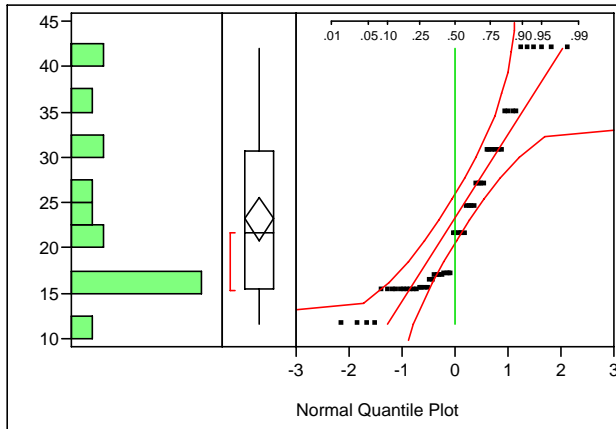
Normal Quantile Plot

Quantiles

100.0%	maximum	41.998
99.5%		41.998
97.5%		41.998
90.0%		41.998
75.0%	quartile	30.715
50.0%	median	21.604
25.0%	quartile	15.536
10.0%		15.328
2.5%		11.656
0.5%		11.656
0.0%	minimum	11.656

Moments

Mean	23.17468
Std Dev	9.247631
Std Err Mean	1.2142734
upper 95% Mean	25.60622
lower 95% Mean	20.743139
N	58

DB (m)

Normal Quantile Plot
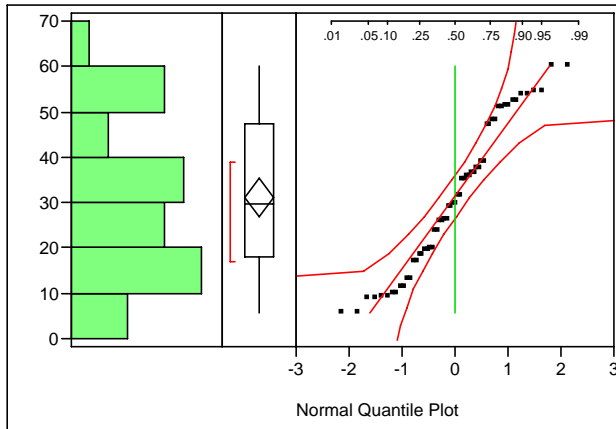
Quantiles

100.0%	maximum	60.195
99.5%		60.195
97.5%		60.195
90.0%		54.029
75.0%	quartile	47.463
50.0%	median	29.700
25.0%	quartile	18.076
10.0%		9.482
2.5%		5.657
0.5%		5.657
0.0%	minimum	5.657

Moments

Mean	31.176941
Std Dev	16.124783
Std Err Mean	2.1172877
upper 95% Mean	35.416737
lower 95% Mean	26.937145
N	58

BS (#)

Normal Quantile Plot
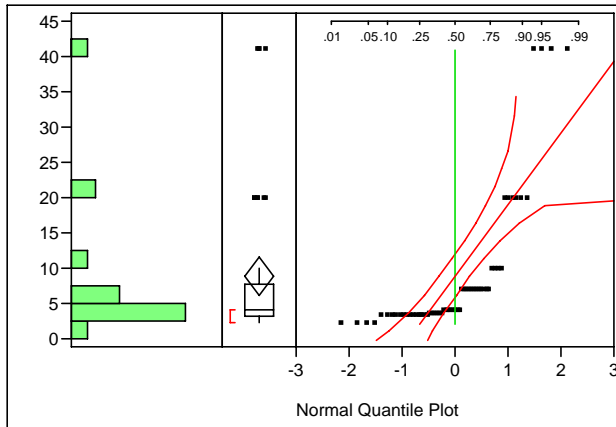
Quantiles

100.0%	maximum	41.000
99.5%		41.000
97.5%		41.000
90.0%		20.000
75.0%	quartile	7.750
50.0%	median	4.000
25.0%	quartile	3.250
10.0%		3.250
2.5%		2.250
0.5%		2.250
0.0%	minimum	2.250

Moments

Mean	8.887931
Std Dev	10.173837
Std Err Mean	1.3358902
upper 95% Mean	11.563005
lower 95% Mean	6.212857
N	58

(B) Pearson Product Moment Correlation Matrix

Multivariate Correlations

	FHI (C)	SHI (C)	Sh (%)	SW (m)	DB (m)	BS (#)
FHI (C)	1.0000	0.9490	-0.3998	-0.3544	-0.3603	0.0112
SHI (C)	0.9490	1.0000	-0.2268	-0.3860	-0.3106	0.0757
Sh (%)	-0.3998	-0.2268	1.0000	0.0685	0.1760	-0.1450
SW (m)	-0.3544	-0.3860	0.0685	1.0000	0.7420	0.1239
DB (m)	-0.3603	-0.3106	0.1760	0.7420	1.0000	0.1964
BS (#)	0.0112	0.0757	-0.1450	0.1239	0.1964	1.0000

Scatterplot Matrix
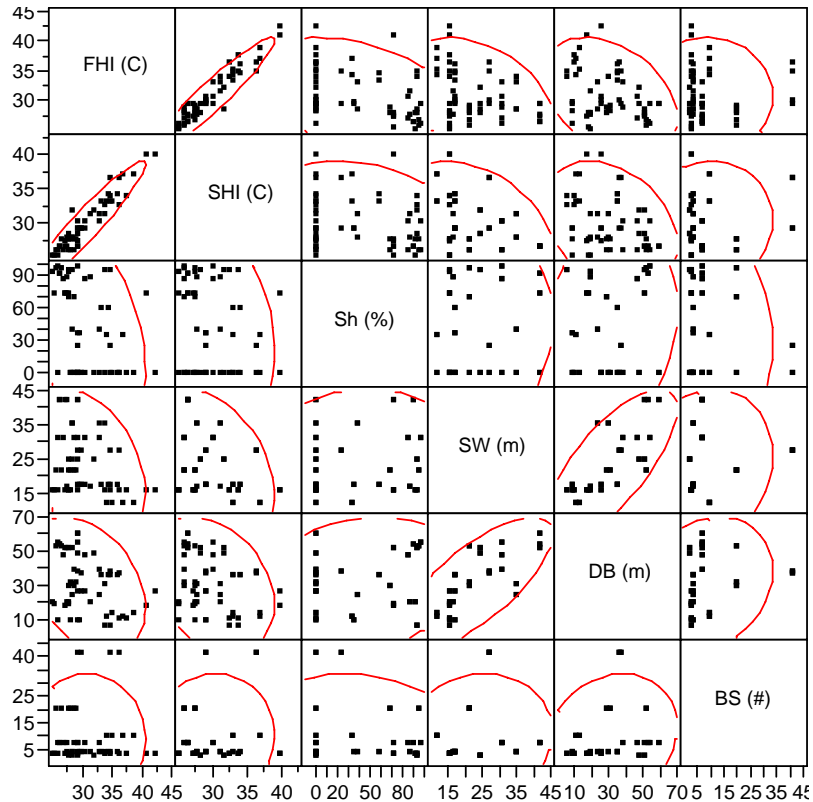
(C) Stepwise Regression

Stepwise Fit
Response: FHI (C)

Current Estimates

	SSE	DFE	MSE	RSquare	RSquare Adj	Cp	AIC
	53.214176	54	0.9854477	0.9441	0.9410	6.3582573	3.005146

Stepwise Regression Control

Lock	Entered	Parameter	Estimate	nDF	SS	F Ratio	Prob>F
X	X	Intercept	2.92501155	1	0	0.000	1.0000
	X	SHI (C)	0.97282375	1	744.1994	755.189	0.0000
	X	Sh (%)	-0.0210016	1	37.7993	38.357	0.0000
		SW (m)	0	1	0.5263	0.529	0.4701
		DB (m)	0	1	0.682315	0.688	0.4104
	X	BS (#)	-0.0351563	1	7.124663	7.230	0.0095

Prob to Enter 0.250
Prob to Leave 0.250

Direction: Mixed

Step History

Step	Parameter	Action	"Sig Prob"	Seq SS	RSquare	Cp	p
1	SHI (C)	Entered	0.0000	857.1439	0.9007	46.12	2
2	Sh (%)	Entered	0.0000	34.19545	0.9366	11.904	3
3	BS (#)	Entered	0.0095	7.124663	0.9441	6.3583	4

(D) OLS Regression

Response FHI (C)
Whole Model
Actual by Predicted Plot

FHI (C) Predicted P<.0001 RSq=0.94
RMSE=0.9927
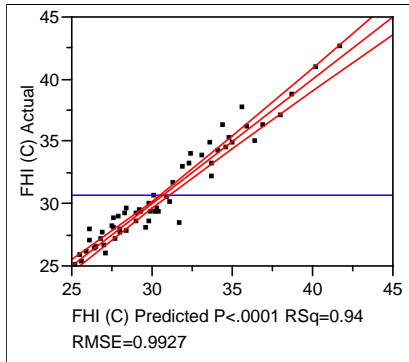
Summary of Fit

RSquare	0.944084
RSquare Adj	0.940977
Root Mean Square Error	0.992697
Mean of Response	30.79156
Observations (or Sum Wgts)	58

Analysis of Variance

Source	DF	Sum of Squares	Mean Square	F Ratio
Model	3	898.46405	299.488	303.9106
Error	54	53.21418	0.985	Prob > F
C. Total	57	951.67823		<.0001

Residual by Predicted Plot

FHI (C) Predicted
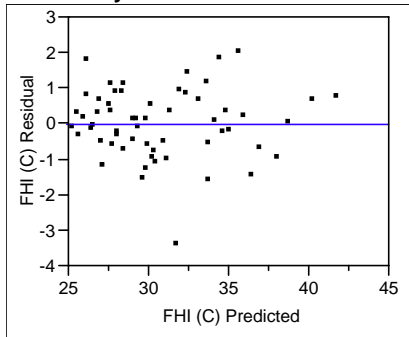
Parameter Estimates

Term	Estimate	Std Error	t Ratio	Prob>|t|	VIF
Intercept	2.9250116	1.108333	2.64	0.0108	.
SHI (C)	0.9728238	0.0354	27.48	<.0001	1.0563044
Sh (%)	-0.021002	0.003391	-6.19	<.0001	1.0727956
BS (#)	-0.035156	0.013075	-2.69	0.0095	1.023499

Effect Tests

Source	Nparm	DF	Sum of Squares	F Ratio	Prob > F
SHI (C)	1	1	744.19942	755.1892	<.0001
Sh (%)	1	1	37.79930	38.3575	<.0001
BS (#)	1	1	7.12466	7.2299	0.0095

Leverage Plot
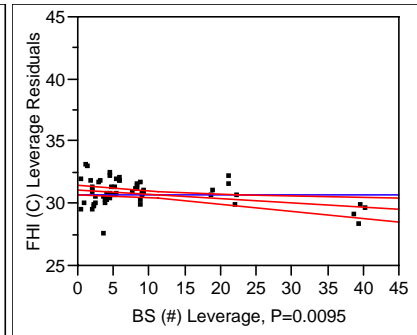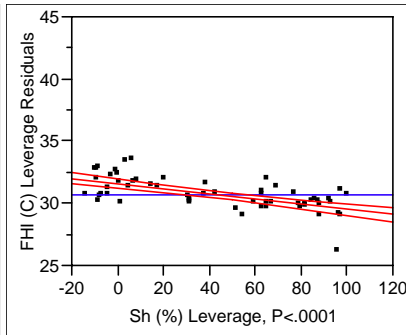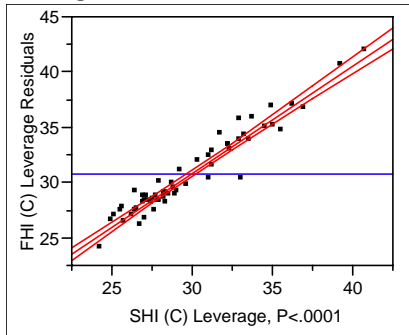
SHI (C) Leverage, P<.0001

Sh (%) Leverage, P<.0001

BS (#) Leverage, P=0.0095

71

(E) Distribution of Residuals derived from OLS Regression

Residual FHI (C) Distributions

	Normal(-8e-15,0.96622)
Quantiles	
100.0% maximum	2.037
99.5%	2.037
97.5%	1.954
90.0%	1.126
75.0% quartile	0.679
50.0% median	0.060
25.0% quartile	-0.573
10.0%	-1.169
2.5%	-2.535
0.5%	-3.404
0.0% minimum	-3.404
Moments	
Mean	-8.45e-15
Std Dev	0.9662205
Std Err Mean	0.126871
upper 95% Mean	0.2540547
lower 95% Mean	-0.254055
N	58
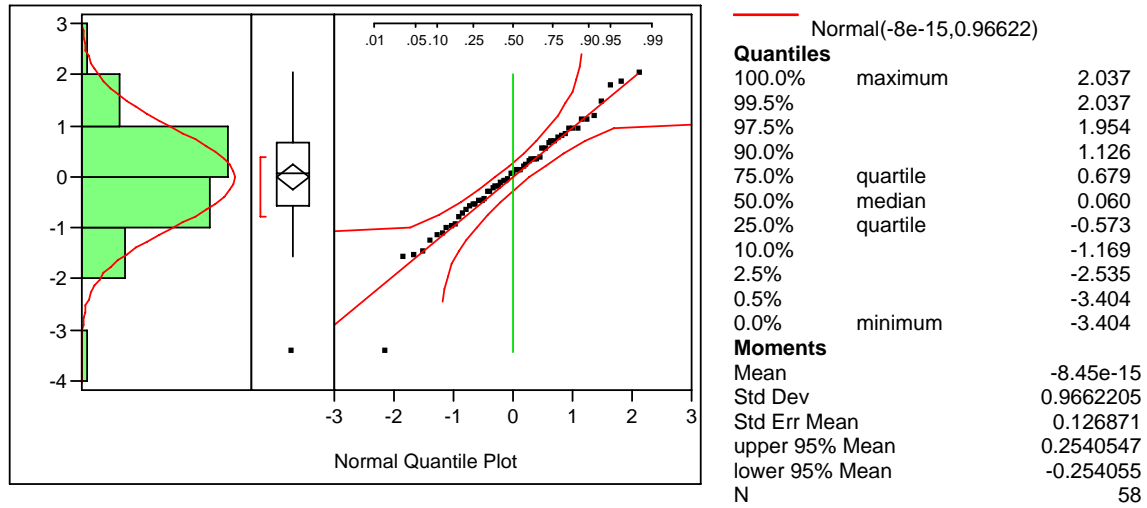
Fitted Normal
Parameter Estimates

Type	Parameter	Estimate	Lower 95%	Upper 95%
Location	Mu	-8.45e-15	-0.254055	0.254055
Dispersion	Sigma	0.966220	0.816850	1.182957

(F) Regressing Residuals on Explanatory Variables

Bivariate Fit of Residual FHI (C) By SHI (C)

— Linear Fit

Linear Fit
Residual FHI (C) = -3.49e-14 + 8.846e-16 SHI (C)
Summary of Fit

RSquare	0
RSquare Adj	-0.01786
Root Mean Square Error	0.974809
Mean of Response	-8.5e-15
Observations (or Sum Wgts)	58

Analysis of Variance

Source	DF	Sum of Squares	Mean Square	F Ratio
Model	1	0.000000	0.000000	0.0000
Error	56	53.214176	0.950253	Prob > F
C. Total	57	53.214176		1.0000

Parameter Estimates

Term	Estimate	Std Error	t Ratio	Prob>|t|
Intercept	-3.49e-14	1.018471	-0.00	1.0000
SHI (C)	8.846e-16	0.033823	0.00	1.0000
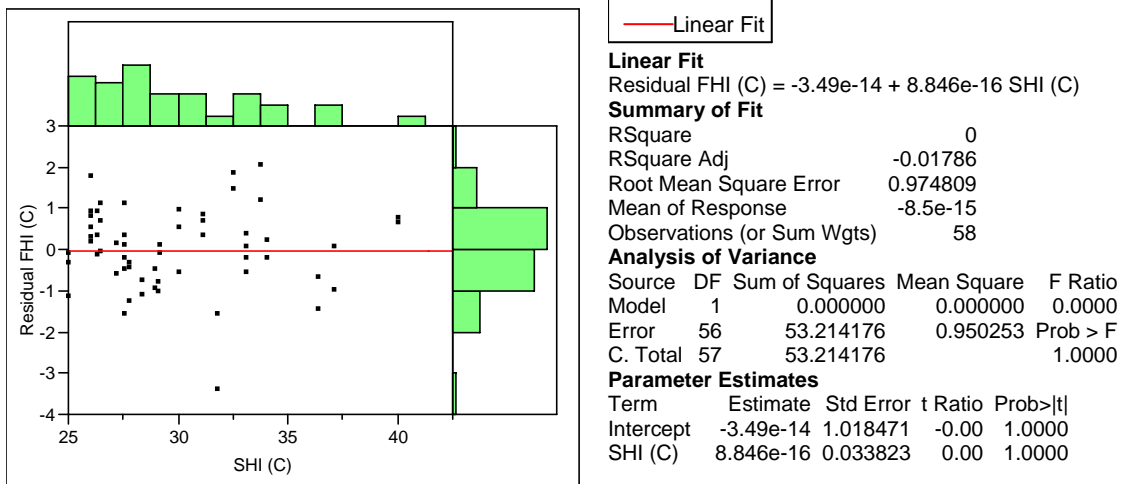
Bivariate Fit of Residual FHI (C) By Sh (%)
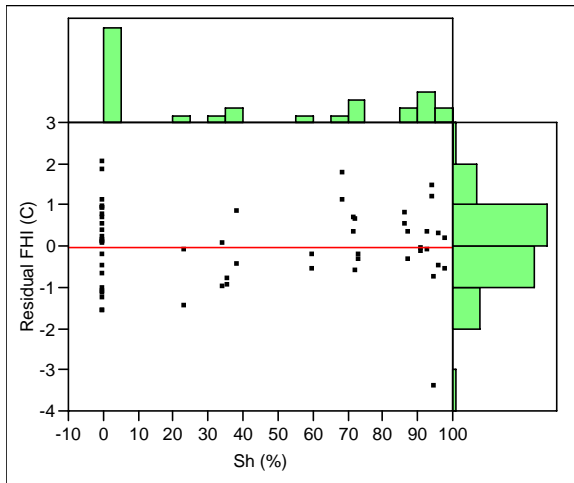
———Linear Fit

Linear Fit
Residual FHI (C) = 1.699e-14 - 6.059e-16 Sh (%)
Summary of Fit

RSquare	0
RSquare Adj	-0.01786
Root Mean Square Error	0.974809
Mean of Response	-8.5e-15
Observations (or Sum Wgts)	58

Analysis of Variance

Source	DF	Sum of Squares	Mean Square	F Ratio
Model	1	0.000000	0.000000	0.0000
Error	56	53.214176	0.950253	Prob > F
C. Total	57	53.214176		1.0000

Parameter Estimates

Term	Estimate	Std Error	t Ratio	Prob>|t|
Intercept	1.699e-14	0.186049	0.00	1.0000
Sh (%)	-6.06e-16	0.003215	-0.00	1.0000

Bivariate Fit of Residual FHI (C) By BS (#)
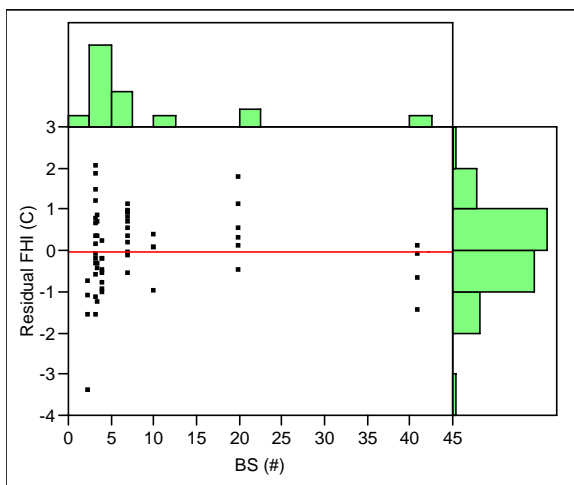
———Linear Fit

Linear Fit
Residual FHI (C) = 2.012e-14 - 3.215e-15 BS (#)
Summary of Fit

RSquare	0
RSquare Adj	-0.01786
Root Mean Square Error	0.974809
Mean of Response	-8.5e-15
Observations (or Sum Wgts)	58

Analysis of Variance

Source	DF	Sum of Squares	Mean Square	F Ratio
Model	1	0.000000	0.000000	0.0000
Error	56	53.214176	0.950253	Prob > F
C. Total	57	53.214176		1.0000

Parameter Estimates

Term	Estimate	Std Error	t Ratio	Prob>|t|
Intercept	2.012e-14	0.170607	0.00	1.0000
BS (#)	-3.22e-15	0.012691	-0.00	1.0000

73

Appendix 4-3. Result of Preliminary Testing for Impervious Surface at Nighttime (22:00).

(A) Distribution of Variables

FHI (C)
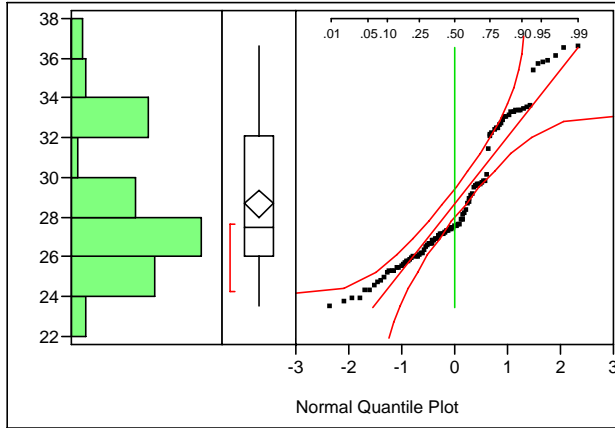
Quantiles		
100.0%	maximum	36.609
99.5%		36.609
97.5%		36.237
90.0%		33.393
75.0%	quartile	32.097
50.0%	median	27.498
25.0%	quartile	26.023
10.0%		25.125
2.5%		23.857
0.5%		23.510
0.0%	minimum	23.510

Moments	
Mean	28.671252
Std Dev	3.3881086
Std Err Mean	0.3290822
upper 95% Mean	29.323761
lower 95% Mean	28.018743
N	106

SHI (C)
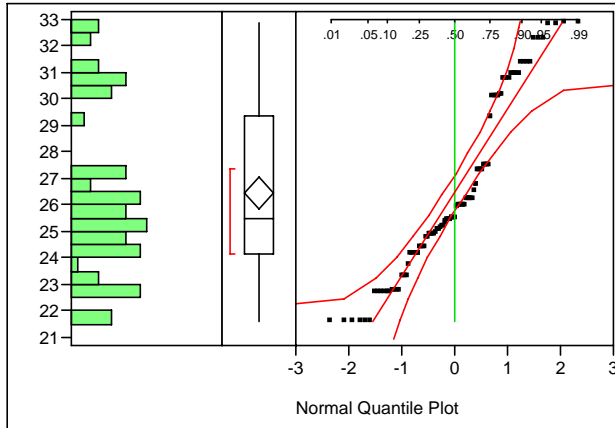
Quantiles		
100.0%	maximum	32.898
99.5%		32.898
97.5%		32.873
90.0%		31.366
75.0%	quartile	29.363
50.0%	median	25.513
25.0%	quartile	24.176
10.0%		22.736
2.5%		21.620
0.5%		21.620
0.0%	minimum	21.620

Moments	
Mean	26.431695
Std Dev	3.1453218
Std Err Mean	0.3055007
upper 95% Mean	27.037446
lower 95% Mean	25.825944
N	106

SW (m)
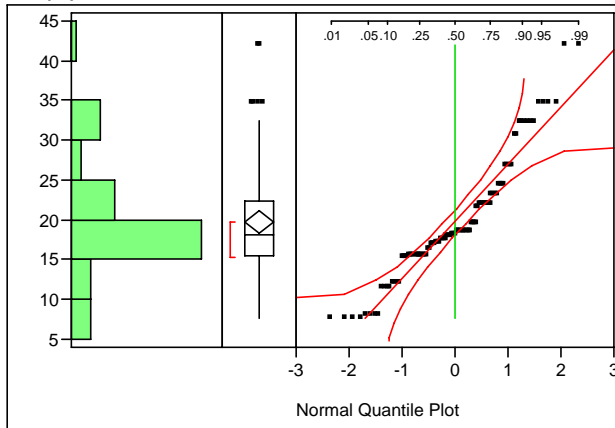
Quantiles		
100.0%	maximum	41.998
99.5%		41.998
97.5%		37.108
90.0%		32.397
75.0%	quartile	22.406
50.0%	median	18.190
25.0%	quartile	15.545
10.0%		11.656
2.5%		7.635
0.5%		7.635
0.0%	minimum	7.635

Moments	
Mean	19.73534
Std Dev	7.257367
Std Err Mean	0.7048978
upper 95% Mean	21.133022
lower 95% Mean	18.337658
N	106

DB (m)

Normal Quantile Plot
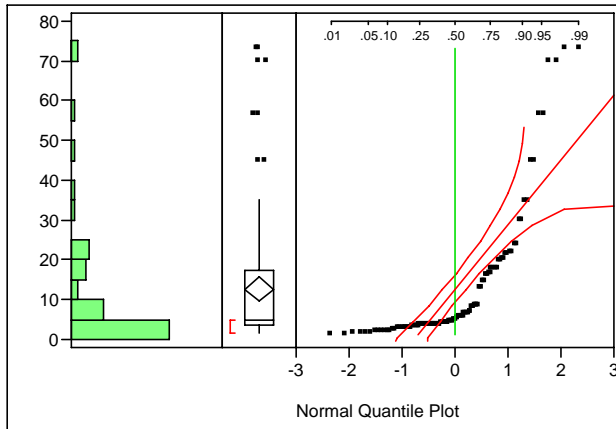
Quantiles

100.0%	maximum	73.173
99.5%		73.173
97.5%		71.134
90.0%		31.686
75.0%	quartile	17.192
50.0%	median	4.999
25.0%	quartile	3.645
10.0%		2.385
2.5%		1.659
0.5%		1.561
0.0%	minimum	1.561

Moments

Mean	12.672319
Std Dev	16.278366
Std Err Mean	1.5810946
upper 95% Mean	15.807337
lower 95% Mean	9.5373002
N	106

BS (#)

Normal Quantile Plot
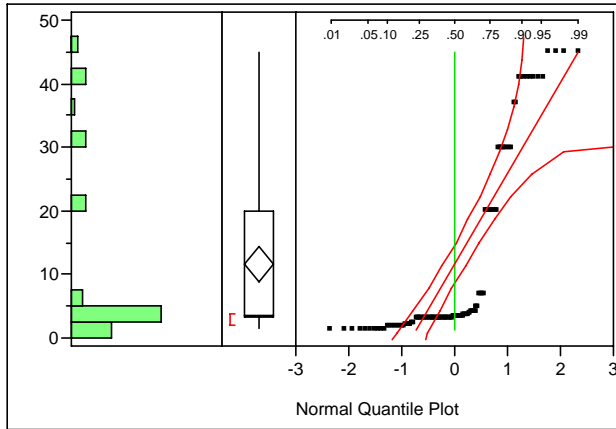
Quantiles

100.0%	maximum	45.000
99.5%		45.000
97.5%		45.000
90.0%		41.000
75.0%	quartile	20.000
50.0%	median	3.500
25.0%	quartile	3.250
10.0%		1.850
2.5%		1.500
0.5%		1.500
0.0%	minimum	1.500

Moments

Mean	11.54717
Std Dev	14.289445
Std Err Mean	1.3879136
upper 95% Mean	14.299146
lower 95% Mean	8.7951936
N	106

(C) Pearson Product Moment Correlation Matrix

Multivariate Correlations

	FHI (C)	SHI (C)	SW (m)	DB (m)	BS (#)
FHI (C)	1.0000	0.9445	0.1783	-0.0788	0.2195
SHI (C)	0.9445	1.0000	0.1654	0.0188	0.2318
SW (m)	0.1783	0.1654	1.0000	0.3597	0.2839
DB (m)	-0.0788	0.0188	0.3597	1.0000	-0.2645
BS (#)	0.2195	0.2318	0.2839	-0.2645	1.0000

Scatterplot Matrix
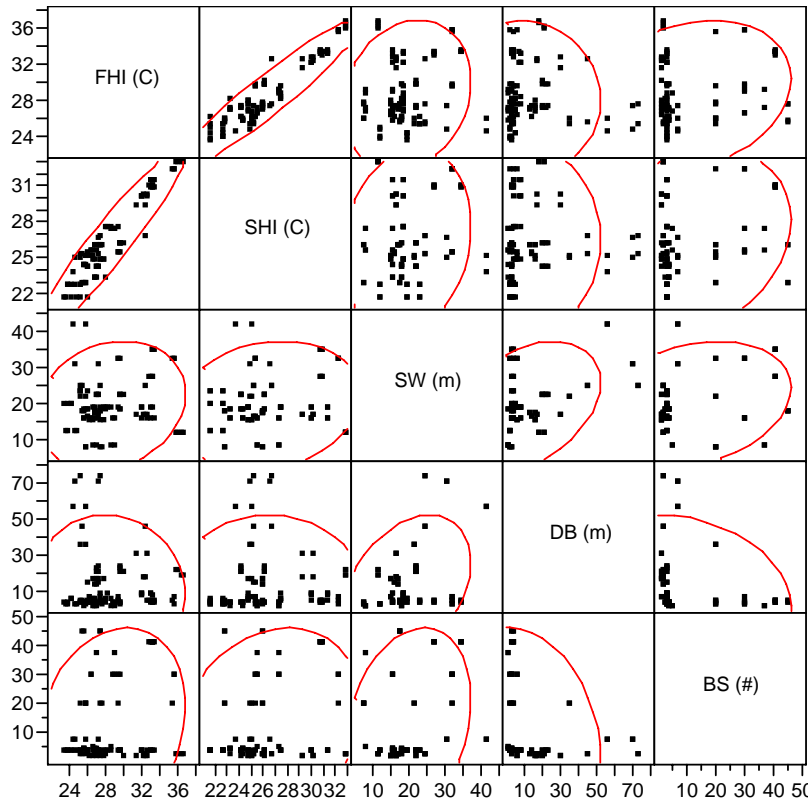
(C) Stepwise Regression

Stepwise Fit
Response: FHI (C)

Stepwise Regression Control

Prob to Enter	0.250
Prob to Leave	0.250

Direction: Mixed

Current Estimates

	SSE	DFE	MSE	RSquare	RSquare Adj	Cp	AIC
	110.49744	101	1.0940341	0.9083	0.9047	5	14.40465

Lock	Entered	Parameter	Estimate	nDF	SS	F Ratio	Prob>F
X	X	Intercept	1.41638324	1	0	0.000	1.0000
	X	SHI (C)	1.02011314	1	1009.599	922.823	0.0000
	X	SW (m)	0.04357491	1	7.476612	6.834	0.0103
	X	DB (m)	-0.030697	1	18.96202	17.332	0.0001
	X	BS (#)	-0.0155374	1	3.809415	3.482	0.0649

Step History

Step	Parameter	Action	"Sig Prob"	Seq SS	RSquare	Cp	p
1	SHI (C)	Entered	0.0000	1075.225	0.8921	16.917	2
2	DB (m)	Entered	0.0023	11.23553	0.9014	8.647	3
3	SW (m)	Entered	0.0464	4.556625	0.9052	6.482	4
4	BS (#)	Entered	0.0649	3.809415	0.9083	5	5

(D) OLS Regression

Response FHI (C)
Whole Model
Actual by Predicted Plot

FHI (C) Predicted P<.0001 RSq=0.91
RMSE=1.046
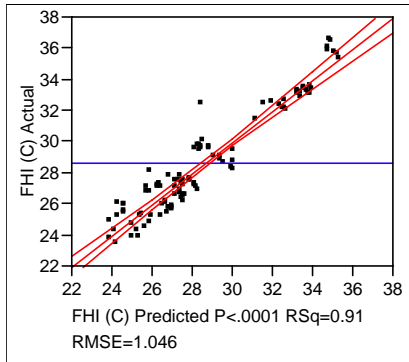
Summary of Fit

RSquare	0.908326
RSquare Adj	0.904695
Root Mean Square Error	1.045961
Mean of Response	28.67125
Observations (or Sum Wgts)	106

Analysis of Variance

Source	DF	Sum of Squares	Mean Square	F Ratio
Model	4	1094.8269	273.707	250.1812
Error	101	110.4974	1.094	Prob > F
C. Total	105	1205.3244		<.0001

Residual by Predicted Plot

FHI (C) Predicted
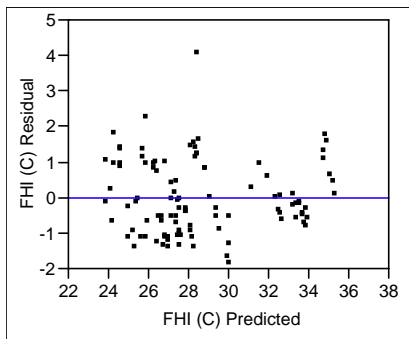
Parameter Estimates

Term	Estimate	Std Error	t Ratio	Prob>|t|	VIF
Intercept	1.4163832	0.890969	1.59	0.1150	.
SHI (C)	1.0201131	0.033581	30.38	<.0001	1.0706983
SW (m)	0.0435749	0.016669	2.61	0.0103	1.4044801
DB (m)	-0.030697	0.007373	-4.16	<.0001	1.3826721
BS (#)	-0.015537	0.008327	-1.87	0.0649	1.3586885

Effect Tests

Source	Nparm	DF	Sum of Squares	F Ratio	Prob > F
SHI (C)	1	1	1009.5993	922.8226	<.0001
SW (m)	1	1	7.4766	6.8340	0.0103
DB (m)	1	1	18.9620	17.3322	<.0001
BS (#)	1	1	3.8094	3.4820	0.0649

Leverage Plot
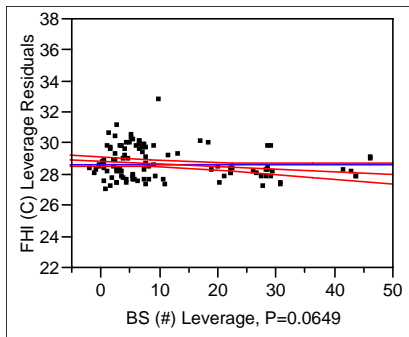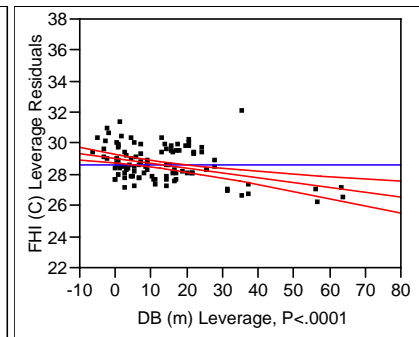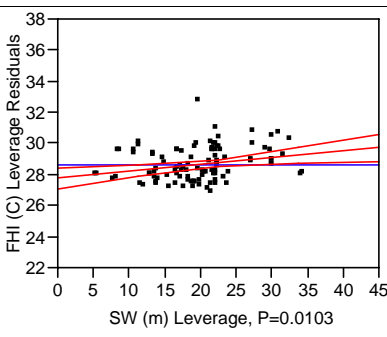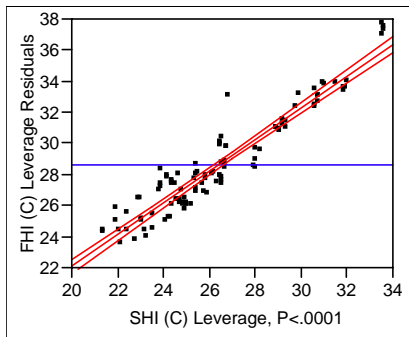
SHI (C) Leverage, P<.0001

SW (m) Leverage, P=0.0103

DB (m) Leverage, P<.0001

BS (#) Leverage, P=0.0649

77

(E) Distribution of Residuals derived from OLS Regression

Residual FHI (C) Distributions

Normal(1.3e-14,1.02584)

Quantiles

100.0%	maximum	4.067
99.5%		4.067
97.5%		1.971
90.0%		1.372
75.0%	quartile	0.899
50.0%	median	-0.199
25.0%	quartile	-0.732
10.0%		-1.150
2.5%		-1.475
0.5%		-1.851
0.0%	minimum	-1.851

Moments

Mean	1.287e-14
Std Dev	1.0258443
Std Err Mean	0.0996388
upper 95% Mean	0.1975654
lower 95% Mean	-0.197565
N	106

Normal Quantile Plot
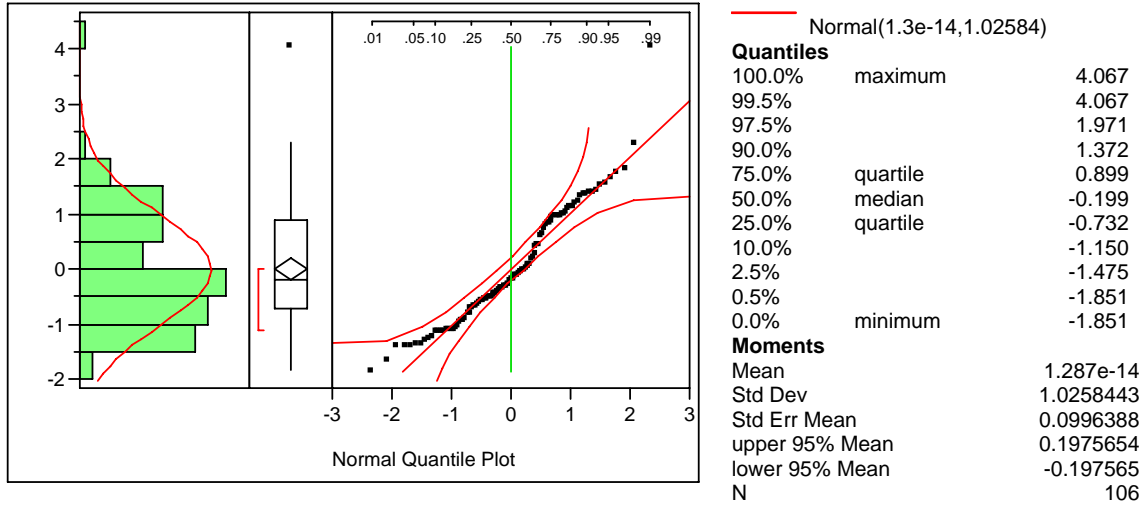
Fitted Normal
Parameter Estimates

Type	Parameter	Estimate	Lower 95%	Upper 95%
Location	Mu	1.287e-14	-0.197565	0.197565
Dispersion	Sigma	1.025844	0.903883	1.186153

(F) Regressing Residuals on Explanatory Variables

Bivariate Fit of Residual FHI (C) By SHI (C)

— Linear Fit

Linear Fit

Residual FHI (C) = -3.37e-13 + 1.325e-14 SHI (C)

Summary of Fit

RSquare	0
RSquare Adj	-0.00962
Root Mean Square Error	1.030764
Mean of Response	1.29e-14
Observations (or Sum Wgts)	106

Analysis of Variance

Source	DF	Sum of Squares	Mean Square	F Ratio
Model	1	0.00000	0.00000	0.0000
Error	104	110.49744	1.06248	Prob > F
C. Total	105	110.49744		1.0000

Parameter Estimates

Term	Estimate	Std Error	t Ratio	Prob>|t|
Intercept	-3.37e-13	0.851235	-0.00	1.0000
SHI (C)	1.325e-14	0.031982	0.00	1.0000
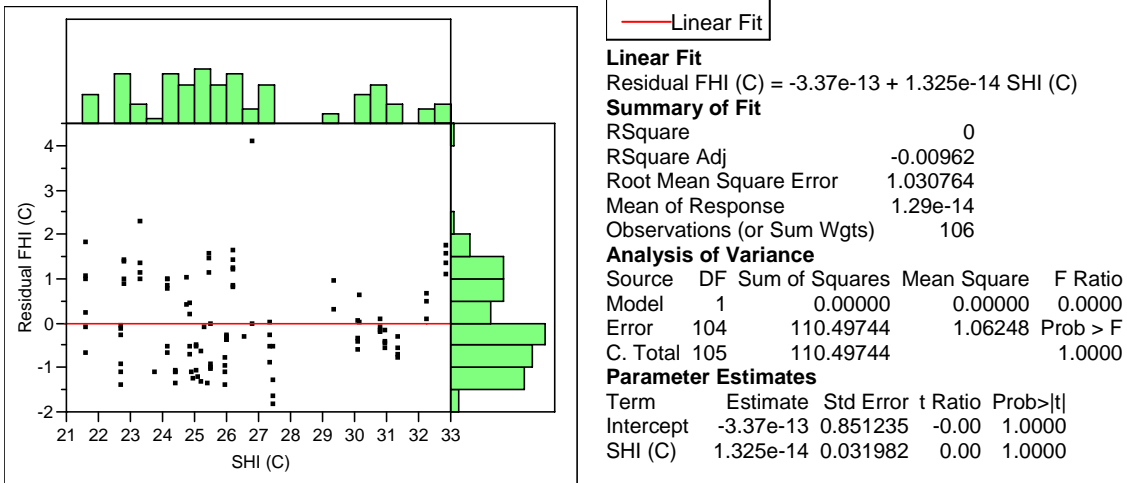
Bivariate Fit of Residual FHI (C) By SW (m)
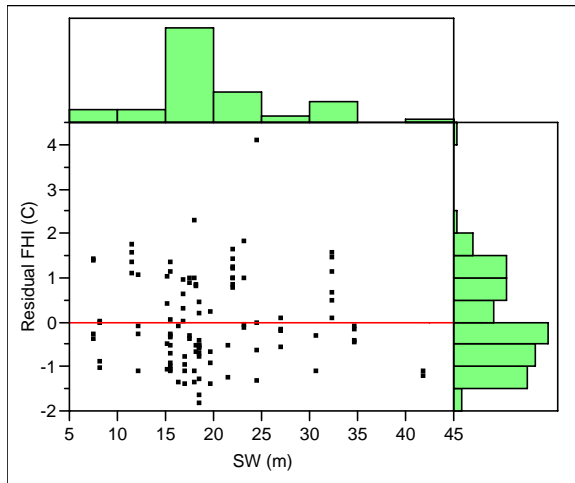
Linear Fit

Linear Fit
Residual FHI (C) = -4.73e-14 + 3.051e-15 SW (m)
Summary of Fit

RSquare	0
RSquare Adj	-0.00962
Root Mean Square Error	1.030764
Mean of Response	1.29e-14
Observations (or Sum Wgts)	106

Analysis of Variance

Source	DF	Sum of Squares	Mean Square	F Ratio
Model	1	0.00000	0.00000	0.0000
Error	104	110.49744	1.06248	Prob > F
C. Total	105	110.49744		1.0000

Parameter Estimates

Term	Estimate	Std Error	t Ratio	Prob>|t|
Intercept	-4.73e-14	0.291292	-0.00	1.0000
SW (m)	3.051e-15	0.013861	0.00	1.0000

Bivariate Fit of Residual FHI (C) By DB (m)
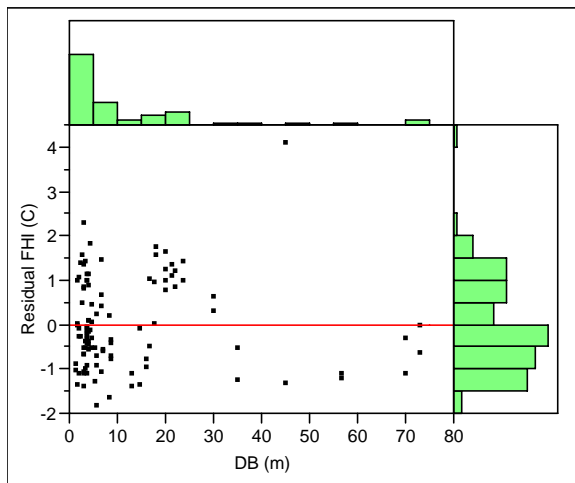
Linear Fit

Linear Fit
Residual FHI (C) = -2.84e-15 + 1.24e-15 DB (m)
Summary of Fit

RSquare	0
RSquare Adj	-0.00962
Root Mean Square Error	1.030764
Mean of Response	1.29e-14
Observations (or Sum Wgts)	106

Analysis of Variance

Source	DF	Sum of Squares	Mean Square	F Ratio
Model	1	0.00000	0.00000	0.0000
Error	104	110.49744	1.06248	Prob > F
C. Total	105	110.49744		1.0000

Parameter Estimates

Term	Estimate	Std Error	t Ratio	Prob>|t|
Intercept	-2.84e-15	0.127105	-0.00	1.0000
DB (m)	1.24e-15	0.00618	0.00	1.0000

Bivariate Fit of Residual FHI (C) By BS (#)
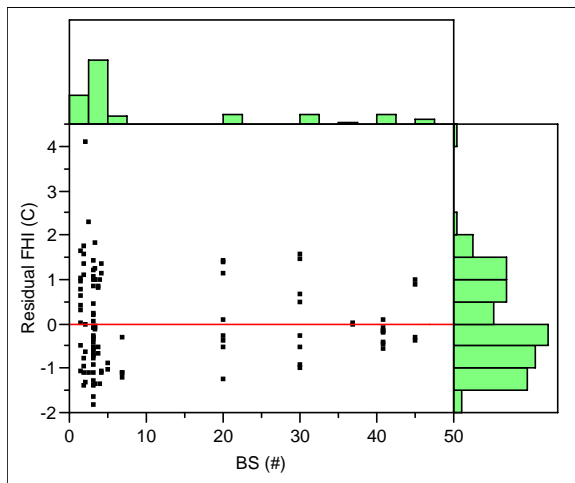
Linear Fit

Linear Fit
Residual FHI (C) = -2.76e-14 + 3.501e-15 BS (#)
Summary of Fit

RSquare	0
RSquare Adj	-0.00962
Root Mean Square Error	1.030764
Mean of Response	1.29e-14
Observations (or Sum Wgts)	106

Analysis of Variance

Source	DF	Sum of Squares	Mean Square	F Ratio
Model	1	0.00000	0.00000	0.0000
Error	104	110.49744	1.06248	Prob > F
C. Total	105	110.49744		1.0000

Parameter Estimates

Term	Estimate	Std Error	t Ratio	Prob>|t|
Intercept	-2.76e-14	0.128961	-0.00	1.0000
BS (#)	3.501e-15	0.00704	0.00	1.0000

Appendix 4-4. Result of Preliminary Testing for Pervious Surface at Nighttime (22:00).

(A) Distribution of Variables

FHI (C)
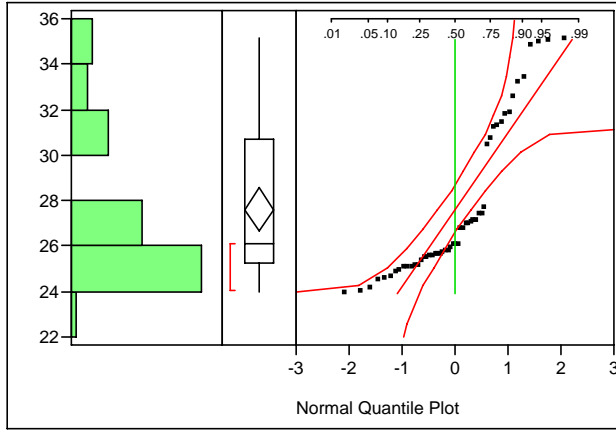
Quantiles

100.0%	maximum	35.125
99.5%		35.125
97.5%		35.098
90.0%		33.367
75.0%	quartile	30.673
50.0%	median	26.075
25.0%	quartile	25.217
10.0%		24.599
2.5%		23.994
0.5%		23.975
0.0%	minimum	23.975

Moments

Mean	27.620308
Std Dev	3.3500173
Std Err Mean	0.4645638
upper 95% Mean	28.552959
lower 95% Mean	26.687657
N	52

SHI (C)
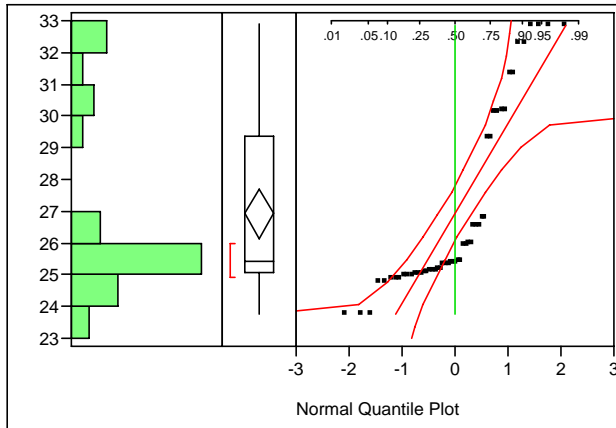
Quantiles

100.0%	maximum	32.898
99.5%		32.898
97.5%		32.898
90.0%		32.294
75.0%	quartile	29.363
50.0%	median	25.417
25.0%	quartile	25.063
10.0%		24.823
2.5%		23.761
0.5%		23.761
0.0%	minimum	23.761

Moments

Mean	26.927788
Std Dev	2.8380835
Std Err Mean	0.3935714
upper 95% Mean	27.717916
lower 95% Mean	26.137661
N	52

SW (m)
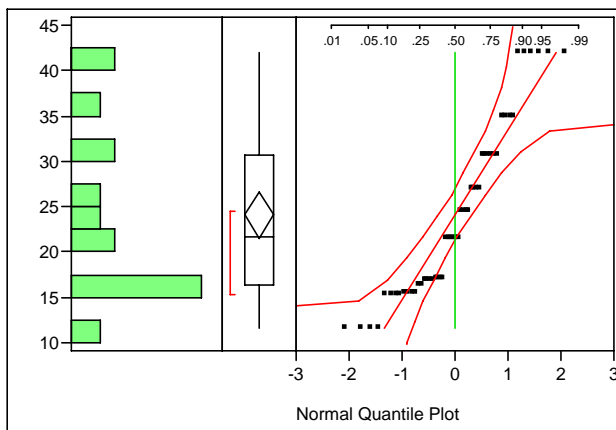
Quantiles

100.0%	maximum	41.998
99.5%		41.998
97.5%		41.998
90.0%		41.998
75.0%	quartile	30.715
50.0%	median	21.604
25.0%	quartile	16.423
10.0%		15.328
2.5%		11.656
0.5%		11.656
0.0%	minimum	11.656

Moments

Mean	24.072635
Std Dev	9.3612181
Std Err Mean	1.2981674
upper 95% Mean	26.678815
lower 95% Mean	21.466455
N	52

DB (m)

Normal Quantile Plot
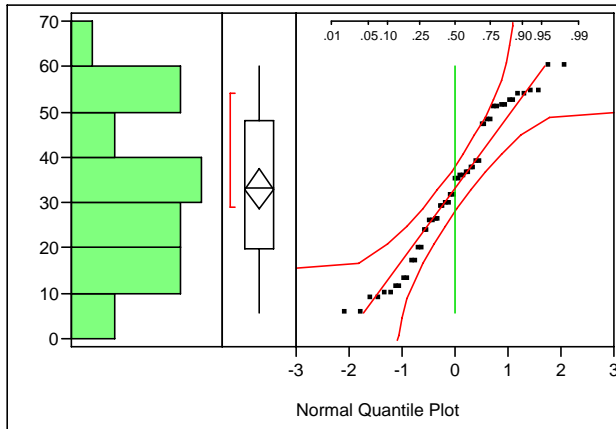
Quantiles

100.0%	maximum	60.195
99.5%		60.195
97.5%		60.195
90.0%		54.029
75.0%	quartile	48.177
50.0%	median	33.400
25.0%	quartile	19.879
10.0%		10.028
2.5%		5.657
0.5%		5.657
0.0%	minimum	5.657

Moments

Mean	32.95439
Std Dev	16.034639
Std Err Mean	2.2236043
upper 95% Mean	37.418462
lower 95% Mean	28.490318
N	52

BS (#)

Normal Quantile Plot
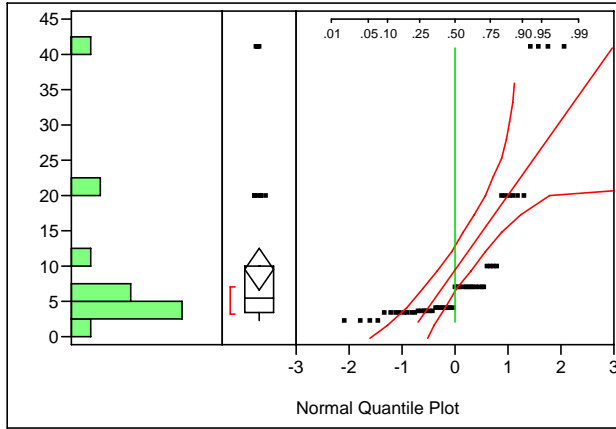
Quantiles

100.0%	maximum	41.000
99.5%		41.000
97.5%		41.000
90.0%		20.000
75.0%	quartile	10.000
50.0%	median	5.500
25.0%	quartile	3.500
10.0%		3.250
2.5%		2.250
0.5%		2.250
0.0%	minimum	2.250

Moments

Mean	9.5384615
Std Dev	10.559981
Std Err Mean	1.4644059
upper 95% Mean	12.478379
lower 95% Mean	6.5985441
N	52

(B) Pearson Product Moment Correlation Matrix

Multivariate Correlations

	FHI (C)	SHI (C)	SW (m)	DB (m)	BS (#)
FHI (C)	1.0000	0.9800	-0.5132	-0.5096	0.1669
SHI (C)	0.9800	1.0000	-0.5320	-0.4882	0.1234
SW (m)	-0.5132	-0.5320	1.0000	0.7190	0.0735
DB (m)	-0.5096	-0.4882	0.7190	1.0000	0.1454
BS (#)	0.1669	0.1234	0.0735	0.1454	1.0000

Scatterplot Matrix
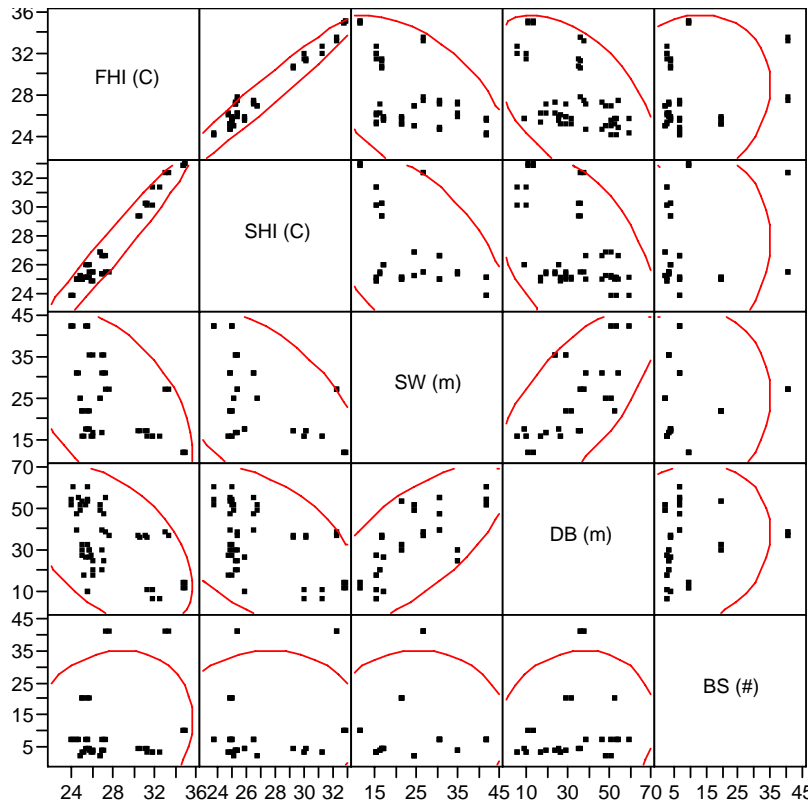
(C) Stepwise Regression

Stepwise Fit
Response: FHI (C)

Current Estimates

	SSE	DFE	MSE	RSquare	RSquare Adj	Cp	AIC
	19.199537	47	0.4085008	0.9665	0.9636	5	-41.8106

Stepwise Regression Control

Lock	Entered	Parameter	Estimate	nDF	SS	F Ratio	Prob>F
X	X	Intercept	-2.9280783	1	0	0.000	1.0000
	X	SHI (C)	1.13256218	1	347.5669	850.835	0.0000
	X	SW (m)	0.02129864	1	0.89147	2.182	0.1463
	X	DB (m)	-0.0192966	1	2.21303	5.417	0.0243
	X	BS (#)	0.01826134	1	1.76132	4.312	0.0433

Prob to Enter 0.250
Prob to Leave 0.250

Direction: Mixed

Step History

Step	Parameter	Action	"Sig Prob"	Seq SS	RSquare	Cp	p
1	SHI (C)	Entered	0.0000	549.7098	0.9604	7.431	2
2	BS (#)	Entered	0.1000	1.228496	0.9626	6.4237	3
3	DB (m)	Entered	0.0816	1.324106	0.9649	5.1823	4
4	SW (m)	Entered	0.1463	0.89147	0.9665	5	5

(D) OLS Regression

Response FHI (C)
Whole Model
Actual by Predicted Plot
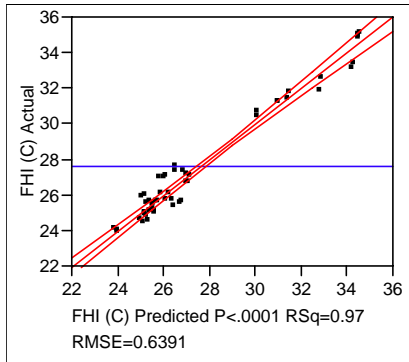
Summary of Fit

RSquare	0.966455
RSquare Adj	0.9636
Root Mean Square Error	0.639141
Mean of Response	27.62031
Observations (or Sum Wgts)	52

Analysis of Variance

Source	DF	Sum of Squares	Mean Square	F Ratio
Model	4	553.15388	138.288	338.5268
Error	47	19.19954	0.409	Prob > F
C. Total	51	572.35342		<.0001

Residual by Predicted Plot
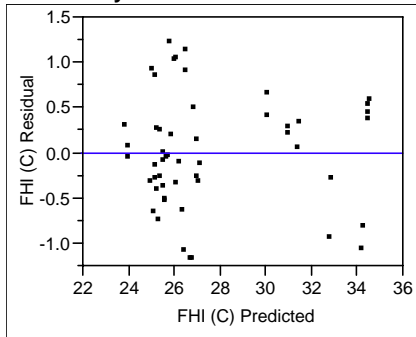
Parameter Estimates

Term	Estimate	Std Error	t Ratio	Prob>|t|	VIF
Intercept	-2.928078	1.214532	-2.41	0.0199	.
SHI (C)	1.1325622	0.038827	29.17	<.0001	1.5160242
SW (m)	0.0212986	0.014418	1.48	0.1463	2.2742164
DB (m)	-0.019297	0.008291	-2.33	0.0243	2.2062912
BS (#)	0.0182613	0.008794	2.08	0.0433	1.0767711

Effect Tests

Source	Nparm	DF	Sum of Squares	F Ratio	Prob > F
SHI (C)	1	1	347.56695	850.8354	<.0001
SW (m)	1	1	0.89147	2.1823	0.1463
DB (m)	1	1	2.21303	5.4174	0.0243
BS (#)	1	1	1.76132	4.3117	0.0433

Leverage Plot
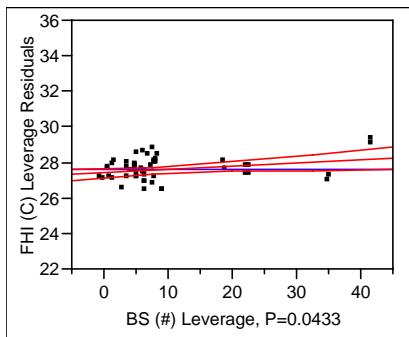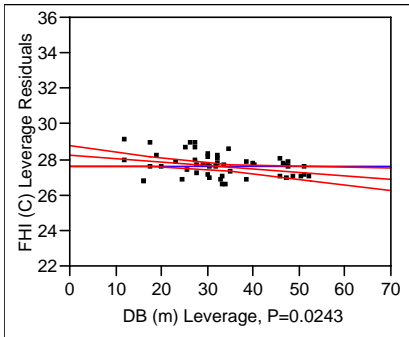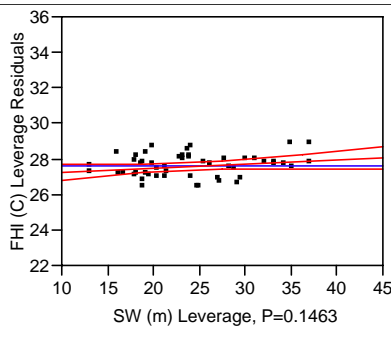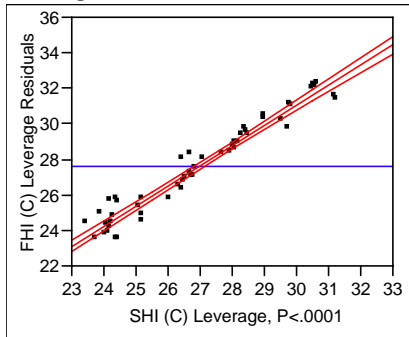
83

(E) Distribution of Residuals derived from OLS Regression

Residual FHI (C) Distributions
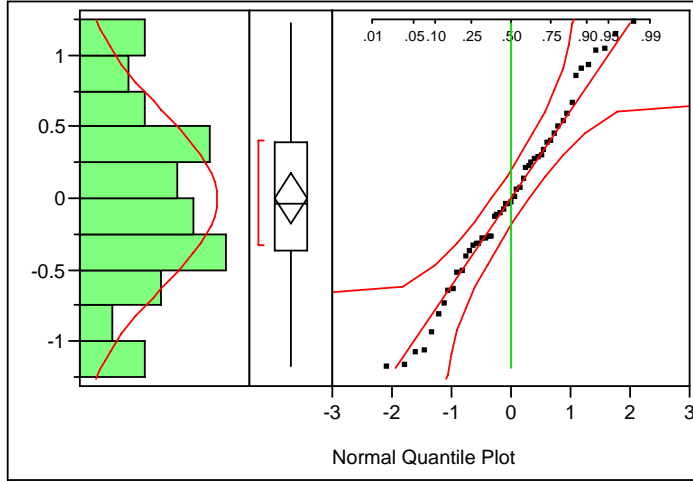
Normal(1.3e-14,0.61356)

Quantiles

100.0%	maximum	1.228
99.5%		1.228
97.5%		1.199
90.0%		0.922
75.0%	quartile	0.396
50.0%	median	-0.040
25.0%	quartile	-0.366
10.0%		-0.904
2.5%		-1.174
0.5%		-1.177
0.0%	minimum	-1.177

Moments

Mean	1.346e-14
Std Dev	0.6135646
Std Err Mean	0.0850861
upper 95% Mean	0.1708175
lower 95% Mean	-0.170817
N	52

Fitted Normal
Parameter Estimates

Type	Parameter	Estimate	Lower 95%	Upper 95%
Location	Mu	1.346e-14	-0.170817	0.1708175
Dispersion	Sigma	0.6135646	0.514197	0.7608980

(E) Regressing Residuals on Explanatory Variables

Bivariate Fit of Residual FHI (C) By SHI (C)
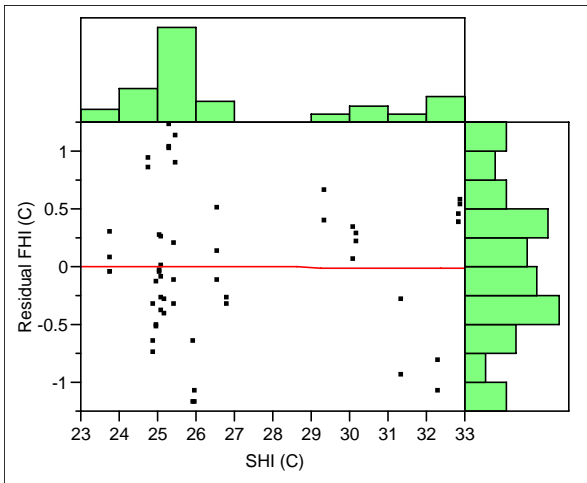
Linear Fit

Linear Fit
Residual FHI (C) = 2.179e-13 - 7.59e-15 SHI (C)

Summary of Fit

RSquare	0
RSquare Adj	-0.02
Root Mean Square Error	0.61967
Mean of Response	1.35e-14
Observations (or Sum Wgts)	52

Analysis of Variance

Source	DF	Sum of Squares	Mean Square	F Ratio
Model	1	0.000000	0.000000	0.0000
Error	50	19.199537	0.383991	Prob > F
C. Total	51	19.199537		1.0000

Parameter Estimates

Term	Estimate	Std Error	t Ratio	Prob>|t|
Intercept	2.179e-13	0.827759	0.00	1.0000
SHI (C)	-7.59e-15	0.030574	-0.00	1.0000

Bivariate Fit of Residual FHI (C) By SW (m)
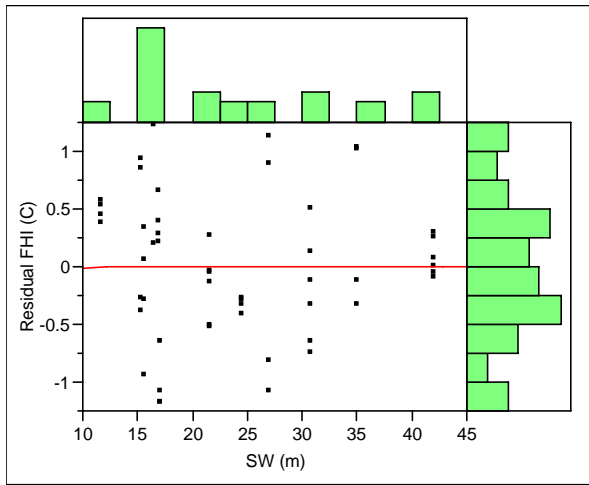
——Linear Fit

Linear Fit
Residual FHI (C) = -9.5e-15 + 9.538e-16 SW (m)
Summary of Fit
RSquare   0
RSquare Adj   -0.02
Root Mean Square Error   0.61967
Mean of Response   1.35e-14
Observations (or Sum Wgts)   52
Analysis of Variance

Source	DF	Sum of Squares	Mean Square	F Ratio
Model	1	0.000000	0.000000	0.0000
Error	50	19.199537	0.383991	Prob > F
C. Total	51	19.199537		1.0000

Parameter Estimates

Term	Estimate	Std Error	t Ratio	Prob>|t|
Intercept	-9.5e-15	0.23911	-0.00	1.0000
SW (m)	9.538e-16	0.009269	0.00	1.0000

Bivariate Fit of Residual FHI (C) By DB (m)
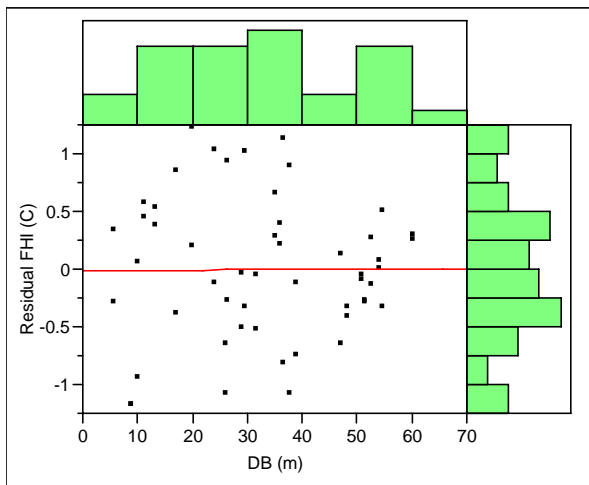
——Linear Fit

Linear Fit
Residual FHI (C) = -2.87e-14 + 1.28e-15 DB (m)
Summary of Fit
RSquare   0
RSquare Adj   -0.02
Root Mean Square Error   0.61967
Mean of Response   1.35e-14
Observations (or Sum Wgts)   52
Analysis of Variance

Source	DF	Sum of Squares	Mean Square	F Ratio
Model	1	0.000000	0.000000	0.0000
Error	50	19.199537	0.383991	Prob > F
C. Total	51	19.199537		1.0000

Parameter Estimates

Term	Estimate	Std Error	t Ratio	Prob>|t|
Intercept	-2.87e-14	0.197956	-0.00	1.0000
DB (m)	1.28e-15	0.005411	0.00	1.0000

Bivariate Fit of Residual FHI (C) By BS (#)
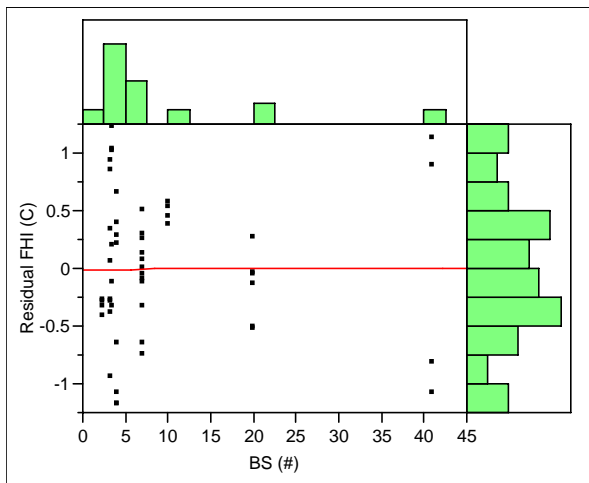
——Linear Fit

Linear Fit
Residual FHI (C) = -2.41e-14 + 3.941e-15 BS (#)
Summary of Fit
RSquare   0
RSquare Adj   -0.02
Root Mean Square Error   0.61967
Mean of Response   1.35e-14
Observations (or Sum Wgts)   52
Analysis of Variance

Source	DF	Sum of Squares	Mean Square	F Ratio
Model	1	0.000000	0.000000	0.0000
Error	50	19.199537	0.383991	Prob > F
C. Total	51	19.199537		1.0000

Parameter Estimates

Term	Estimate	Std Error	t Ratio	Prob>|t|
Intercept	-2.41e-14	0.116308	-0.00	1.0000
BS (#)	3.941e-15	0.008217	0.00	1.0000

Appendix 5-1. Commands and Results of MATLAB for Impervious Surface at 13:00.

Commands:	**>> sar(y,X,W,vnames);**
>> W=zeros(102); >> W(52:end,1:51)=eye(51); >> vnames=strvcat('SHI (C)','Sh (%)','BS (#)'); >> names=strvcat('FHI (C)',vnames); >> y=data(:,1);X=data(:,2:4); >> ols_ts(y,X,names); >> sar(y,X,W,vnames);	FINAL REGRESSION RESULTS: VAR COEFF Z-VAL PROB const 0.897437 0.799467 0.424020 SHI (C) 1.099025 30.648404 0.000000 Sh (%) -0.033024 -9.319274 0.000000 BS (#) -0.043505 -3.398399 0.000678 AUTOCORRELATION RESULTS:

>> ols_ts(y,X,names);

Ordinary Least-squares Estimates
Dependent Variable =   FHI (C)
R-squared   =   0.9050
R-squared Adj   =   0.9021
AIC   =   351.4259
AIC_corrected   =   352.0509
sigma^2   =   1.7323
Durbin-Watson   =   1.3128
Nobs, Nvars   =   102,   4
****

Variable	Coefficient	t-statistic	t-probability
Constant	0.440386	0.357058	0.721816
SHI (C)	1.111740	27.827940	0.000000
Sh (%)	-0.032555	-10.535124	0.000000
BS (#)	-0.040655	-3.609266	0.000486

AUTOCORRELATION RESULTS:

	VAL	Z-VAL	PROB
rho	0.466649	3.332544	0.000861

GOODNESS-OF-FIT RESULTS:

Pseudo R-Square   =   0.98559
Pseudo R-Square Adj   =   0.98515
Squared_Correlation   =   0.9048
Log Likelihood Value =   -164.1677
AIC   =   340.3355
AIC_corrected   =   341.2197

TESTS OF SAR MODEL:

TEST	VAL	PROB
LR	13.090449	0.000297
Com-LR	19.820985	0.000185

Appendix 5-2. Commands and Results of MATLAB for Pervious Surface at 13:00.

Commands:	**>> sar(y,X,W,vnames);**
>>W=zeros(58); >>W(30:end,1:29)=eye(29); >>vnames=strvcat('SHI (C)','Sh (%)','BS (#)'); >>names=strvcat('FHI (C)',vnames); >>y=data(:,1);X=data(:,2:4); >>ols_ts(y,X,names); >>sar(y,X,W,vnames);	FINAL REGRESSION RESULTS: VAR COEFF Z-VAL PROB Const 2.806569 3.173098 0.001508 SHI (C) 0.985783 36.055478 0.000000 Sh (%) -0.021753 -5.876609 0.000000 BS (#) -0.055871 -3.585368 0.000337 AUTOCORRELATION RESULTS:

>> ols_ts(y,X,names);

Ordinary Least-squares Estimates
Dependent Variable   =   FHI (C)
R-squared   =   0.9441
R-squared Adj   =   0.9410
AIC   =   169.6020
AIC_corrected   =   170.7559
sigma^2   =   0.9854
Durbin-Watson   =   1.4327
Nobs, Nvars   =   58,   4
****

Variable	Coefficient	t-statistic	t-probability
Constant	2.925012	2.639109	0.010841
SHI (C)	0.972824	27.480705	0.000000
Sh (%)	-0.021002	-6.193342	0.000000
BS (#)	-0.035156	-2.688843	0.009516

AUTOCORRELATION RESULTS:

	VAL	Z-VAL	PROB
rho	0.913871	4.921348	0.000001

GOODNESS-OF-FIT RESULTS:

Pseudo R-Square   =   0.99728
Pseudo R-Square Adj   =   0.99712
Squared_Correlation   =   0.94167
Log Likelihood Value =   -71.9462
AIC   =   155.8924
AIC_corrected   =   157.5394

TESTS OF SAR MODEL:

TEST	VAL	PROB
LR	15.709630	0.000074
Com-LR	111.816707	0.000000

Appendix 5-3. Commands and Results of MATLAB for Impervious Surface at 22:00.

<table>
<tr><td>

Commands:
```
>>W=zeros(106);
>>W(54:end,1:53)=eye(53);
>>vnames=strvcat('SHI (C)','SW (m)','DB (m)','BS (#)');
>>names=strvcat('FHI (C)',vnames);
>>y=data(:,1);X=data(:,2:5);
>>ols_ts(y,X,names);
>>sar(y,X,W,vnames);
```

</td><td>

>> sar(y,X,W,vnames);

FINAL REGRESSION RESULTS:

VAR	COEFF	Z-VAL	PROB
Const	1.560483	1.726435	0.084269
SHI (C)	1.014258	29.830028	0.000000
SW (m)	0.043774	2.549879	0.010776
DB (m)	-0.030611	-4.030951	0.000056
BS (#)	-0.015229	-1.776752	0.075609

AUTOCORRELATION RESULTS:

	VAL	Z-VAL	PROB
rho	0.112460	0.818721	0.412946

</td></tr>
<tr><td>

>> ols_ts(y,X,names);

Ordinary Least-squares Estimates
Dependent Variable	=	FHI (C)
R-squared	=	0.9083
R-squared Adj	=	0.9047
AIC	=	317.2196
AIC_corrected	=	318.0681
sigma^2	=	1.0940
Durbin-Watson	=	1.1193
Nobs, Nvars	=	106, 5

****

Variable	Coefficient	t-statistic	t-probability
Constant	1.416383	1.589711	0.115025
SHI (C)	1.020113	30.377995	0.000000
SW (m)	0.043575	2.614189	0.010312
DB (m)	-0.030697	-4.163196	0.000066
BS (#)	-0.015537	-1.866009	0.064942

</td><td>

GOODNESS-OF-FIT RESULTS:

Pseudo R-Square	=	0.92756
Pseudo R-Square Adj	=	0.92469
Squared_Correlation	=	0.90832
Log Likelihood Value	=	-152.354
AIC	=	318.708
AIC_corrected	=	319.8508

TESTS OF SAR MODEL:

TEST	VAL	PROB
LR	0.511638	0.474431
Com-LR	8.023420	0.090724

</td></tr>
</table>

Appendix 5-4. Commands and Results of MATLAB for Pervious Surface at 22:00

<table>
<tr><td>

Commands:
```
>>W=zeros(52);
>>W(27:end,1:26)=eye(26);
>>vnames=strvcat('SHI (C)','SW (m)','DB (m)','BS (#)');
>>names=strvcat('FHI (m)',vnames);
>>y=data(:,1);X=data(:,2:5);
>>ols_ts(y,X,names);
>>sar(y,X,W,vnames);
```

</td><td>

>> sar(y,X,W,vnames);

FINAL REGRESSION RESULTS:

VAR	COEFF	Z-VAL	PROB
Const	-2.885863	-2.489227	0.012802
SHI (C)	1.131182	30.524478	0.000000
SW (m)	0.021148	1.532591	0.125377
DB (m)	-0.019359	-2.439459	0.014709
BS (#)	0.018328	2.177254	0.029462

AUTOCORRELATION RESULTS:

	VAL	Z-VAL	PROB
rho	0.013992	0.071348	0.943121

</td></tr>
<tr><td>

>> ols_ts(y,X,names);

Ordinary Least-squares Estimates
Dependent Variable	=	FHI (C)
R-squared	=	0.9665
R-squared Adj	=	0.9636
AIC	=	107.7590
AIC_corrected	=	109.6257
sigma^2	=	0.4085
Durbin-Watson	=	1.0828
Nobs, Nvars	=	52, 5

****

Variable	Coefficient	t-statistic	t-probability
Constant	-2.928078	-2.410870	0.019878
SHI (C)	1.132562	29.169083	0.000000
SW (m)	0.021299	1.477260	0.146276
DB (m)	-0.019297	-2.327540	0.024293
BS (#)	0.018261	2.076456	0.043345

</td><td>

GOODNESS-OF-FIT RESULTS:

Pseudo R-Square	=	0.96665
Pseudo R-Square Adj	=	0.96381
Squared_Correlation	=	0.96645
Log Likelihood Value	=	-47.8776
AIC	=	109.7552
AIC_corrected	=	112.3006

TESTS OF SAR MODEL:

TEST	VAL	PROB
LR	0.003866	0.950423
Com-LR	12.719988	0.012728

</td></tr>
</table>